NBSIR 81-2407 (R)

Intruder Tagging and Identification Using Luminescent Particles

U.S. DEPARTMENT OF COMMERCE
National Bureau of Standards
Center for Analytical Chemistry
Washington, DC 20234

Prepared by
Law Enforcement Standards Laboratory
National Engineering Laboratory
National Bureau of Standards
Washington, DC 20234

September 1982

Final Report

Prepared for
Defense Nuclear Agency
ATTN: OPNS
Washington, DC 20305

OFFICIAL USE ONLY

NBSIR 81-2407 (R)

INTRUDER TAGGING AND IDENTIFICATION USING LUMINESCENT PARTICLES

J. R. DeVoe
R. A. Velapoldi
J. K. Langland
D. K. Hancock

U.S. DEPARTMENT OF COMMERCE
National Bureau of Standards
Center for Analytical Chemistry
Washington, DC 20234

Prepared by
Law Enforcement Standards Laboratory
National Engineering Laboratory
National Bureau of Standards
Washington, DC 20234

September 1982

Final Report

.

Prepared for
Defense Nuclear Agency
Attn: OPNS
Washington, DC 20305

OFFICIAL USE ONLY

U.S. DEPARTMENT OF COMMERCE, Malcolm Baldrige, *Secretary*

NATIONAL BUREAU OF STANDARDS, Ernest Ambler, *Director*

FOREWORD

The Defense Nuclear Agency (DNA) is engaged in a continuing effort to enhance the security of nuclear weapons storage. In this effort, it is receiving technical support from the National Bureau of Standards' Law Enforcement Standards Laboratory (LESL), whose overall program involves the application of science and technology to the problems of crime prevention, law enforcement and criminal justice.

LESL is assisting DNA's physical security program with support in chemical sciences, and the barrier and ballistic materials areas.

Among the tasks being performed by LESL for DNA are the preparation and publication of several series of technical reports on the results of its researches. This document is one such report.

Technical comments and suggestions are invited from all interested parties. They may be addressed to the authors, or the Law Enforcement Standards Laboratory, National Bureau of Standards, Washington, DC 20234.

Lawrence K. Eliason, Chief
Law Enforcement Standards Laboratory

INTRUDER TAGGING AND IDENTIFICATION
USING LUMINESCENT PARTICLES

Contents

LIST OF TABLES

Page

INTRUDER TAGGING AND IDENTIFICATION
USING LUMINESCENT PARTICLES

J. R. DeVoe, R. A. Velapoldi, J. K. Langland, D. K. Hancock*

National Bureau of Standards
Washington, DC 20234

This is the final report on the development of a unique particle tagging system that can allow one to follow the egress of a person who violates a secured area. The intruder comes into contact with glass beads (20 μm diam) which are of two types: one type acts as light reflectors allowing immediate visual detection; the second type contains rare earths whose emission spectra and quantity can be measured in a microspectrofluorimeter. Each site is tagged with beads containing a unique concentration ratio of two rare earths, thereby enabling hundreds of unique codes. The efficiency for detecting these particles has been measured and particle densities as low as 5 particles/cm^2 can be detected. Particle concentration techniques were also developed. Practical tests demonstrated the portability of the equipment and that this system is effective in such environments as normal buildings and houses as well as in an ammunition storage bunker.

Key words: fluorescence; intruder tagging and identification; microspectrofluorimeter; particles; tagging material.

I. INTRODUCTION

Conventional security systems rely upon a combination of intrusion alarms and response forces to protect facilities and government property. Present day intrusion detection systems sense the presence or action of an intruder and signal an alarm for appropriate action by the response force. The need for improved site security is often recognized, and several overall intrusion detection systems have been developed. While these systems may have application for improving the security of a site, it is desirable to augment such systems with components that react to the penetration attempts of an intruder, not simply signal an alarm.

The Defense Nuclear Agency has sponsored the development of a security system concept called Forced Entry Deterrent Systems (FEDS). The objective of this development is to deny access to a secured site by impairing the senses of an intruder sufficiently to cause him to discontinue his penetration attempt (psychological deterrence), while at the same time affording a tactical advantage to the response force personnel.

Assuming that an intruder has activated a FEDS component, it would be desirable to tag or label the individual so that the person could be positively identified as having attempted to intrude into the site and aid in apprehension should the intruder escape from the scene before response forces arrive. In addition, a tagging material that is dispensed at the perimeter of a site could assist in tracking the intruder towards the target.

An intruder enters a secured area and then leaves with or without the object or information that was to be stolen. The question to be answered is whether or not a tag can be used to uniquely identify the intruder even if apprehension occurred much later and quite remote from the secured area. This report describes one solution to the problem, which is the use of luminescent particles that can be made so as to cause them to be uniquely identifiable from all other types of particles.

The luminescent particles must be physically placed on or within the intruder. There are two obvious ways that this can be accomplished. The surface areas of interest (e.g., inventory, tables, walls, parts of the floor) can be coated with a film of these particles. Alternatively, a sensor can trigger the ejection of particles in a cloud that fills the area. The intruders then get the particles on

---

*Center for Analytical Chemistry, National Measurement Laboratory.

their person and/or in the nostrils and lungs, and of course leave a trail. The particles can be made so that immediate detection of even a few particles with a simple lamp is possible. To identify conclusively that the particles came from the violated secured space, the particles must be analyzed with a microspectrofluorimeter.

There are only a few techniques available for identification involving measurement of elemental concentration ratios of rare earths within single particles [1][1]. Electron or ion probes are expensive, but can be used in this application. Very sensitive analytical techniques such as activation analysis could be used, but the availability of facilities is limited. Other sensitive methods which dissolve the sample could be used, but the cost of analyses at the expected resultant 100 pg/mL of solution is high due to the technical difficulties in analyzing at such low concentrations.

Producing and measuring luminescence of particles involve the use of a special microscope in which particles are irradiated with ultraviolet (UV) light. This UV energy excites the luminescent substance causing it to emit radiation of a different wavelength than the incident radiation. Measurement of the emission or luminescence spectrum verifies the identity of the substance and in this work the ratio of specified peaks in the emission spectrum of two luminescent substances provides the unique identification of the particle. Peak intensities in the emission spectra are proportional to the concentration of the luminescent species. Spectra can be obtained from rare earth glass spheres as small as 10 um in diameter.

There has been a limited amount of work done on this idea in the past. Luminescent particles have been incorporated into explosives for the purpose of tracing their origins. The Aerospace Corp. [2] contracted with Westinghouse Corp. and 3 M Corp. to produce appropriate particles. Westinghouse used ceramic spheres with a luminescent coating, while 3 M used irregular-shaped particles made of layered luminescent substances. The layered system provides for a large number of possibly unique codes, but the particle sizes are quite large, often greater than 100 um. This may limit dispersal except when explosives are used. Many of the luminophors that were used in these systems were organic compounds whose luminescence can be expected to fade when exposed to sunlight.

The glass spheres selected in this project incorporate the rare earth luminophors as a solid solution and are more stable than the organic species. In addition, it is much easier to detect via microscopic examination completely spherical particles (as contrasted to the irregular shape of the layered particles) from the various odd shapes of particles normally found in common house dust, for example. Although no studies were made during this project, it is suspected that there will be minimal dangers from particles inhaled into the lungs or nasal passages. This assumption is based upon the fact that the surface composition of the glass sphere, unlike the coated ceramic spheres, is mostly SiO_2, which is like road dust or sand, and it has been established to be relatively safe.

A benefit from this study has been the generation of a luminescent particle as a reference material. There is a need in several areas of science for an accurate calibration of instruments that measure luminescence intensity produced by small particles. For example in the field of immunocytology, the use of a luminescent tag of blood cells is commonplace, but there is a need for calibrating the apparatus which measures the intensity of luminescence from a single cell. The glass spheres developed in this work are ideally suited for this. They are very stable, spherical, and can be measured reproducibly.

The five phases identified in this project were carried out in sequence with the understanding that a satisfactory conclusion would have to be derived from each phase before beginning the next one.

The phases are:

1. Identify and characterize candidate particles, fabricate some of the promising ones, and test their properties of luminescence (sec. III).

---

[1]Numbers in brackets refer to references on page 65.

2. Explore the extent of unique types of tagged particles that can be used (sec. IV).

3. Investigate various methods for particle deployment (sec. V).

4. Evaluate the sensitivity for detecting particles (sec. VI).

5. Evaluate the effectiveness of the system by simulated field tests (sec. VII).

The subsequent sections of this report briefly describe the field of microspectrofluorimetry, the work done in each of the phases, and finally, the potential and future development of the system.[2]

II. SPECTROFLUORIMETRY

A. History, Description, and Application

The photoluminescence of molecules was first noted by Monaides in the early 1500's [3], and in 1852, Stokes [4] correctly described this phenomenon and labeled it fluorescence. Luminescence is a general term that includes phosphorescence and fluorescence and will be used throughout this report. Luminescence techniques are extremely sensitive and selective, and are used in both the macro or micro sense in diverse disciplines including: environmental pollution, forensic science, biochemistry, geochemistry, clinical chemistry, molecular biology, and cytology.

It is the application in these latter areas that has led to the development of microscopic techniques and associated instrumentation to measure luminescence. Before addressing this topic, a brief description of the luminescence process and its important variables is in order so that the bases for luminescent particle selection and measurement are established.

Photoluminescence is the emission of radiation (light) by atoms, ions, or molecules excited by an external source (in this case, excitation is through photon absorption). A simplified energy diagram, presented in figure 1, illustrates the basic processes of radiation absorption and emission.

The ground state (S_0), the excited states S_1, S_2---S_n, and the vibrational-rotational levels (for molecules) designated by 0, 1, 2---n are shown schematically in figure 1. Radiation is absorbed in the ground state S_0. The molecule, atom, or ion is raised to some excited state, e.g., S_1 or S_2. In general, the molecule, atom, or ion loses energy through interaction with adjacent atoms, ions, or molecules and thus reverts to the lower energy levels. Two examples of this process, called internal conversion, are represented by I_c in figure 1. Internal conversion is usually quite rapid with respect to photoemission from excited states higher than S_1, and consequently little photoemission is observed from these states. However, the time for I_c from S_1 to S_0 is of the same order of magnitude as photoemission I_L because S_1 and S_0 are separated by a fairly large ΔE, which in turn results in a low probability for I_c. Thus, I_c and I_L from S_1 to S_0 occur within the same time frame and are competing processes. Note: For simplicity, we have neglected other processes competing with photoemission such as intersystem crossing and quenching. Additional information can be obtained from C. A. Parker's classic work as well as other treatises [5]. Each ion, atom, or molecule has different energy levels which result in different excitation (absorbance) and luminescence spectra.

The definition of luminescence emission is:

$$I_L = Q_L \ I_a \tag{1}$$

---

[2]Mention of trade names throughout this report is made to improve clarity of presentation and does not constitute endorsement by any agency of the U.S. Government.

3

where I_L = rate of light emitted in photons/s,
 Q_L = quantum efficiency of luminescence, and
 I_a = rate of light absorbed in photons/s.

The light absorbed can be shown to be

$$I_a = I_0 \ (1-e^{-kc'\ell}) \tag{2}$$

where I_0 is the intensity of the excitation radiation,
 k is the cross-sectional area for absorption,
 c' is the concentration of the luminophor in molecules/cc, and
 ℓ is the length of the absorption path.

Substitution of eq (2) into eq (1) followed by power series expansion and units conversion yields

$$I_L = I_0 \ (2.3 \ \varepsilon c \ell) \left[1 - \frac{2.3 \ \varepsilon c \ell}{2} + \frac{(2.3 \ \varepsilon c \ell)^2}{6} - \ldots \ldots \right] Q_L \tag{3}$$

where ε is the molar absorptivity and c is the concentration in moles/L.
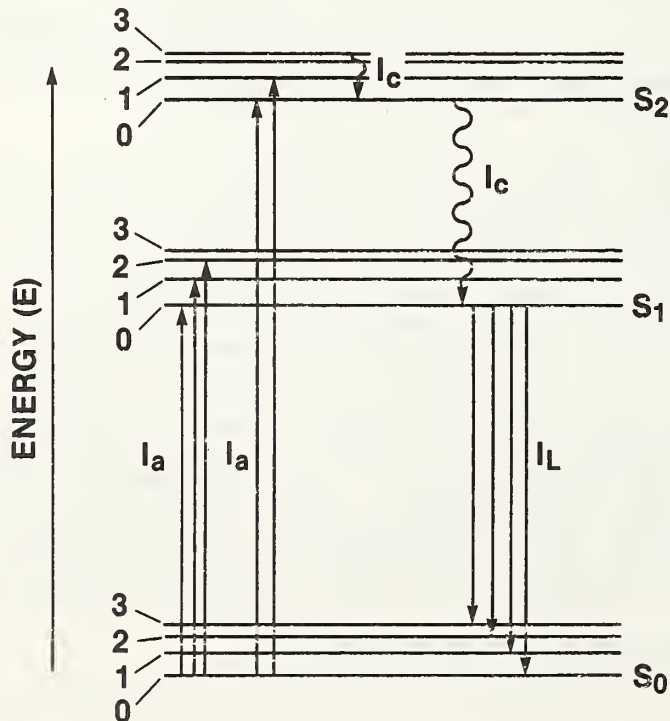
Figure 1. Simplified Jablonski energy level diagram showing the processes of photon absorption (I_a), internal conversion (I_c), and luminescence (I_L).

4

A dilute solution approximation can be made with little error [5(a)] yielding a simplified eq (4):

$$I_L = I_0 \ (2.3 \ \varepsilon c \ell) Q_L \tag{4}$$

which shows that the radiation emitted by a solution is proportional to I_0, Q_L, and the absorbance which equals $\varepsilon c \ell$. Increasing any of these parameters increases the intensity of the emitted radiation. For the same species in the same matrix, ε and Q_L are usually constant. Assuming I_0 and ℓ also to be constant, the equation defining luminescence or the radiation emitted by a solid or solution simplifies to:

$$I_L \propto C \tag{5}$$

which specifies that the intensity of the emitted radiation is proportional to the concentration of the luminescent species.

As a result of having different energy levels, each luminescent material has an excitation spectrum (absorbance spectrum, I_a as a function of wavelength, λ) and an emission spectrum (I_L as a function of λ) that is indicative of the energy levels within the molecule or ion in that particular matrix. These spectra may be measured by using a spectrofluorimeter. A simplified schematic of a spectrofluorimeter is given in figure 2.
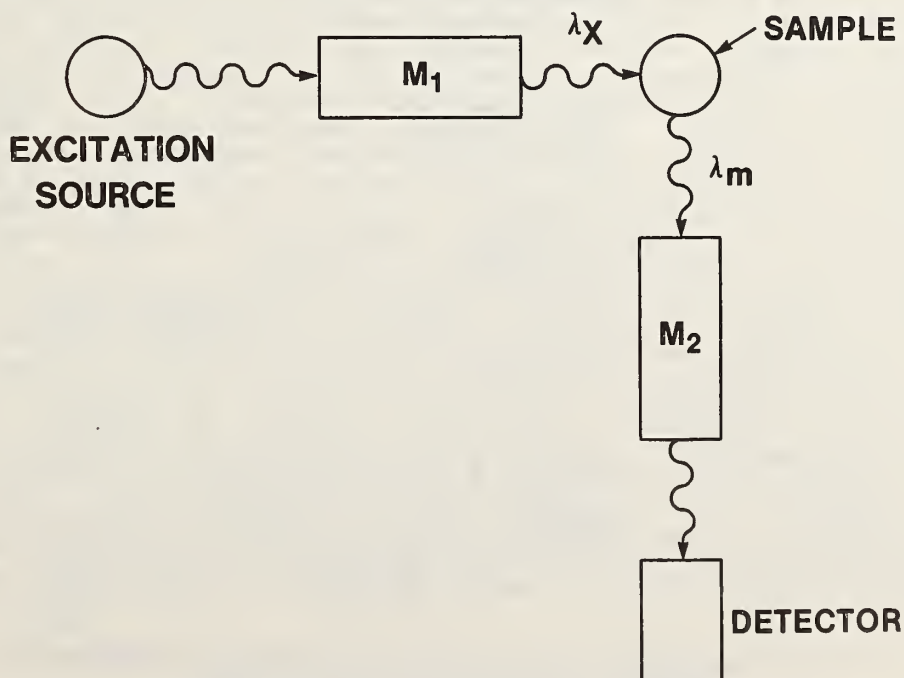
Figure 2. Schematic for a spectrofluorimeter; M can be monochromators or selective filters, λ_x = exciting wavelength, λ_m = emission wavelength.

Radiation (λ_x) from an excitation source (xenon arc, mercury arc, laser, etc.) is selected by M_1 (bandpass filters or monochromator) and is absorbed by the sample. Radiation (λ_m) is emitted by the sample (luminescence) and the spectral distribution of this radiation is analyzed by M_2 (bandpass filters or monochromator) and detected by a photomultiplier tube. For the purpose of this discussion, M_1 and M_2 are considered to be monochromators such that wavelengths for λ_x and λ_m with fairly narrow bandwidths (half-height bandwidths, hhbw) of 1-16 nm can be easily measured. Filter hhbw's are fairly broad (10-200 nm) except for special narrow-bandpass filters. An emission spectrum is obtained by scanning M_2 while holding M_1 constant at some wavelength λ_x at which the species absorbs radiation. Similarly, an excitation spectrum is obtained by scanning M_1 while holding M_2 constant at some wavelength λ_m at which the species emits.

Since different species have different excitation and emission spectra, and since the intensity of the emission (or excitation) spectrum is proportional to species concentration, the luminescence spectrum and the relative intensity of that spectrum can be used to identify a specific luminophor and thus a specific particle. If two luminescent ions with different emission spectra are dissolved in a glass that is fabricated into a sphere, it is probable that the sphere can be unambiguously identified using spectrofluorimetric techniques. In this case the ratio of the major emission peak heights for each luminophor would be determined by measuring the combined emission spectrum and comparing it to known spectra for standard luminophor-doped glass spheres. To accomplish this, a microspectrofluorimeter was designed and constructed from commercially available parts.

B. Description of the Microspectrofluorimeter

A microscope (Orthoplan, Ernst Leitz Wetzlar GMBH, W. Germany) equipped with a Ploemopak vertical illuminator [6] for epi-illumination (incident excitation) and a microscope photometer (MPV, E. Leitz) was used as the basic microspectrofluorimeter (fig. 3). The excitation radiation, produced by a xenon (150 W) or mercury (100 or 200 W) arc lamp, is passed through a BG 38 red suppression filter and through a Ploem illuminator cube system consisting of bandpass (a) and barrier filters (c) and a dichroic mirror (b). The bandpass filter transmits only the UV-blue exciting radiation. The dichroic mirror reflects the UV-blue exciting radiation and transmits the longer wavelength radiation emitted by the sample. The barrier filter is used to screen out the scattered excitation radiation while transmitting the longer emission wavelengths. The optical characteristics of the filters and dichroic mirrors in the cubes used in this work are summarized in table 1. The selected excitation radiation then passes through the microscope objective (25 and 50 magnification with numerical apertures of 0.50 and 0.80, respectively) and irradiates the glass sphere. The luminophor absorbs the exciting radiation and emits characteristic radiation at longer wavelengths (> 400 nm). The emitted radiation is collected by the same microscope objective, passes through the dichroic mirror, barrier filter, a measuring aperture, focusing optics, a scanning monochromator (0.1 m grating monochromator GM 100, Schoeffel Instruments, Westwood, NJ), and finally impinges on a photomultiplier tube (S-20 response, EMI 9659QB extended red, EMI Electronics, Middlesex, England). The signal is amplified and directed to an x-y recorder which plots a curve of intensity vs. emission wavelength. Alternatively, a voltage to frequency converter (V-F) and a multichannel analyzer (MCA) operated in a multiscaling mode can be used to record the emission spectrum. To increase signal reproducibility, the ratio of the luminescence intensity to the intensity of the excitation radiation can also be directed to the recorder or V-F converter - MCA combination. Note: Detailed operating instructions for this instrument are given in a subsequent section.

III. PREPARATION AND EMISSION CHARACTERISTICS OF VARIOUS LUMINOPHOR-DOPED GLASSES

A. Glass Preparation

The glasses and the glass spheres or beads used in this study were prepared by the Inorganic Glass Group at the NBS. The appropriate weights of the individual metal oxides were melted and stirred at 1000-1100°C until a homogeneous mixture was obtained. The melt was poured into a form and allowed to cool slowly to produce a block of glass of approximately 350 g. About 100 g of the block was crushed using a stainless steel mortar and pestle type of apparatus until jagged particles 200 μm and below were produced.

Two base glasses were used that have low intrinsic luminescence properties. Their compositions are in weight percent: Base 1 = SiO_2 - 68.17, Na_2O - 14.07, BaO - 11.50, and ZnO - 6.26; Base 2 = SiO_2 - 39.00, BaO - 44.00, and ZnO - 17.00. (Note: Base glass #1 was used previously [7]). Luminophors such as the lanthanides, uranium, copper, etc., which emit in the green to red spectral regions, were substituted in specific amounts for part of the BaO component.

B. Emission Characteristics

The emission spectra for several of the luminophor glasses are given in figures 4 and 5. The combinations shown as well as others could be used to provide hundreds of different, uniquely identifiable spheres by varying the luminophors and the ratio of the luminophor concentrations.
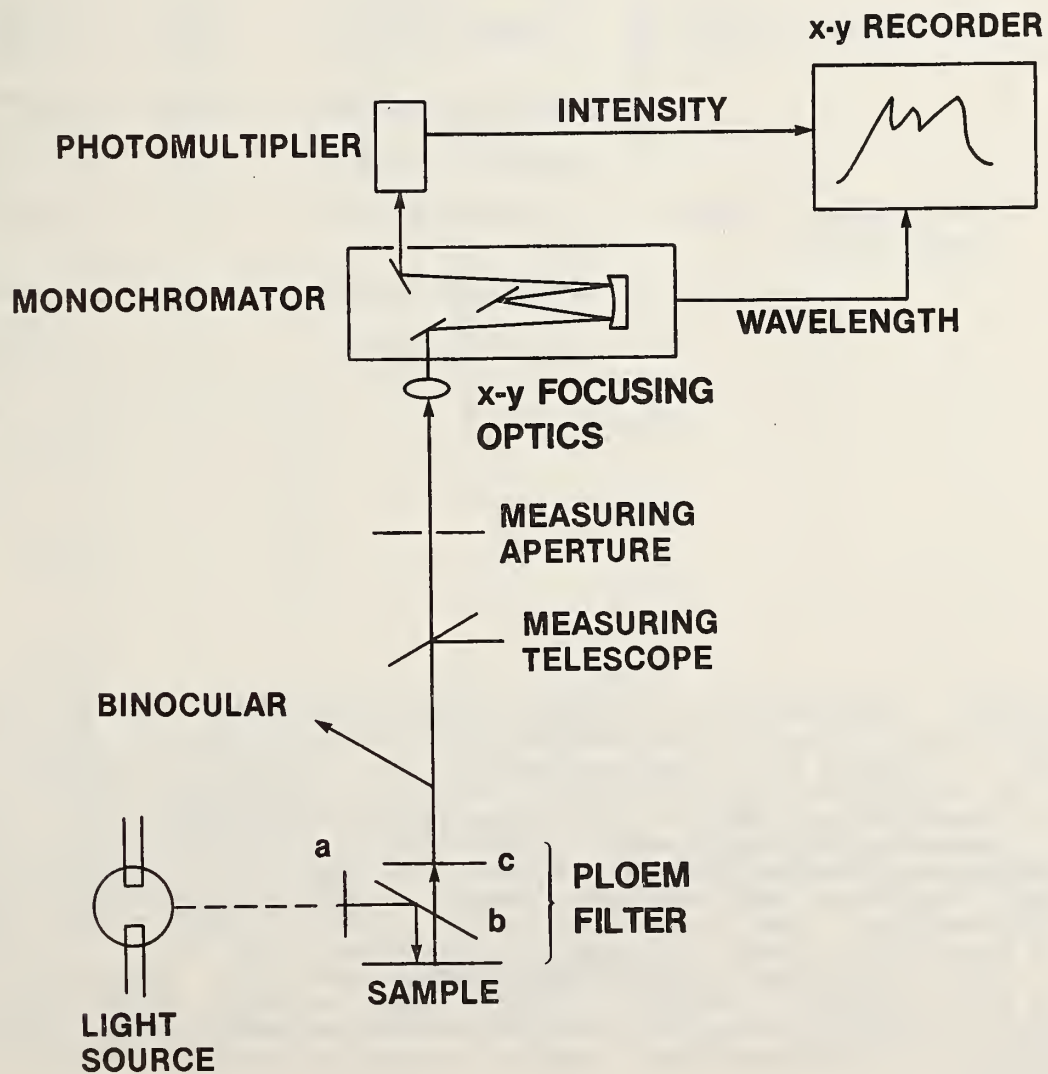
Figure 3. Diagram of microspectrofluorimeter used in this work.

Table 1. Optical characteristics of the Ploemopak filter cubes
used for the selection of excitation radiation

| Cube | Excitation range 50% transmittance | Component | Approximate wavelength in nm for designated transmission (%) | |
			2	50
A	UV 340-380 nm	Bandpass filter	330	340
			390	380
		Dichroic mirror	380	400
		Barrier filter	415	430
D	UV + violet 355-425 nm	Bandpass filter	340	355
			435	425
		Dichroic mirror	420	455
		Barrier filter	445	460
G	UV + violet + blue 350-460 nm	Bandpass filter	---	350
		Dichroic mirror	---	460
		Barrier filter	---	510
			---	515

Preliminary compositions of the glasses containing two luminophors are summarized in table 2, and the emission spectra from these specific melts are given in figures 6 through 18. From these spectra, it is obvious that melts K-1031, K-1032, K-1064, K-1124, K-1125, and K-1128 containing the Tb-Eu, Tb-Sm, and U-Eu luminophor combinations could be easily developed to produce uniquely identifiable glasses. Dysprosium containing melts K-1078, K-1087, and K-1126 may be suitable for use but further work has to be done. On the other hand, melts containing copper (K-1045, K-1079) would need additional development to produce a glass with discernible copper luminescence. The major problem is that luminescence from copper-doped glasses is produced by copper in the +1 oxidation state [8]. Procedures for producing and stabilizing Cu^{+1} glasses would have to be developed. The melts containing Eu^{+3} and Sm^{+3} (K-1077, K-1079) have emission peaks which overlap extensively and although these two luminophors could be used together, sophisticated instrumentation with extremely high spectral resolution would be needed to obtain usable spectra.

C. Testing of Final Glass Composition

Based on the above data and other considerations such as ease of material handling and glass preparation, the glass containing a combination of Tb^{3+} and Eu^{3+} (melt K-1125) was chosen for extensive testing. A series of glasses with varying Tb^{3+} and Eu^{3+} concentrations was prepared and their compositions are summarized in table 3.
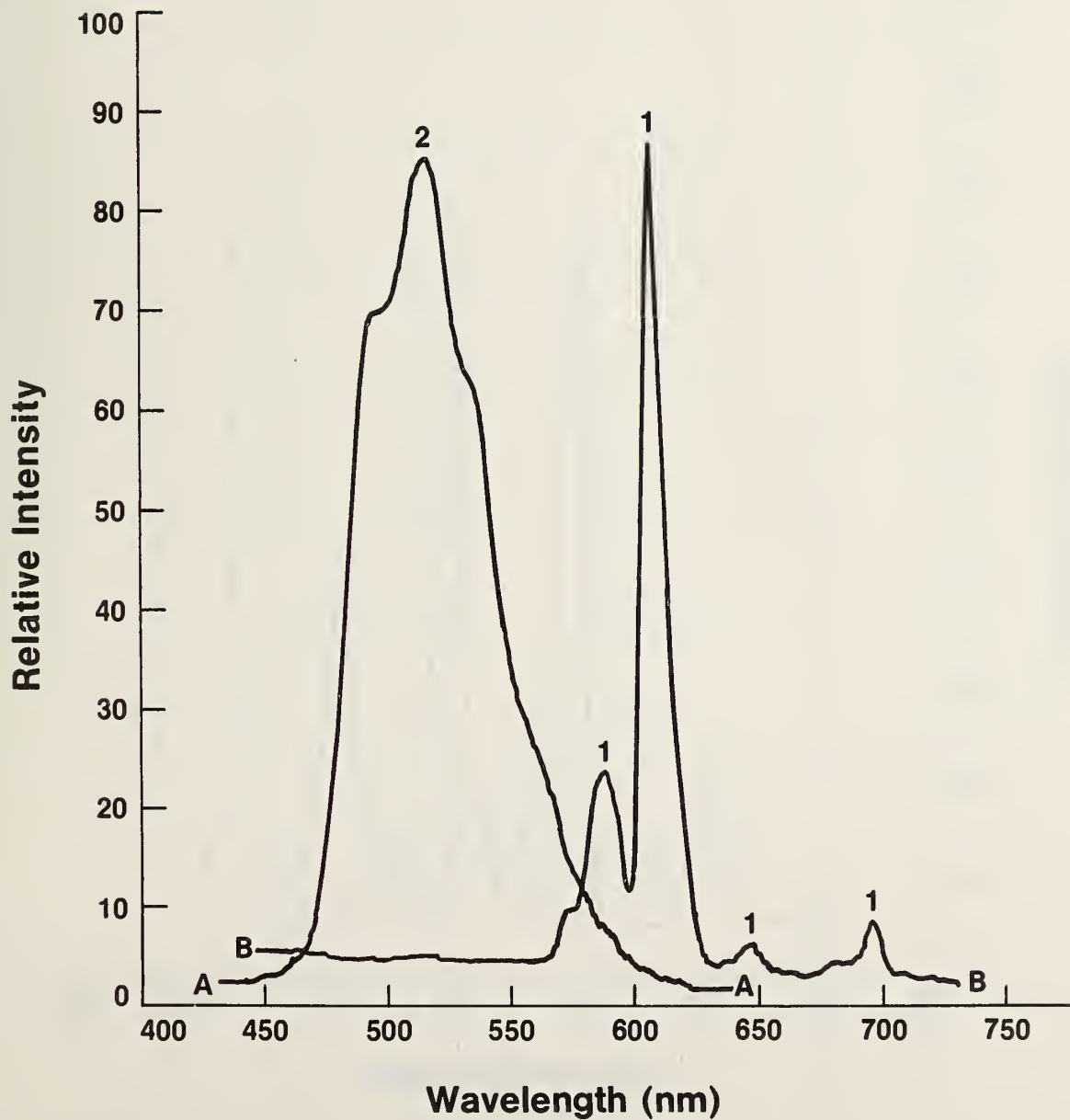
Figure 4. Luminescence spectra of glasses containing U_3O_8 (curve A) and Eu_2O_3 (curve B); (2.5 mole %); cube A; photomultiplier voltage; curve A = 900 V, curve B = 890 V.

9
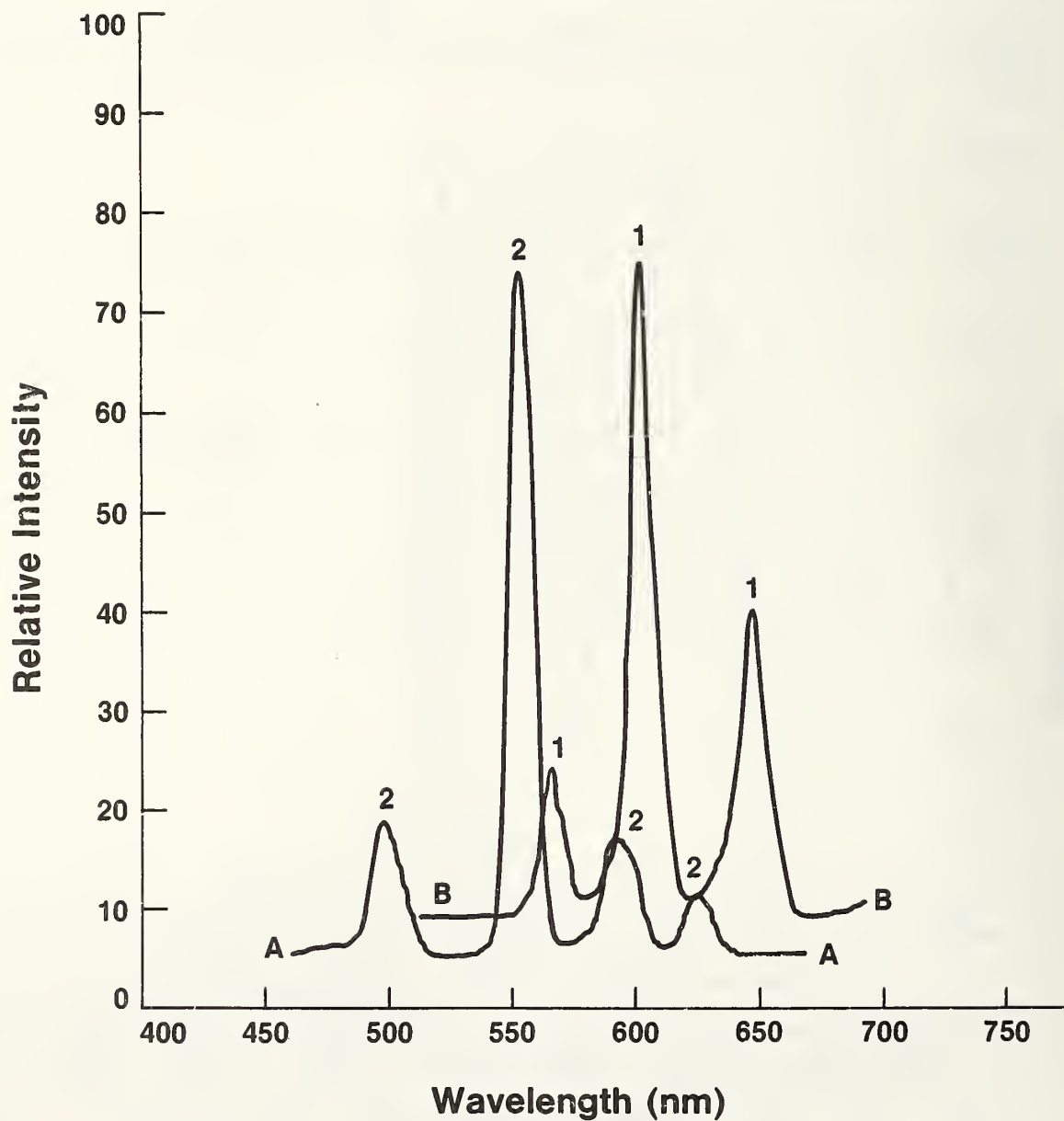
Figure 5. Luminescence spectra of glasses containing Tb_2O_3 (curve A) and Sm_2O_3 (curve B) at 4.0 and 1.1 mole percent, respectively; cube A; photo-multiplier voltage; curve A = 800 V, curve B = 930 V.

Table 2. Compositions of preliminary glass melts

Component	Melt number, composition, weight percent												
	K-1031	K-1032	K-1045	K-1064	K-1077	K-1078	K-1079	K-1087	K-1088	K-1124	K-1125	K-1126	K-1128
SiO_2	34.96	35.92	36.37	36.15	35.60	34.70	36.00	35.07	36.47	65.44	64.76	65.78	65.72
BaO	42.23	42.56	43.76	43.33	41.36	38.74	42.49	39.96	43.88	11.14	11.02	11.19	11.18
ZnO	13.53	13.90	14.07	13.99	13.77	13.43	13.93	13.56	14.11	5.91	5.85	5.95	5.94
Na_2O	--	--	--	--	--	--	--	--	--	13.51	13.37	13.58	13.56
Tb_2O_3	3.80	3.91	--	--	--	--	--	--	--	2.00	2.00	--	--
Eu_2O_3	5.49	--	5.71	5.67	5.58	5.44	3.77	--	--	--	3.00	1.50	3.00
Sm_2O_3	--	3.72	--	--	3.69	--	3.73	3.64	3.78	2.00	--	--	--
Dy_2O_3	--	--	--	--	--	7.69	--	7.77	--	--	--	2.00	--
U_3O_8	--	--	--	0.87	--	--	--	--	0.60	--	--	--	0.60
CuO	--	--	0.09	--	--	--	0.09	--	--	--	--	--	--
Figure (Emission spectrum)	6	7	8	9	10	11	12	13	14	15	16	17	18

11
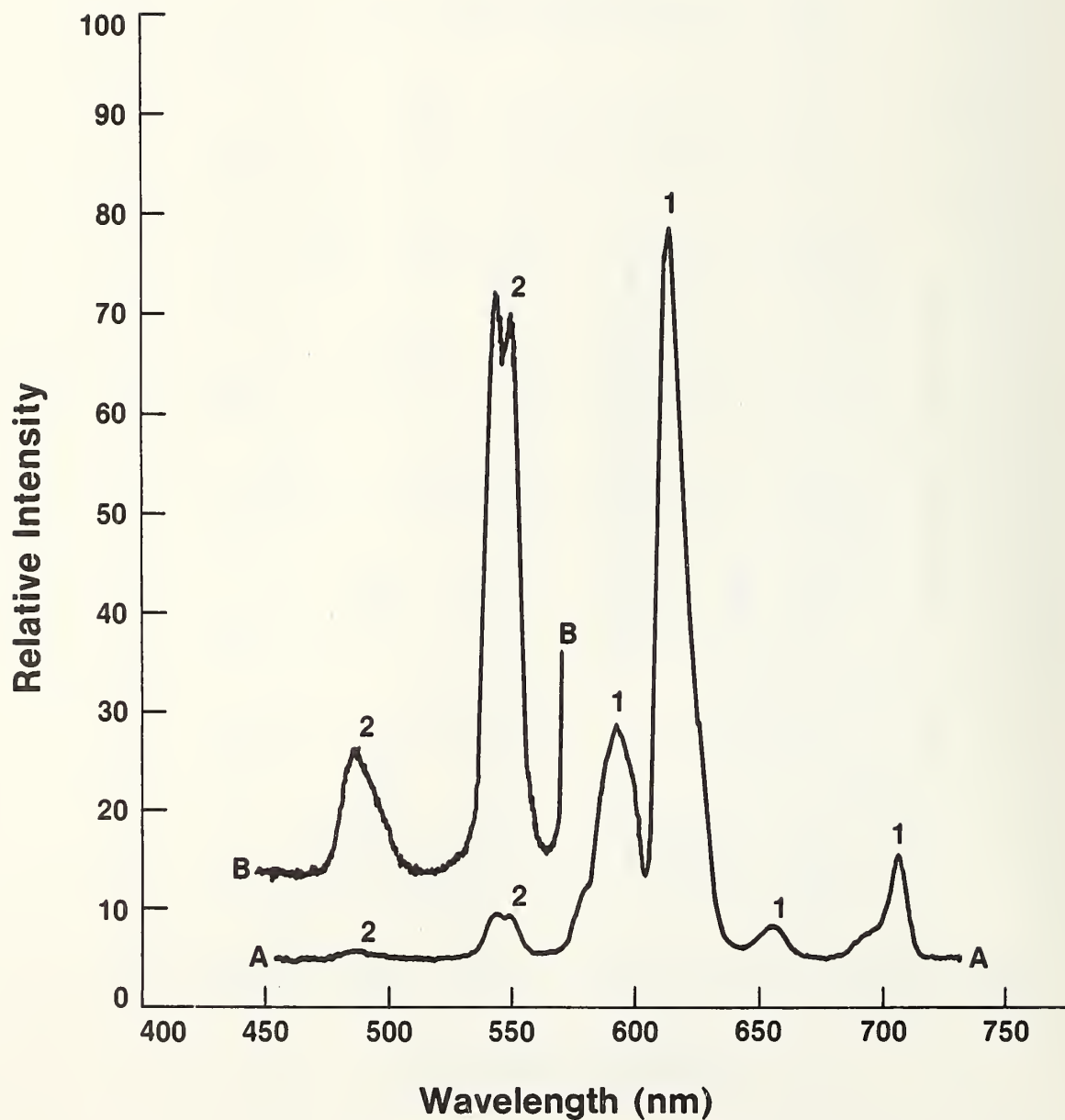
Figure 6. Luminescence spectrum of glass, melt K-1031 containing Eu_2O_3, peaks labeled 1 and Tb_2O_3, peaks labeled 2; 1.5 and 1.0 mole percent, respectively; cube A; photomultiplier voltage; curve A = 970 V, curve B = 1300 V; monochromator slits = 0.5, 0.5 mm.
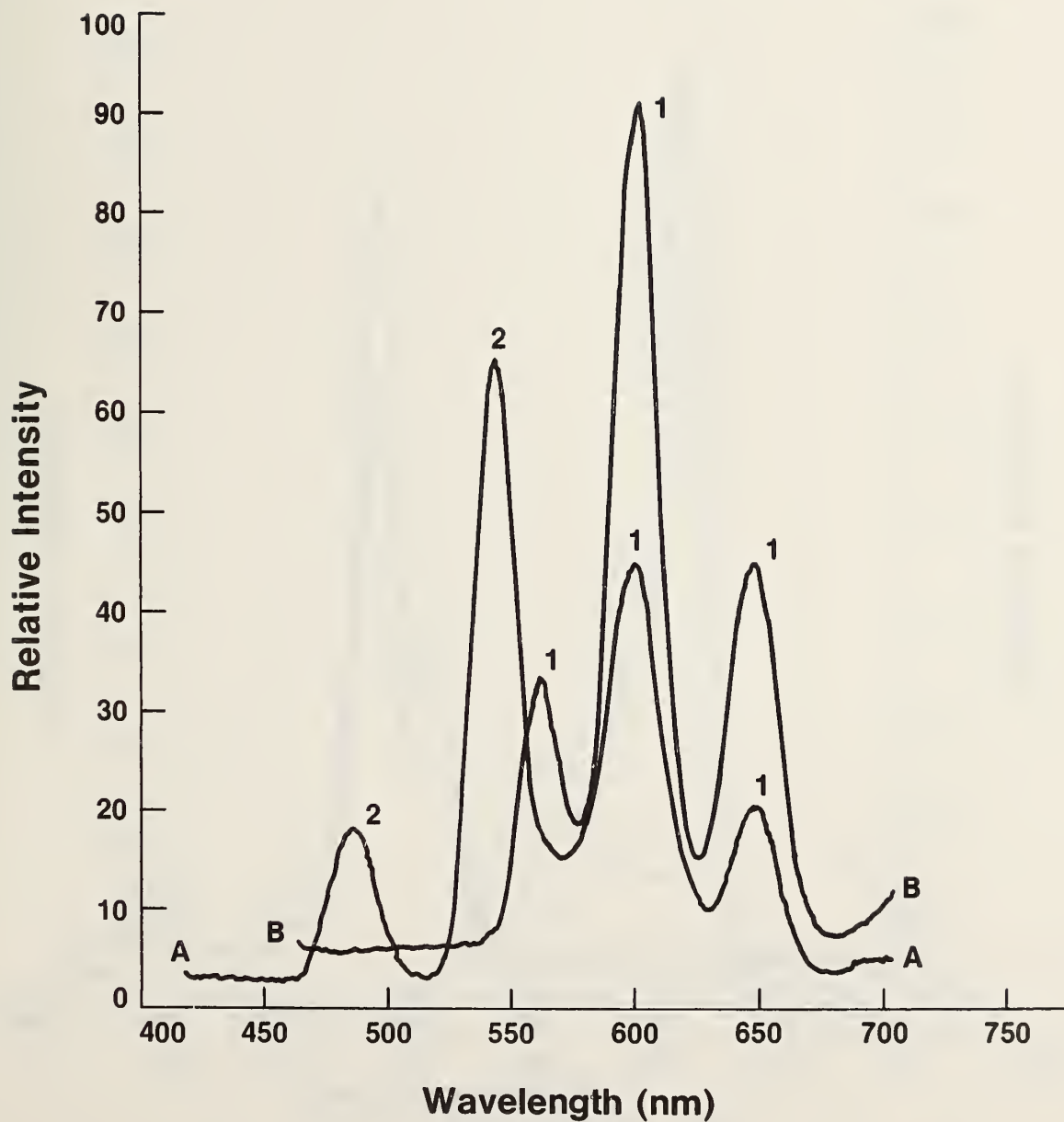
Figure 7. Luminescence spectra of glass, melt K-1032, containing Sm_2O_3, peaks labeled 1 and Tb_2O_3, peaks labeled 2; 1.0 mole percent each; photomultiplier voltage and cube used; curve A = 1020 V, cube A; curve B = 960 V, cube D; monochromator slits = 2,2 mm.
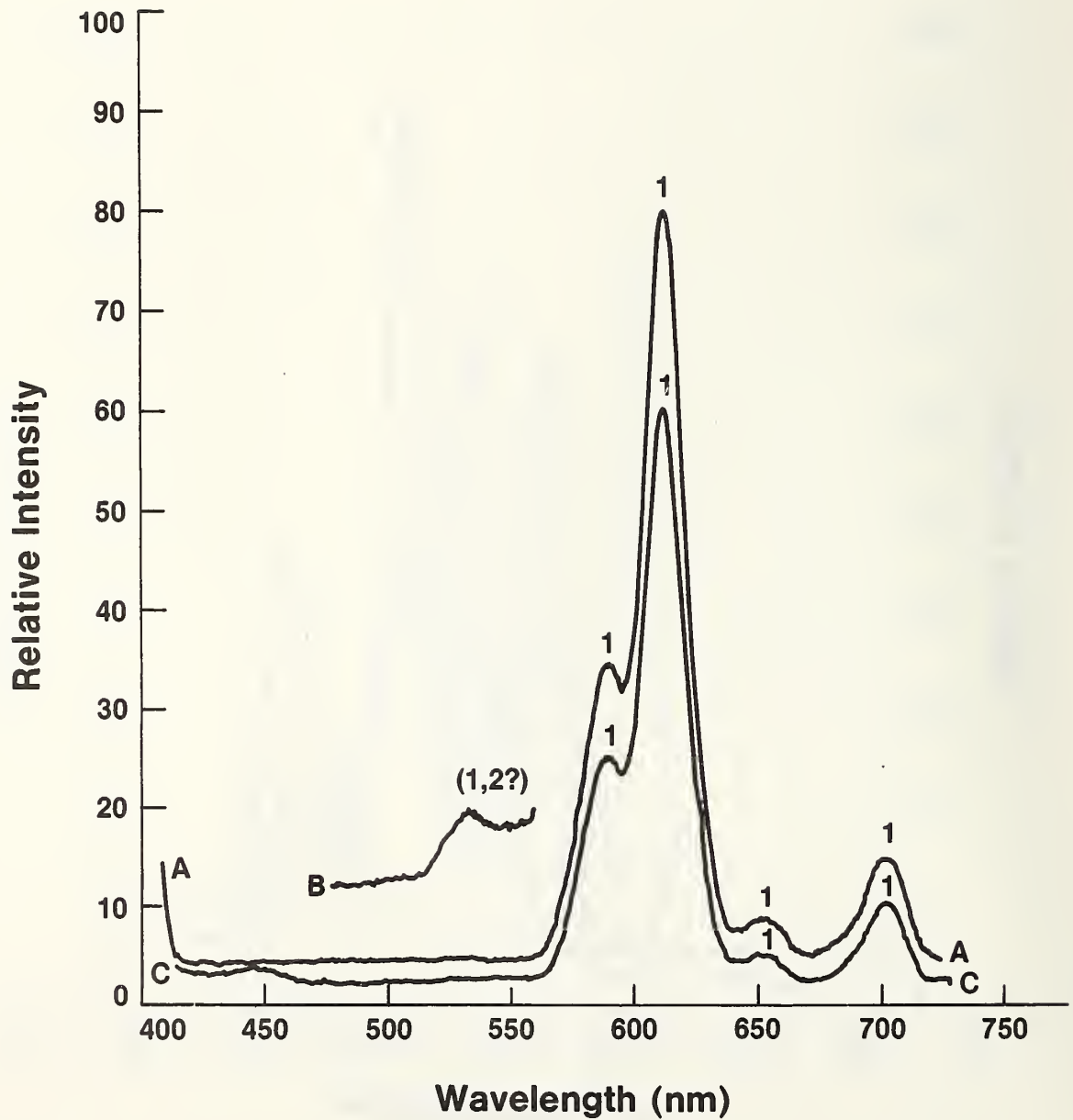
Figure 8.   Luminescence spectra of glass, melt K-1045, containing Eu_2O_3, peaks labeled 1 and CuO; 1.5 and 0.1 mole percent, respectively; photomultiplier voltage and cube used; curve A = 840 V, cube A; curve B = 1200 V, cube A; curve C = 830 V, cube D; monochromator slit widths = 2,2 mm
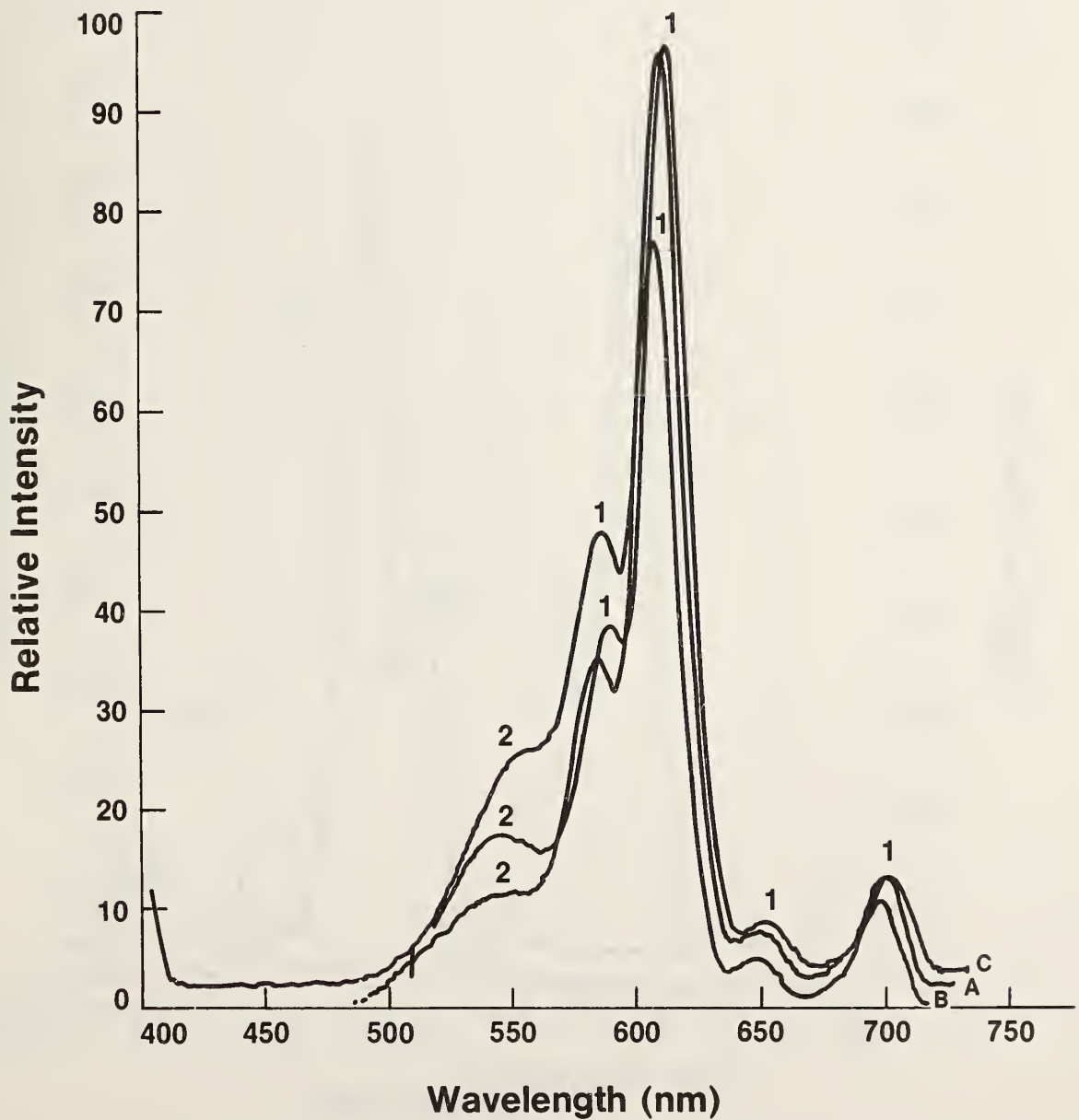
Figure 9. Luminescence spectra of glass, melt K-1064, containing Eu_2O_3 peaks labeled 1 and U_3O_8 peaks labeled 2; 1.5 and 0.3 mole percent, respectively; photomultiplier voltage and cube used; curve A = 780 V, cube A; curve B = 730 V, cube D; curve C = 607 V, cube G; monochromator slit widths = 2,2 mm.
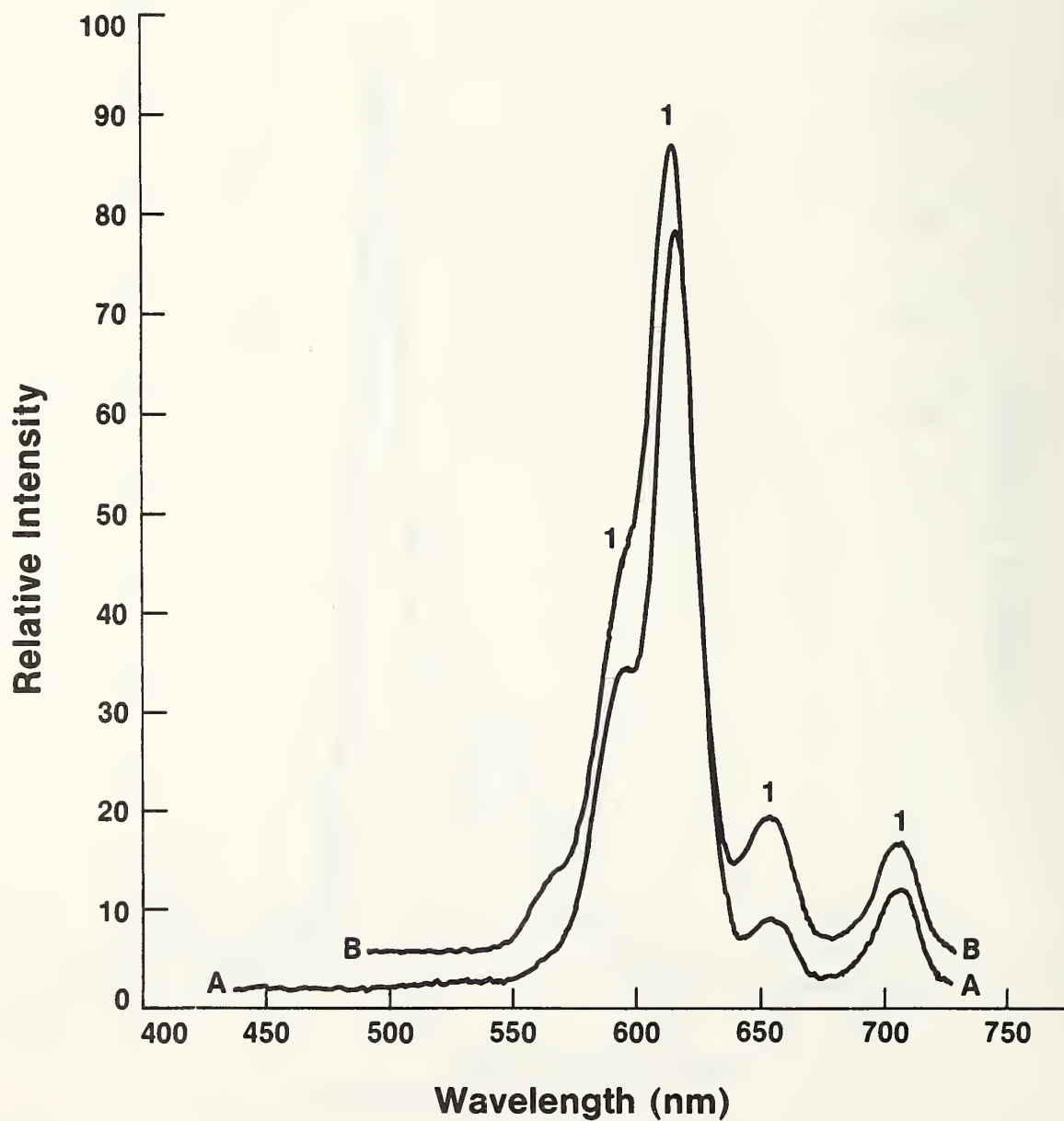
Figure 10. Luminescence spectra of glass, melt K-1077, containing Eu_2O_3, peaks labeled 1, and Sm_2O_3; 1.5 and 1.0 mole percent, respectively; photomultiplier voltage; curve A = 767 V, monochromator slit widths = 2,2 mm.
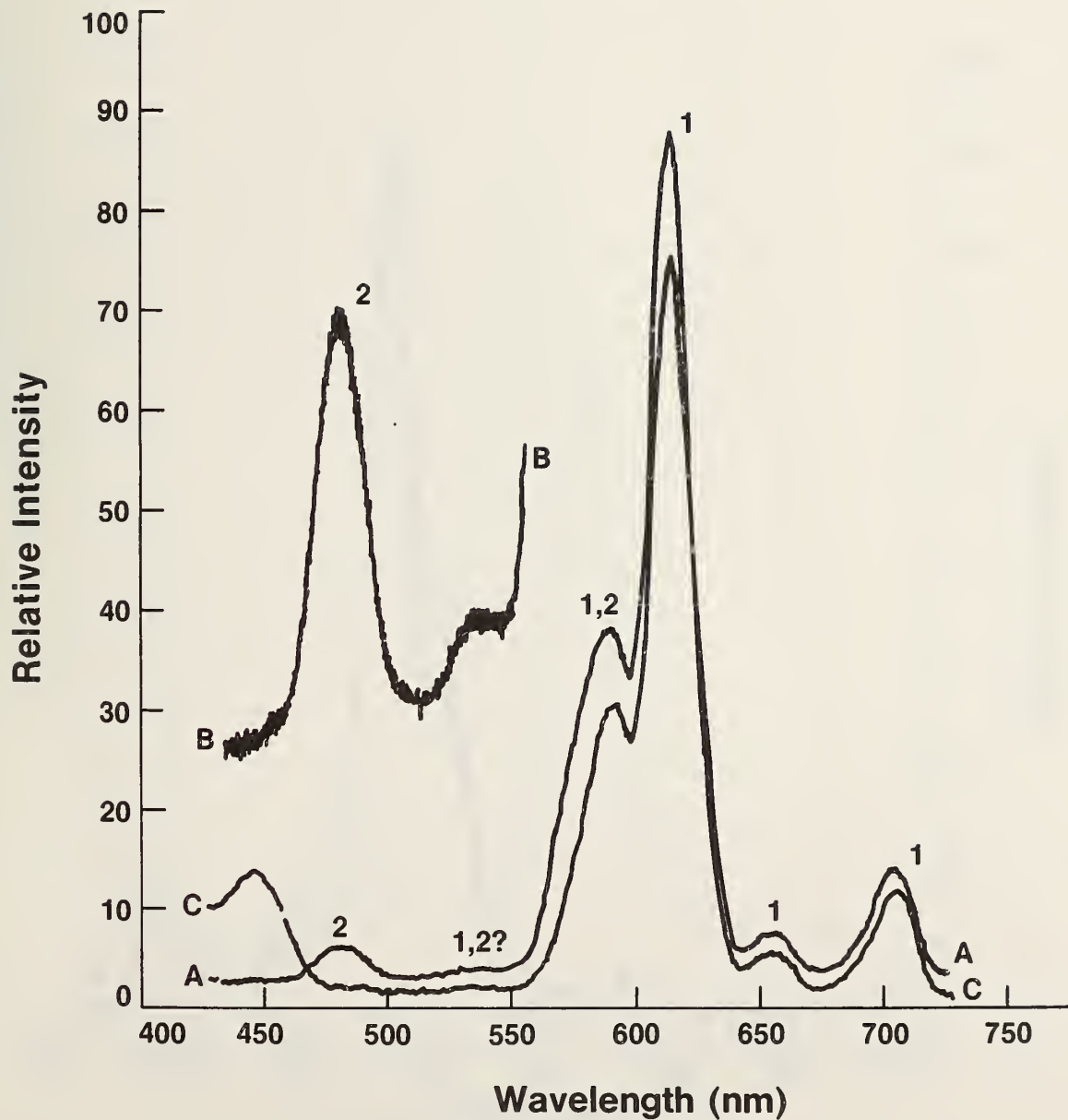
Figure 11. Luminescence spectra of glass, melt K-1078, containing Eu_2O_3, peaks labeled 1 and Dy_2O_3 peaks labeled 2; 1.5 and 2.0 mole percent, respectively; photomultiplier voltage and cube used; curve A = 1100 V, cube A; curve B = 1500 V, cube A scale expanded X10; curve C = 1130 V, cube D; monochromator slit widths = 2,2 mm.

17
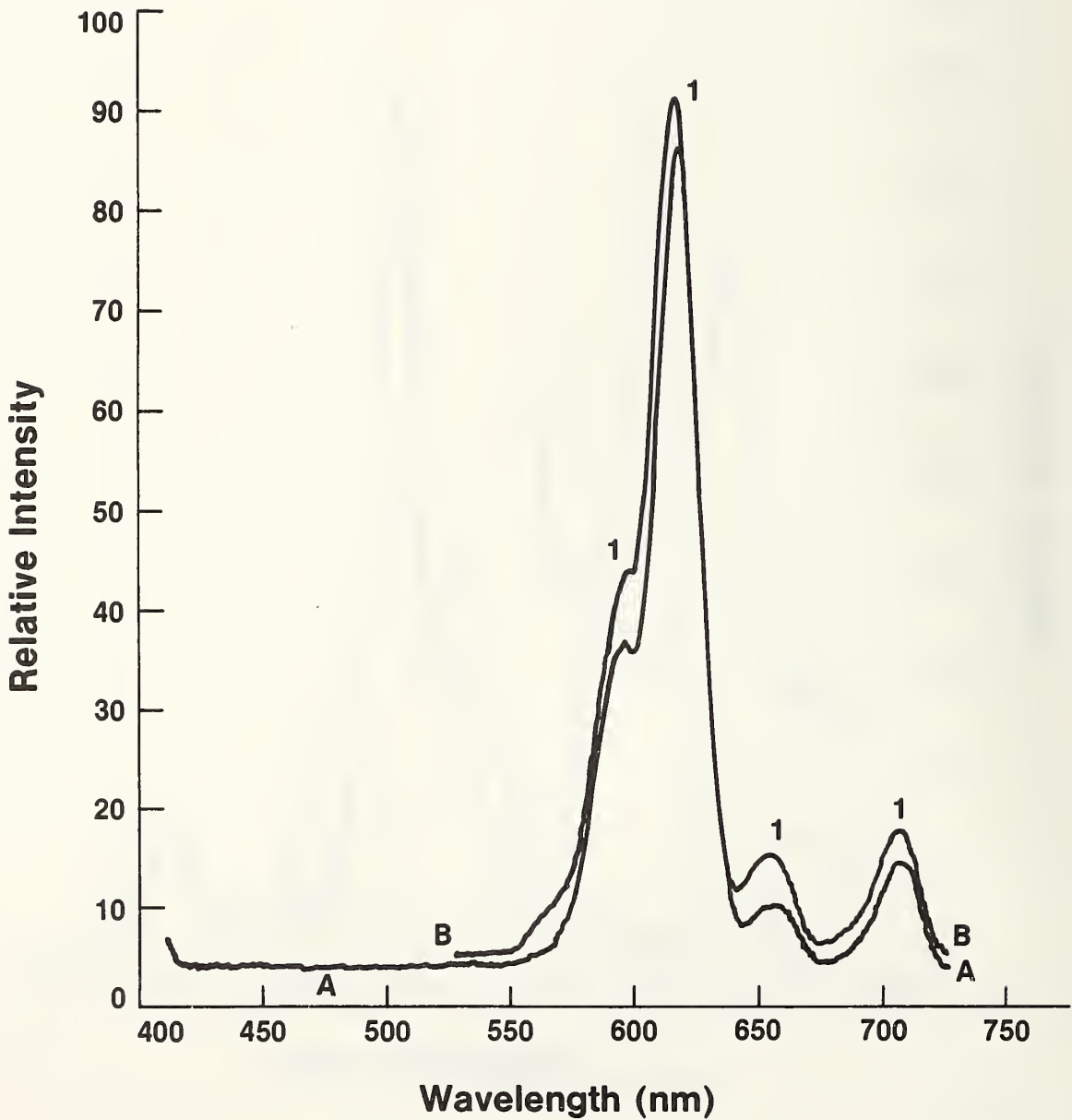
Figure 12. Luminescence spectra of glass, melt K-1079, containing Eu_2O_3, peaks labeled 1; Sm_2O_3, and CuO; 1.0, 1.0, and 0.1 mole percent, respectively; photomultiplier voltage and cube used; curve A = 890 V, cube A; curve B = 890 V, cube D; monochromator slit widths = 2,2 mm.
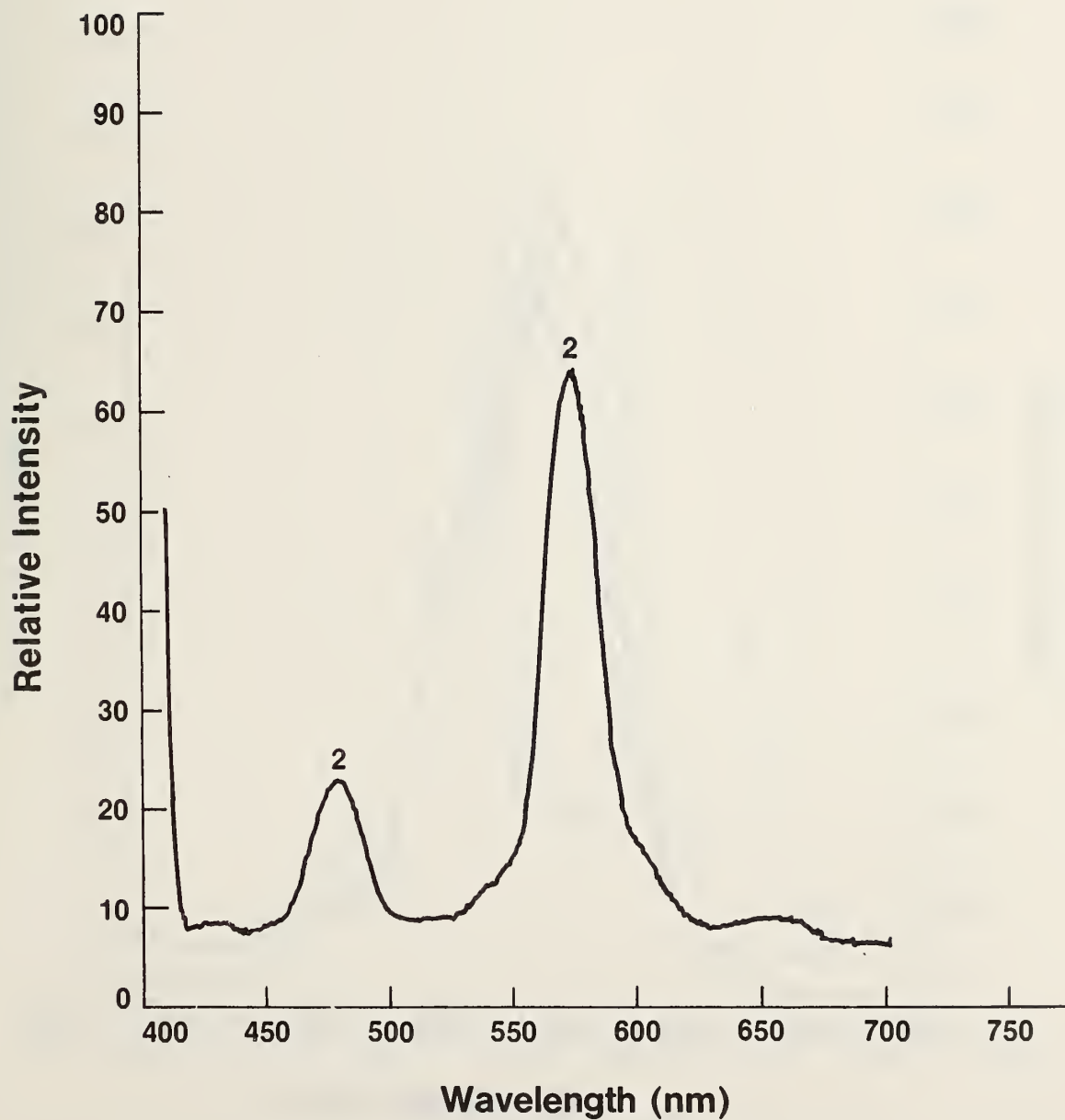
Figure 13. Luminescence spectrum of glass, melt K-1087, containing Sm_2O_3, and Dy_2O_3, peaks labeled 2; 1.0 and 2.0 mole percent, respectively; photomultiplier voltage = 1460 V; monochromator slit widths = 2,2 mm.

Figure 14. Luminescence spectra of glass, melt K-1088, containing U_3O_8, peaks labeled 2 and Sm_2O_3, peaks labeled 1; 0.6 and 1.0 mole percent, respectively; photomultiplier voltage and monochromator slit widths; curve A = 1300 V, 2,2 mm; curve B = 1700 V, 0.5,0.5 mm.
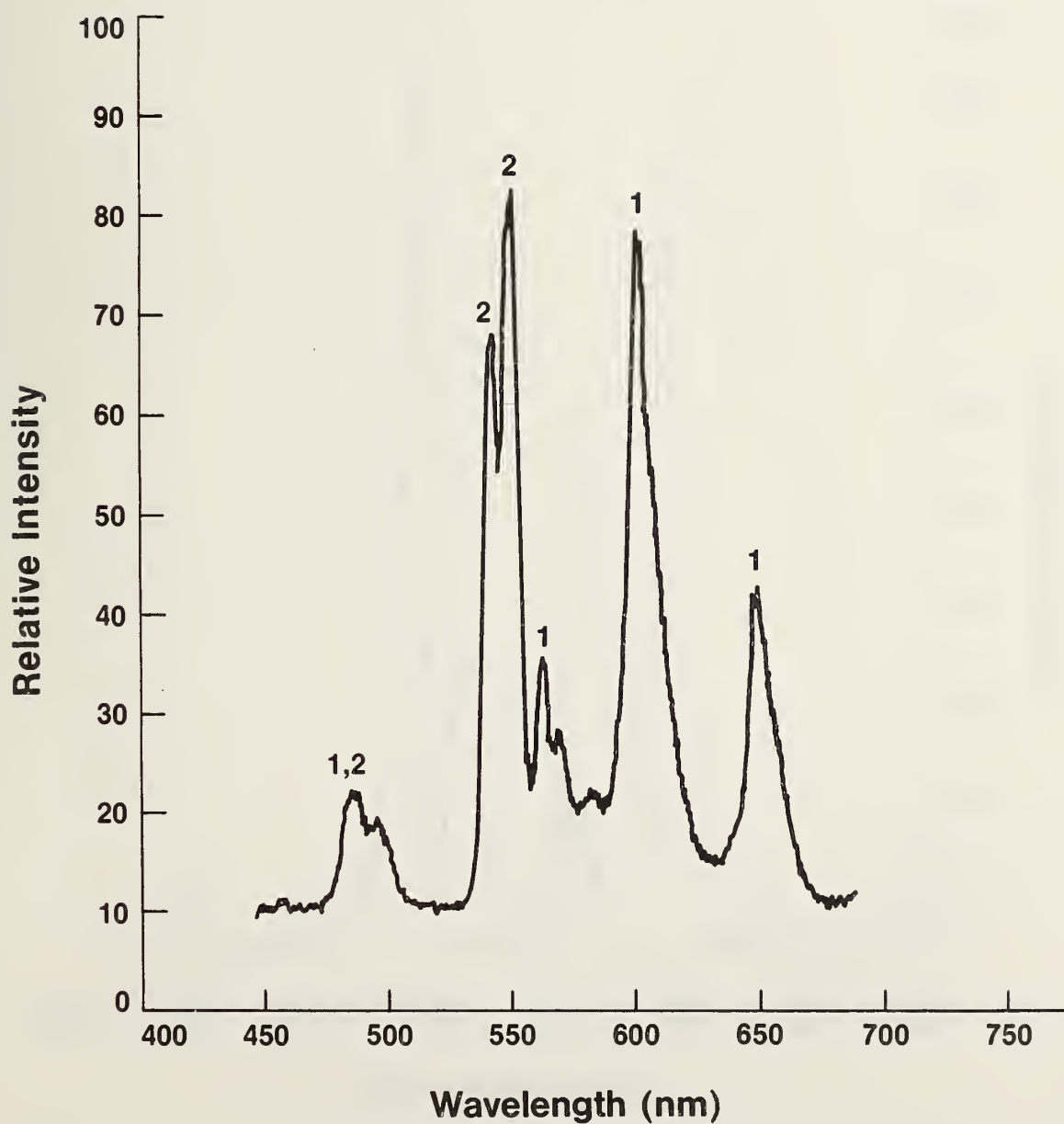
Figure 15. Luminescence spectrum of glass, melt K-1124, containing Tb_2O_3, peaks labeled 2 and Sm_2O_3 peaks labeled 1; 2.0 weight percent; photomultiplier voltage = 1350 V; monochromator slit widths = 0.5,0.5 mm.
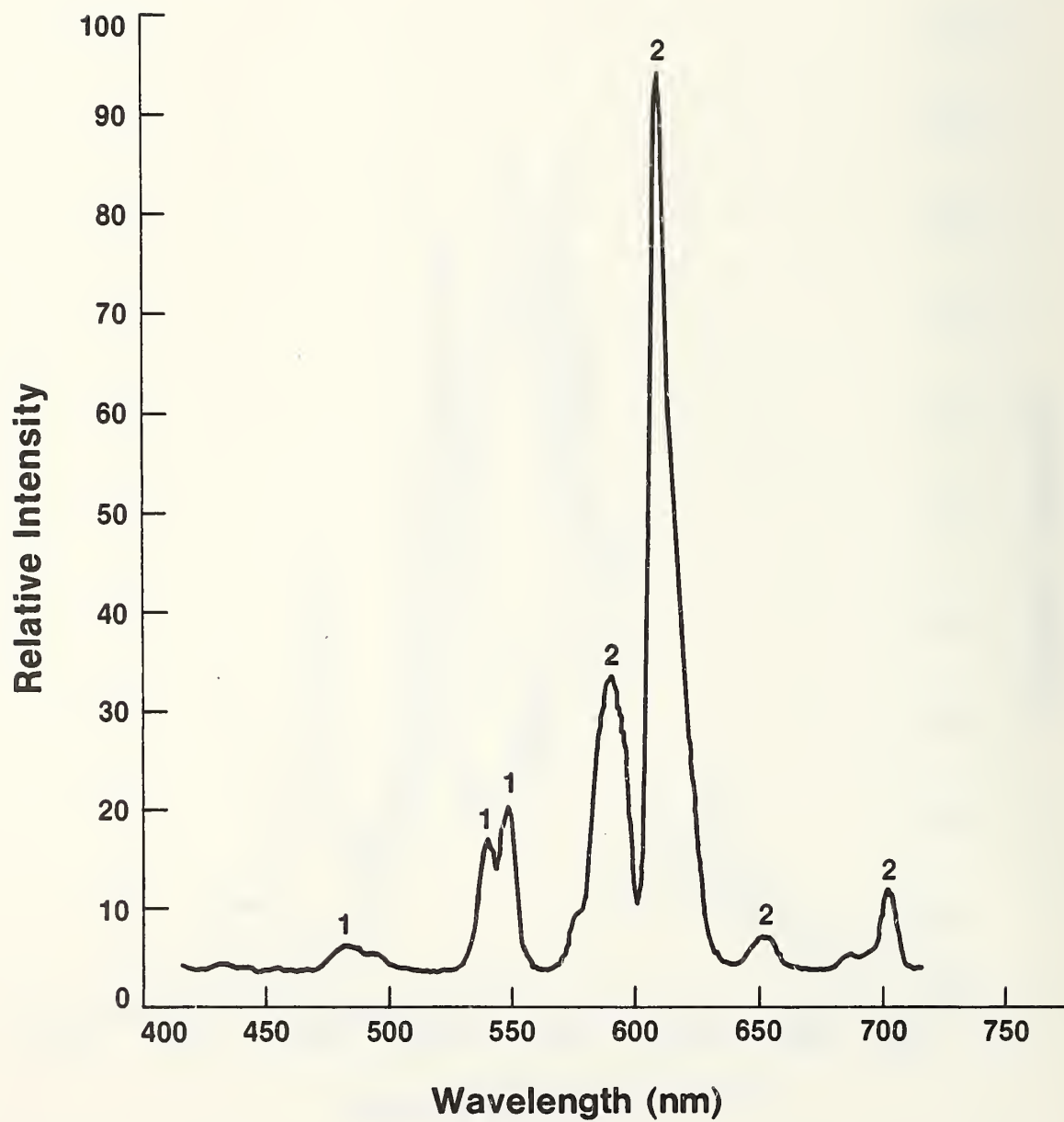
Figure 16. Luminescence spectrum of glass, melt K-1125, containing Tb_2O_3, peaks labeled 1, and Eu_2O_3 peaks labeled 2; 2.0 and 3.0 weight percent, respectively; photomultiplier voltage = 1250 V; monochromator slit widths = 0.5,0.5 mm.
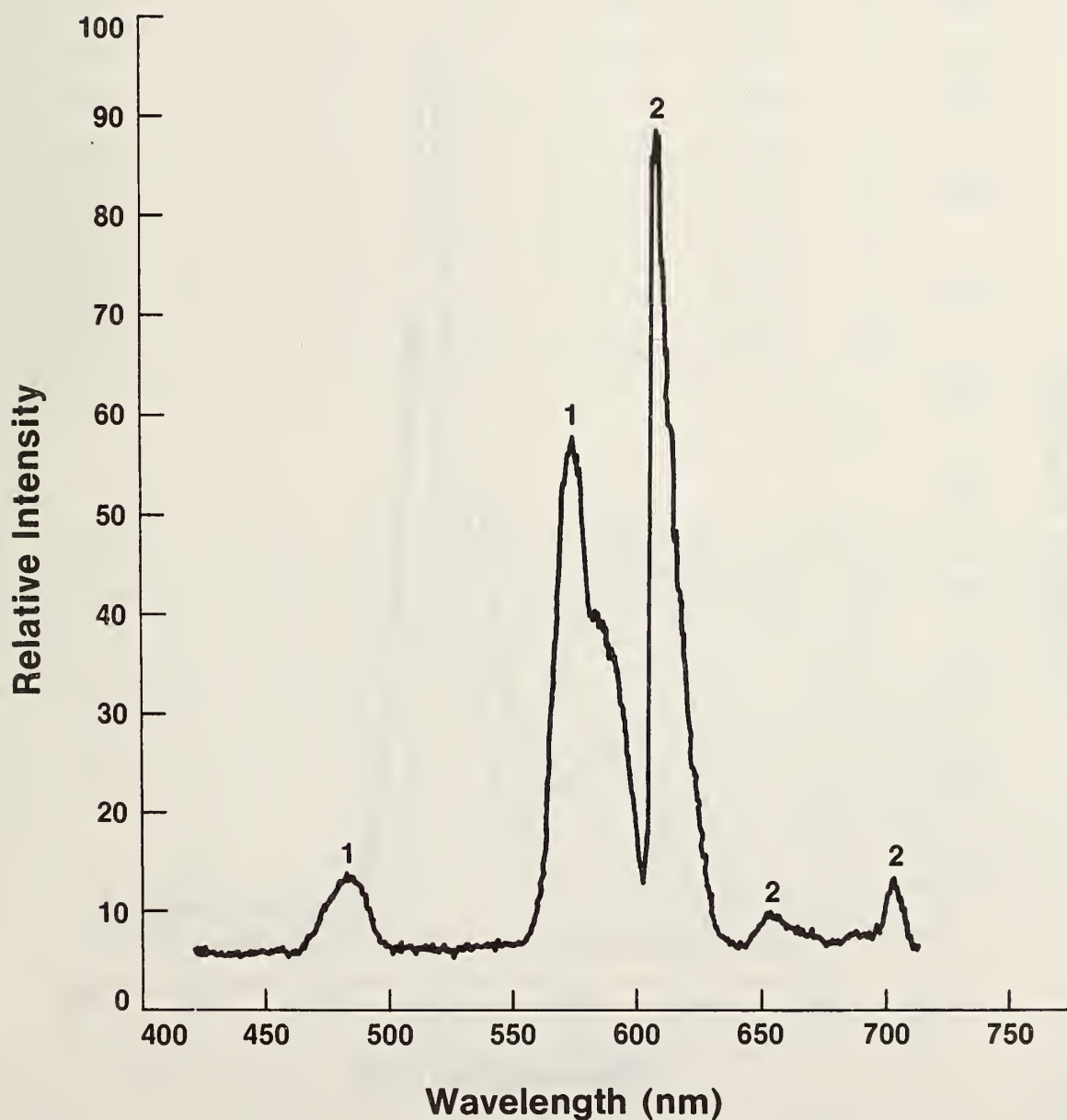
Figure 17. Luminescence spectrum of glass, melt K-1126, containing Dy_2O_3, peaks labeled 1, and Eu_2O_3, peaks labeled 2; 2.0 and 1.5 weight percent, respectively; photomultiplier voltage = 1490 V; monochromator slit widths = 0.5,0.5 mm.
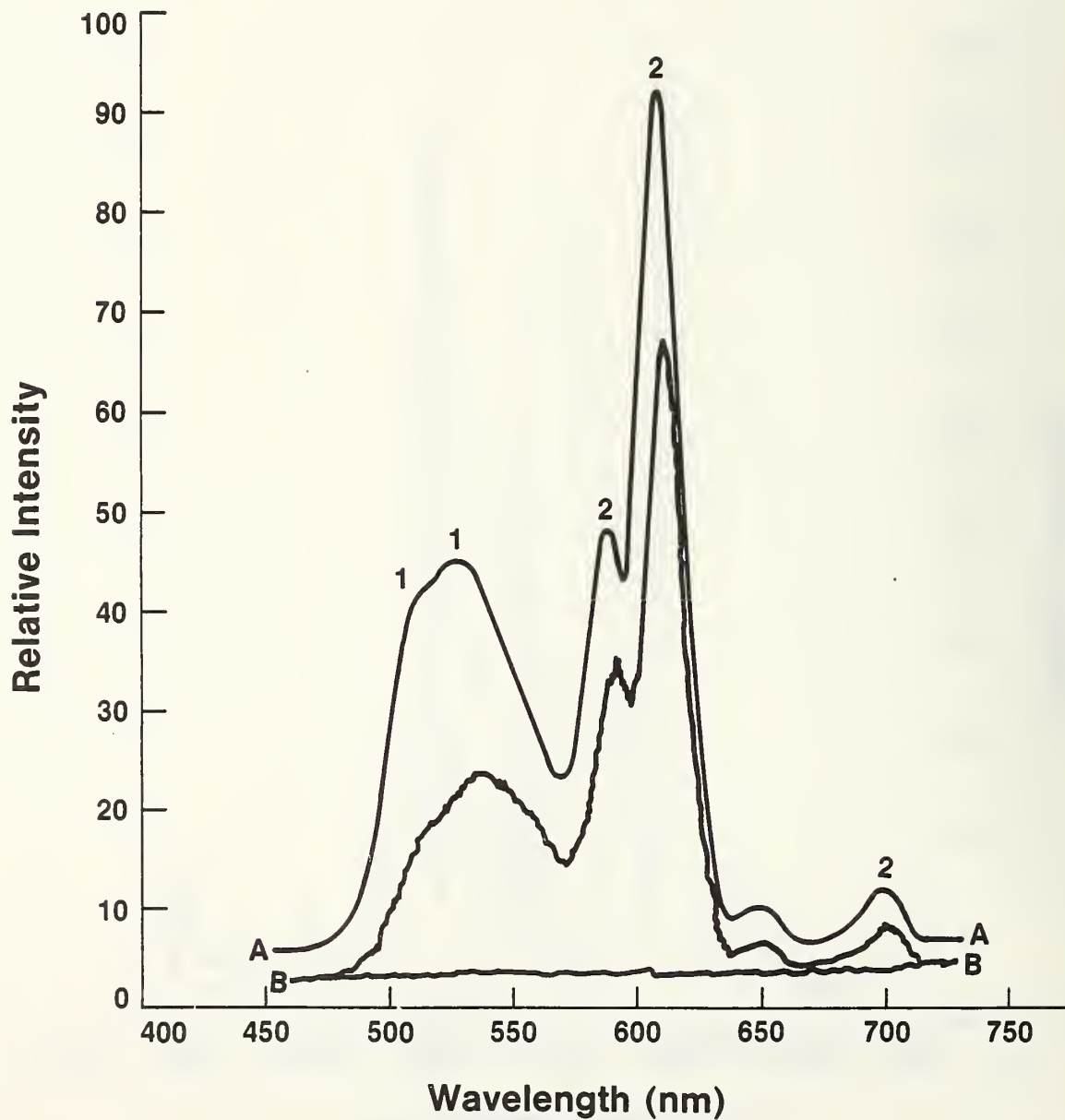
Figure 18. Luminescence spectra of glass, melt K-1128, containing U_3O_8, peaks labeled 1, and Eu_2O_3, peaks labeled 2; 0.6 and 3.0 weight percent, respectively; photomultiplier voltage and monochromator slits; curve A = 1000 V, 2,2 mm; curve B = 1380 V, 2,2 mm.

Table 3. Composition of Tb_2O_3-Eu_2O_3 doped glasses

Melt	Tb_2O_3	Eu_2O_3	SiO_2	Na_2O	BaO	ZnO	Tb/Eu
			Composition, weight percent				
K-1192	3.00	--	66.13	13.65	11.25	5.97	--
K-1198	5.00	0.50	64.43	13.29	10.96	5.82	10.0
K-1200	5.00	1.00	64.09	13.22	10.90	5.79	5.0
K-1202	4.00	1.00	64.76	13.37	11.02	5.85	4.0
K-1186	3.00	1.00	65.44	13.51	11.14	5.91	3.0
K-1201	3.00	2.00	64.76	13.37	11.02	5.85	1.5
K-1125	2.00	3.00	64.76	13.37	11.02	5.85	0.67
K-1194	--	2.00	66.81	13.79	11.37	6.03	--

The emission spectra for melts with Tb^{3+} (K-1192) or Eu^{3+} (K-1194) are given in figure 19. The assigned electronic transitions and approximate maxima for the peaks are summarized in figure 20 [9]. The major transitions that are immediately identifiable to Tb^{3+} are $^5D_4 \rightarrow ^7F_{1,2,3,4,5,}$ and 6 and to Eu^{3+} are $^5D_0 \rightarrow ^7F_{1,2,3,4,5,}$ and 6. Additional transitions for each luminophor have been seen , (e.g., for Eu^{3+} $^5D_0 \rightarrow$ $^7F_{5,6}$, $^5D_1 \rightarrow ^7F_{0,1,2}$ and for Tb^{3+}, $^5D_4 \rightarrow ^7F_0$, $^5D_3 \rightarrow ^7F_{2,3,4,5,6}$); however, under present instrument operating conditions, these are not visible. The transitions shown in figure 20 indicate that several less intense peaks in the Tb^{3+} spectrum overlap intense peaks in the Eu^{3+} spectrum and, as expected, cannot be identified in a melt containing both luminophors. The major peaks are immediately discernable in figure 21 at 542 nm (Tb^{3+}) and 610 nm (Eu^{3+}). These two peaks are those on which the ratio measurements will be made. Emission spectra for the eight melts listed in table 3 are given in figure 22 to show the relative peak maxima; although some contributions to the 610 nm Eu^{3+} peak intensity are made by the Tb^{3+} peaks at ~589 and ~623 nm, no corrections for these contributions will be made since a) the ratio is a relative measurement, and most importantly, b) the peak ratios are dependent on instrumental conditions and must be made relative to the ratio for known standards.

D. Instrumental Factors Affecting Peak Ratios

1. Excitation Bands. Typical excitation spectra for Eu^{3+} and Tb^{3+} in glasses are given in figure 23. The excitation bands selected by Cubes A and D also are superimposed as rectangular areas on the two spectra at the approximate wavelengths (also see table 1). As can be seen, if Cube A is used to select exciting radiation, very little or no radiation is passed to excite Eu^{3+} through the major absorbance peak at 394 nm. Use of Cube D, on the other hand, allows radiation of this wavelength to impinge on the sample. The use of Cube D would be expected to yield a larger Eu/Tb peak ratio measurement than the ratio obtained by use of Cube A. This is verified by the spectra given in figure 24. Thus, use of different cubes to select exciting radiation has significant impact on the measured peak ratios. In addition, if monochromatic radiation at 394 nm rather than a broad band of exciting radiation were used to excite a glass containing both Eu^{3+} and Tb^{3+} ions, only a Eu^{3+} emission spectrum would be observed since Tb^{3+} has very little if any absorbance at this wavelength. To show the relative effects of using Cubes A and D, the spectra for all melts using Cube A are illustrated in figure 25, while those obtained using Cube D are given in figure 22.

25
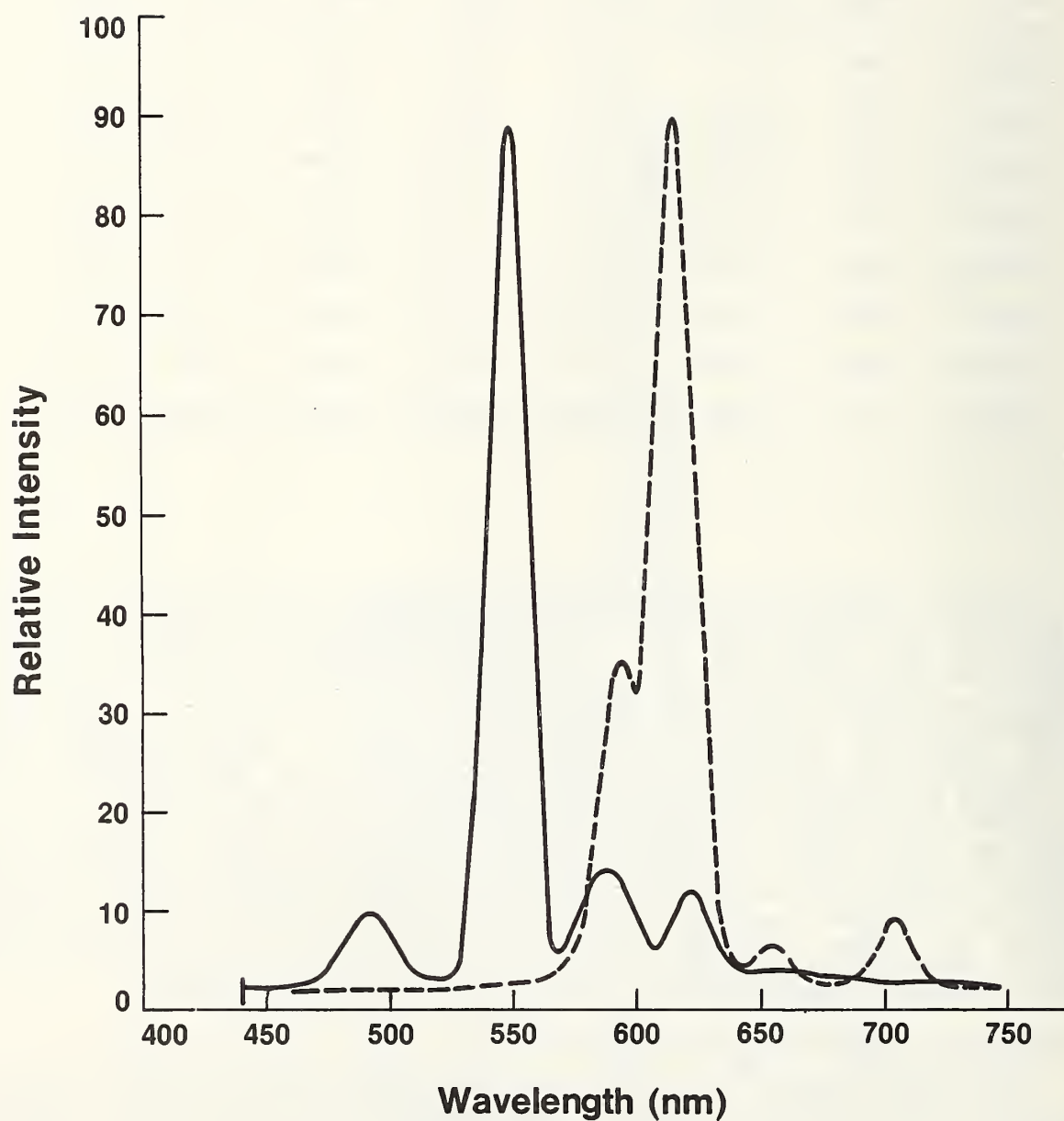
Figure 19. Luminescence spectra of glasses containing Tb^{3+} solid line, Eu^{3+} dashed line, cube D; monochromator slit widths = 2,2 mm.
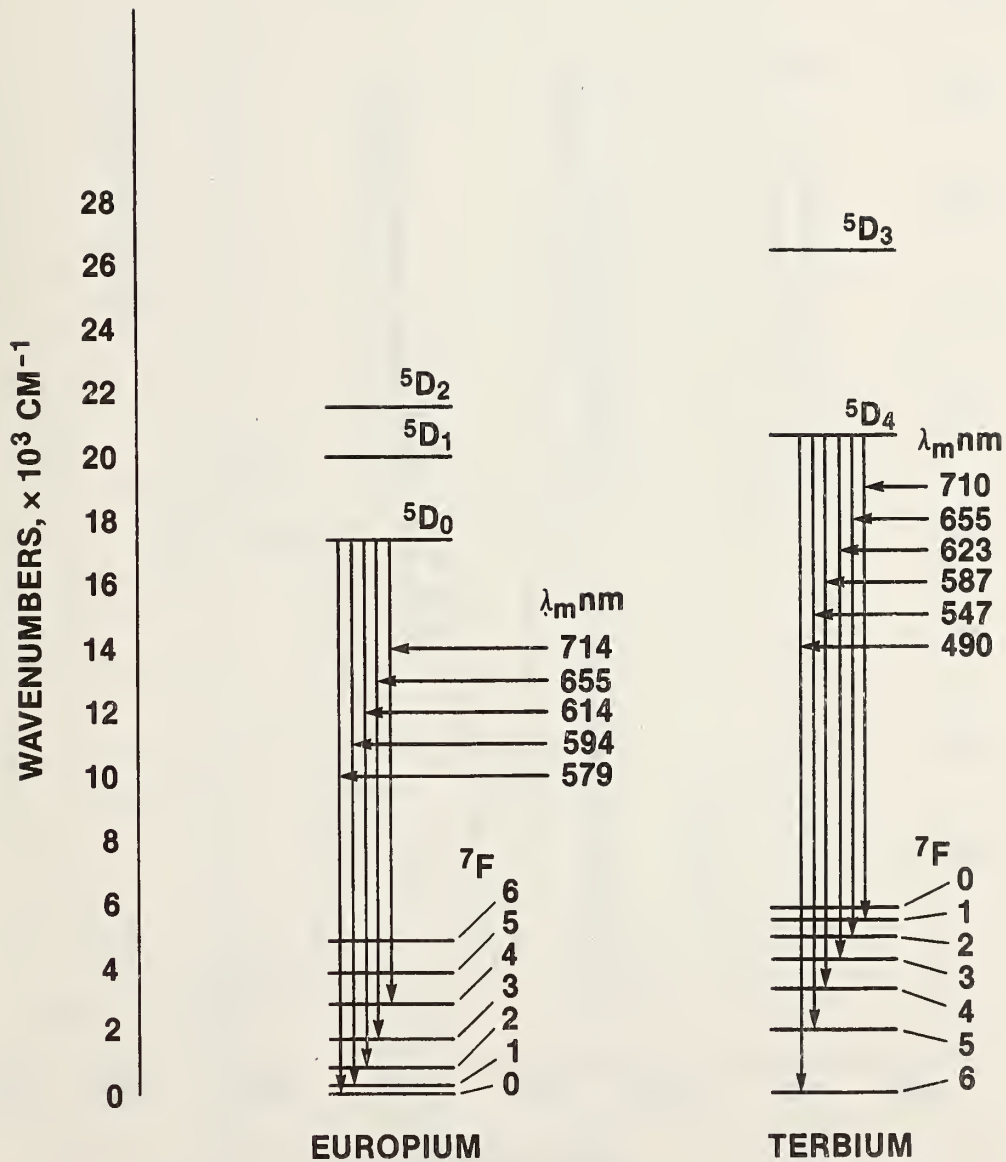
Figure 20. Partial Jablonski energy level diagram of europium and terbium showing the transitions observed in the luminescence spectra of figure 19.
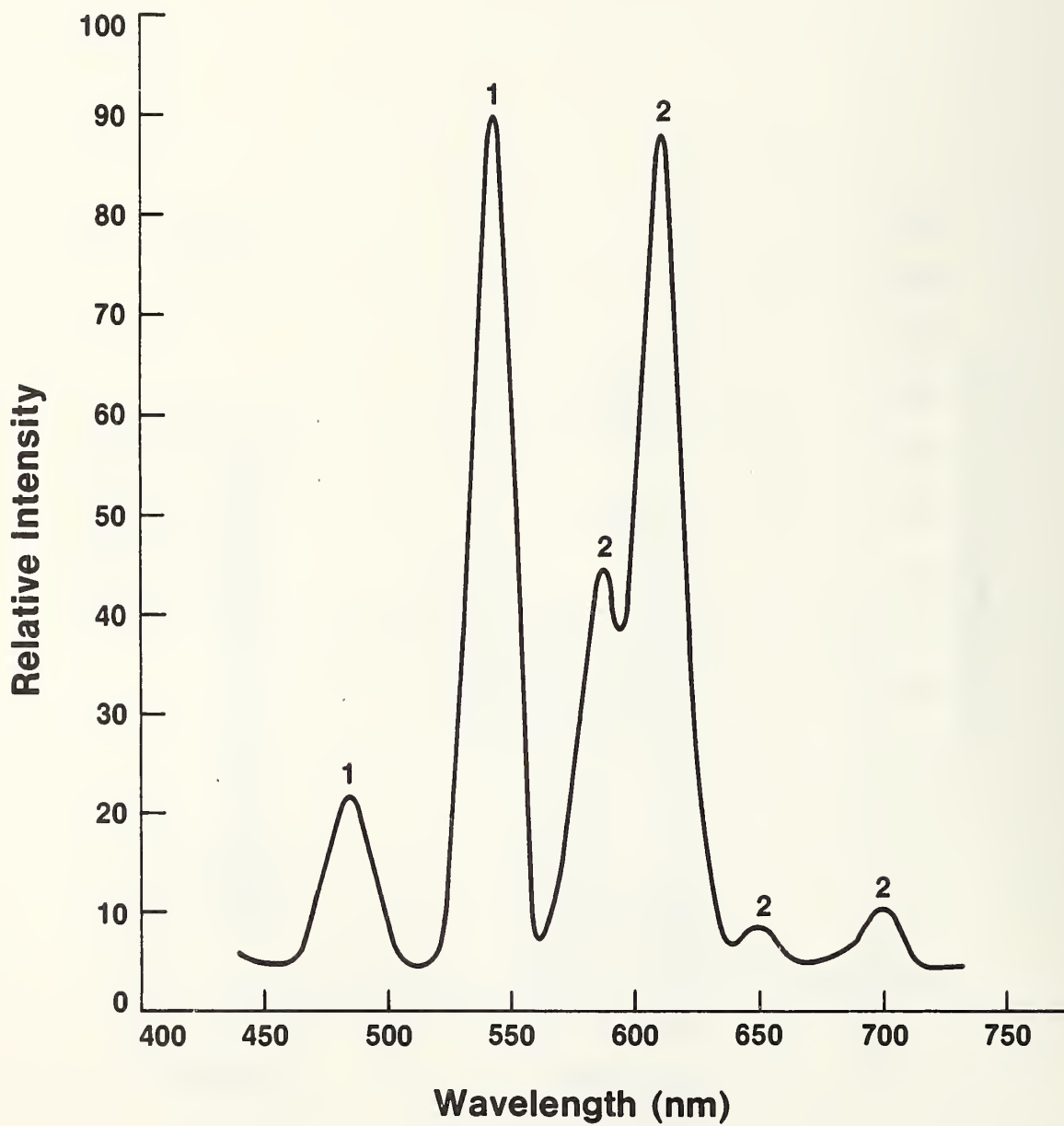
Figure 21. Typical luminescence spectrum of a glass doped with Tb_2O_3, peaks labeled 1, and Eu_2O_3, peaks labeled 2; 3.0 and 1.0 weight percent, respectively; photomultiplier voltage = 1000 V; monochromator slit widths = 2,2 mm.

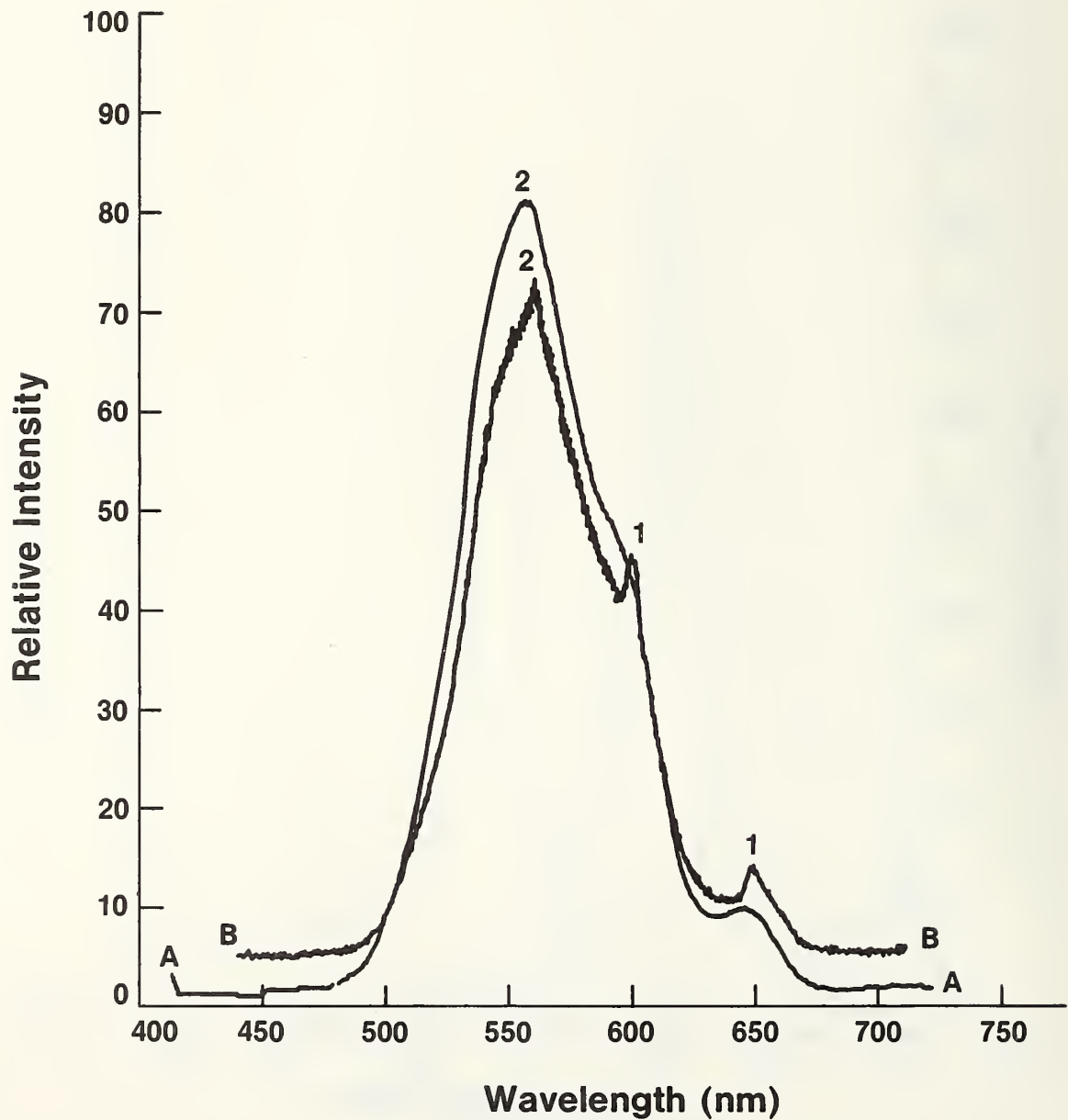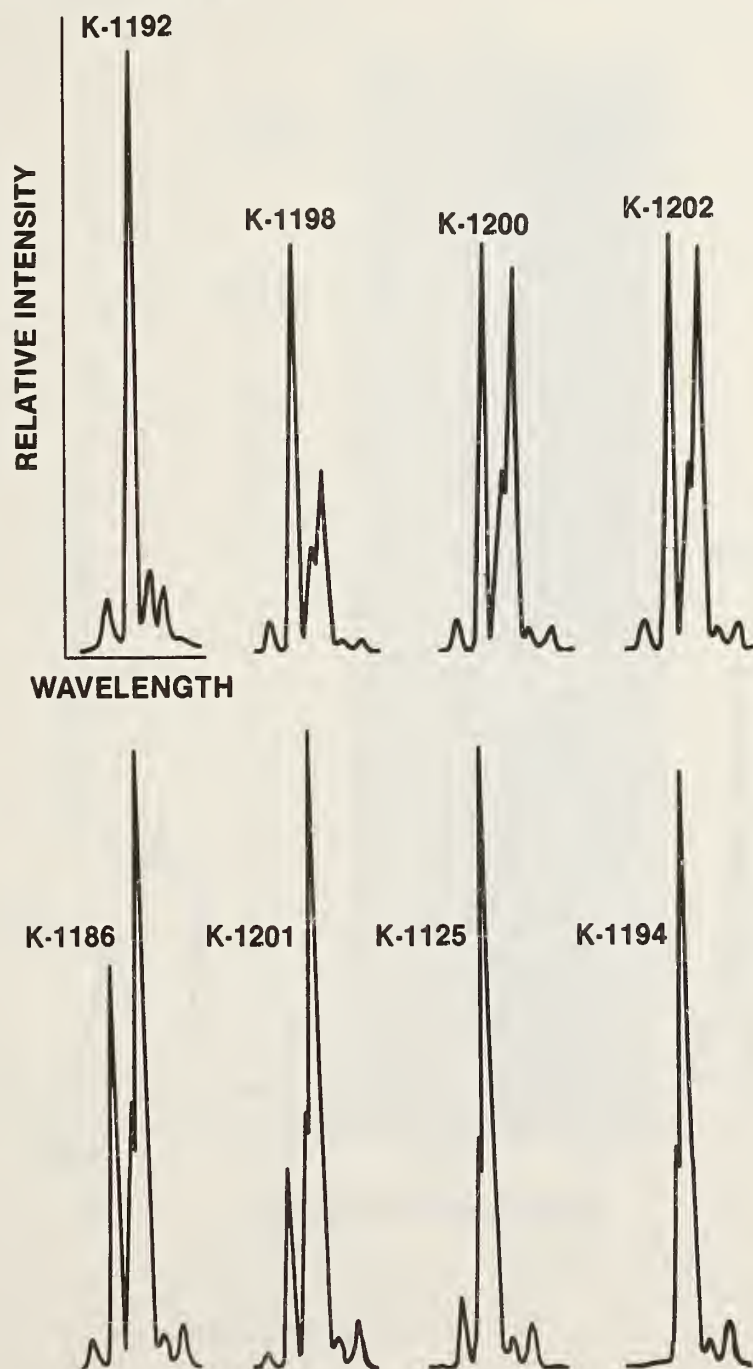Figure 22. Luminescence spectra of glasses containing Tb^{3+} and of Eu^{3+} using cube D (table 1). The numbers refer to the melt designations listed in table 3. Each spectrum was recorded at different gain settings. Relative peak intensities in each spectrum are illustrated.
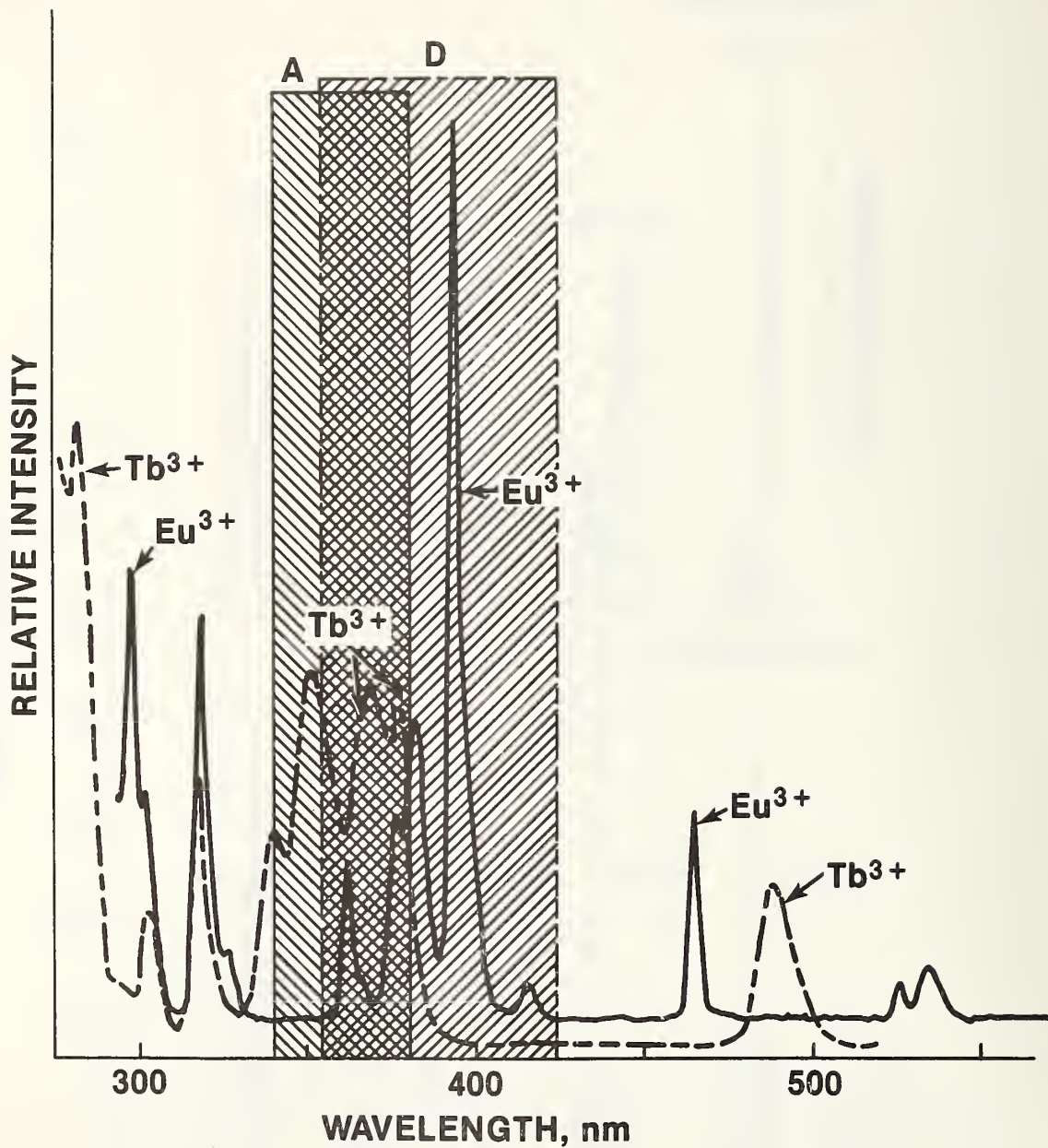
Figure 23. Typical excitation spectra for Tb^{3+} (dashed line) and Eu^{3+} (solid line) in a glass matrix. Approximate excitation wavelength bandwidths are shown by the boxed in areas using filter cubes A and D (see appropriate cross dashing and table 1).
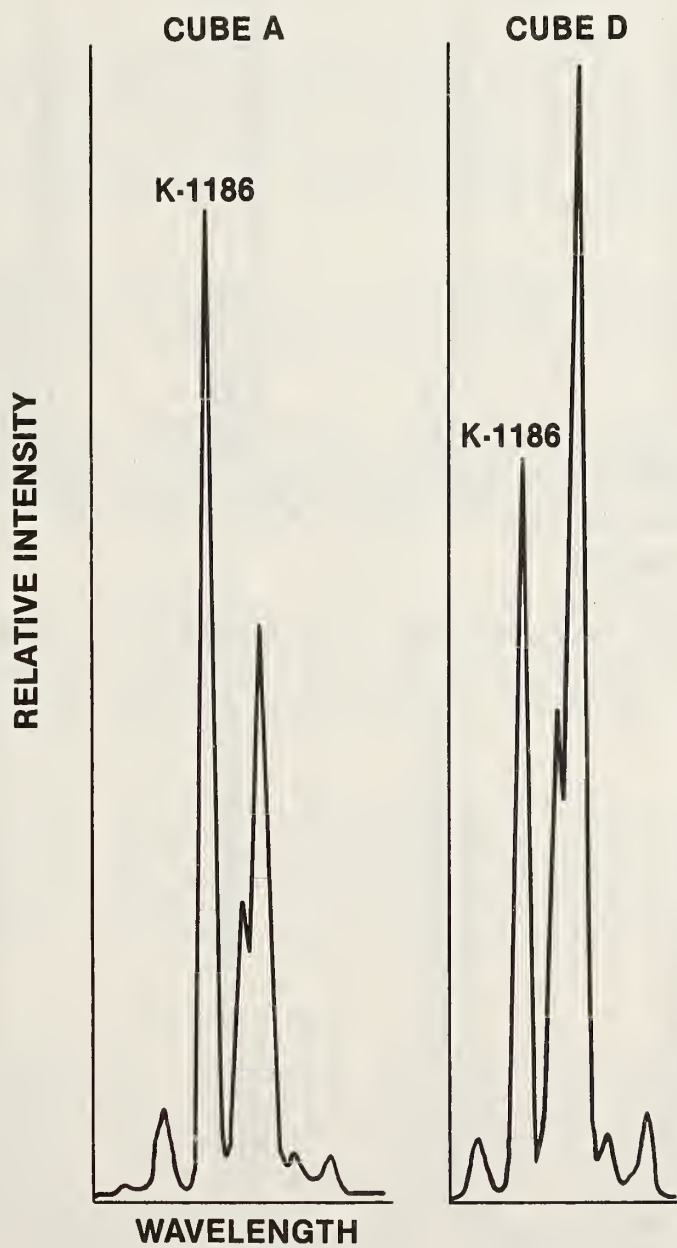
Figure 24. Luminescence spectra of melt K-1186 using cubes A and D (table 1) to select excitation radiation and show difference in peak ratios for the same melt.
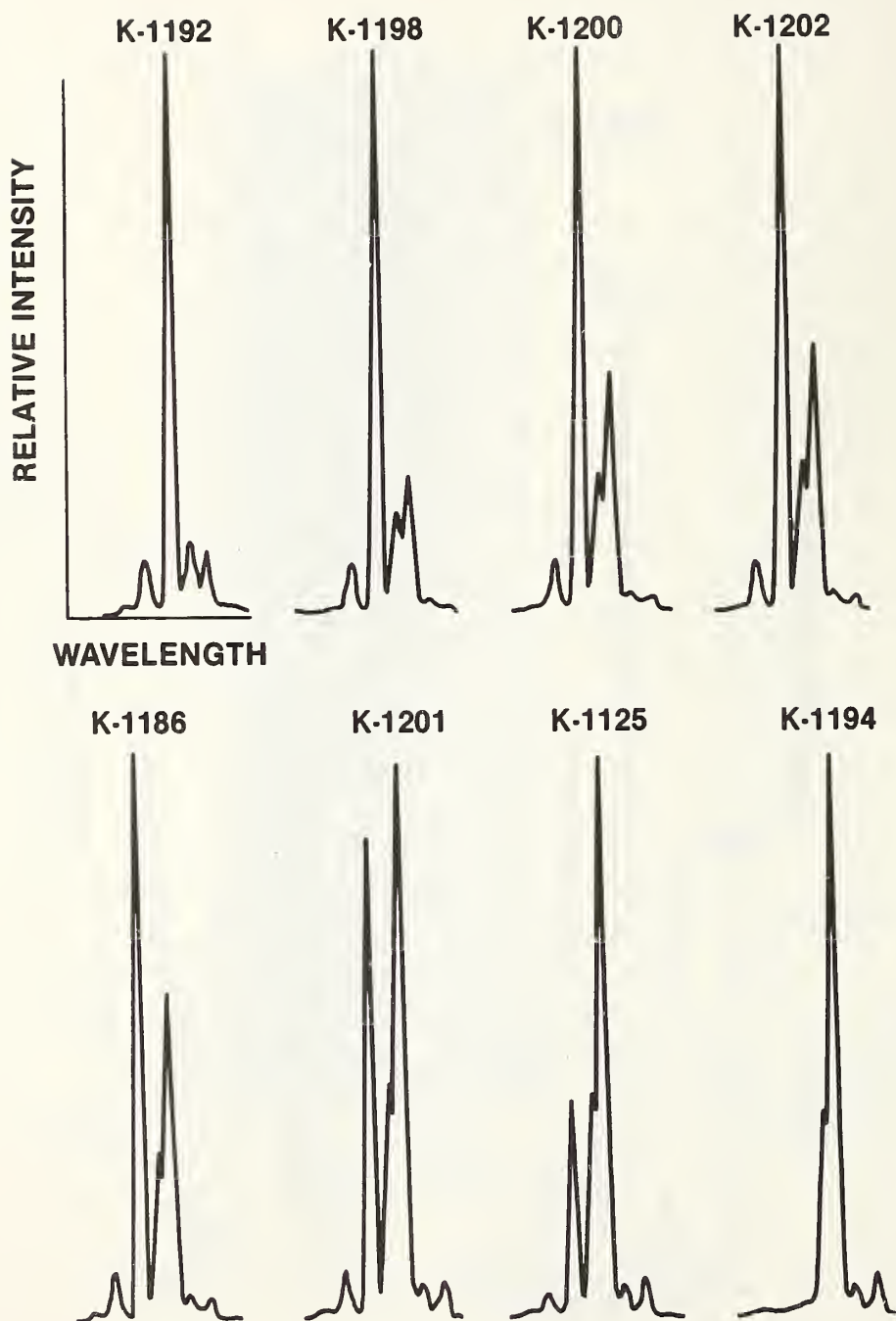
Figure 25. Luminescence spectra of all glass melts of composition listed in table 3 using cube A (table 1). Each spectrum was recorded at different gain settings. Relative peak intensities in each spectrum are illustrated.

2.   Age of Excitation Source. Aging of the excitation source generally reduces the intensities of the shorter wavelengths; thus, the Eu/Tb peak ratio would increase because the Tb^{3+} excitation would decrease more than the Eu^{3+} excitation.

3.   Monochromator Slit Widths. In general, as the monochromator slit widths are decreased, resolution increases and the luminescence intensity passing through the monochromator decreases.   This phenomenon is illustrated in figure 26 which shows the emission spectra of a single melt using four different monochromator slits.

Specifically, as the slit width decreases from 2 mm to 0.2 mm, the resolution increases from 16 nm to 1.6 nm (hhbw) and the Tb^{3+} peaks at ~475 and ~545 nm are split into double peaks. Similarly, shoulders appear at ~580 and ~615 nm on the Eu^{3+} peaks which were not apparent previously. As a result of this splitting, the Eu/Tb peak ratio changes from ~1.30 for 2 - mm slits to ~0.7 for 0.2-mm slits. The luminescence intensity decreases to such an extent that the signal-measuring equipment must be operated at close to maximum gain thereby reducing the signal to noise ratio.

Thus for comparative purposes, it is recommended that the monochromator resolution be as large (~16 nm hhbw) and sensitivities be as low as practicable to obtain spectra that have broad peaks and low noise to facilitate the peak ratio measurements.

4.   Detection System Responsivities. The optical transmission or sensitivity characteristics vary among optical devices (e.g., microscopes, monochromators, etc.).   Photomultiplier responses produced by different manufacturers vary even for similar equipment produced by the same manufacturer due to production differences and component aging. Thus, different peak ratios will be obtained as a function of equipment or time.

In summary, it is imperative that a series of standards (spheres of known composition) is available to be used for the unambiguous identification of an unknown sphere.   The emission spectrum of the unknown must be measured on the same instrument, with the same instrumental parameters, and close in time to that of the standard so that calculations and comparisons of the Eu/Tb peak ratios will not be instrument or time dependent.

To facilitate the following discussions of sphere parameters, specific measurements were made using 2-mm monochromator slits (giving a hhbw resolution of ~16 nm) with a series of melts, or a particular melt being used at the same time on the same instrument. Thus the ratio measurements and discussions relate only to the effect of that single parameter on the stability of the spheres, luminescence intensity as a function of luminophor concentrations, sphere size, or instrument parameters.

E.   Sphere Preparation and Characterization

1.   Sphere Preparation.   Initially the spheres were prepared by placing the crushed glass particles in a "hopper" attached to an oxy-acetylene flame gun.   The particles were passed through the flame at temperatures of 2000-3000 °C and were collected in a water-filled container.   Determination of the Eu/Tb ratios for various sized spheres (10 - 100 μm) showed that the ratios were dependent on sphere diameter. It is believed that the high formation temperatures caused selective luminophor loss at smaller sphere sizes resulting in individual luminophor concentration differences and thus different luminophor intensity ratios.

An alternative procedure was developed to produce spheres [10]. This process prepares spheres by passing an air suspension of crushed glass particles through an oven with an equilibration temperature at which the glass just becomes fluid (900-1400 °C, depending on glass composition). The particles are formed into a spherical shape by surface tension. The particles are collected on filters and passed through appropriate sieves to yield glass spheres of specific size ranges.

2.   Luminophor Homogeneity.   Since the total sphere volume and thus all luminophors are excited by the source, a mass proportional emission flux is obtained. General eq (4) for the emission flux may be modified to yield

$$I_L = I_0 [(2.303 \ \epsilon l \ m/v)] \ O_L \qquad (6)$$

33
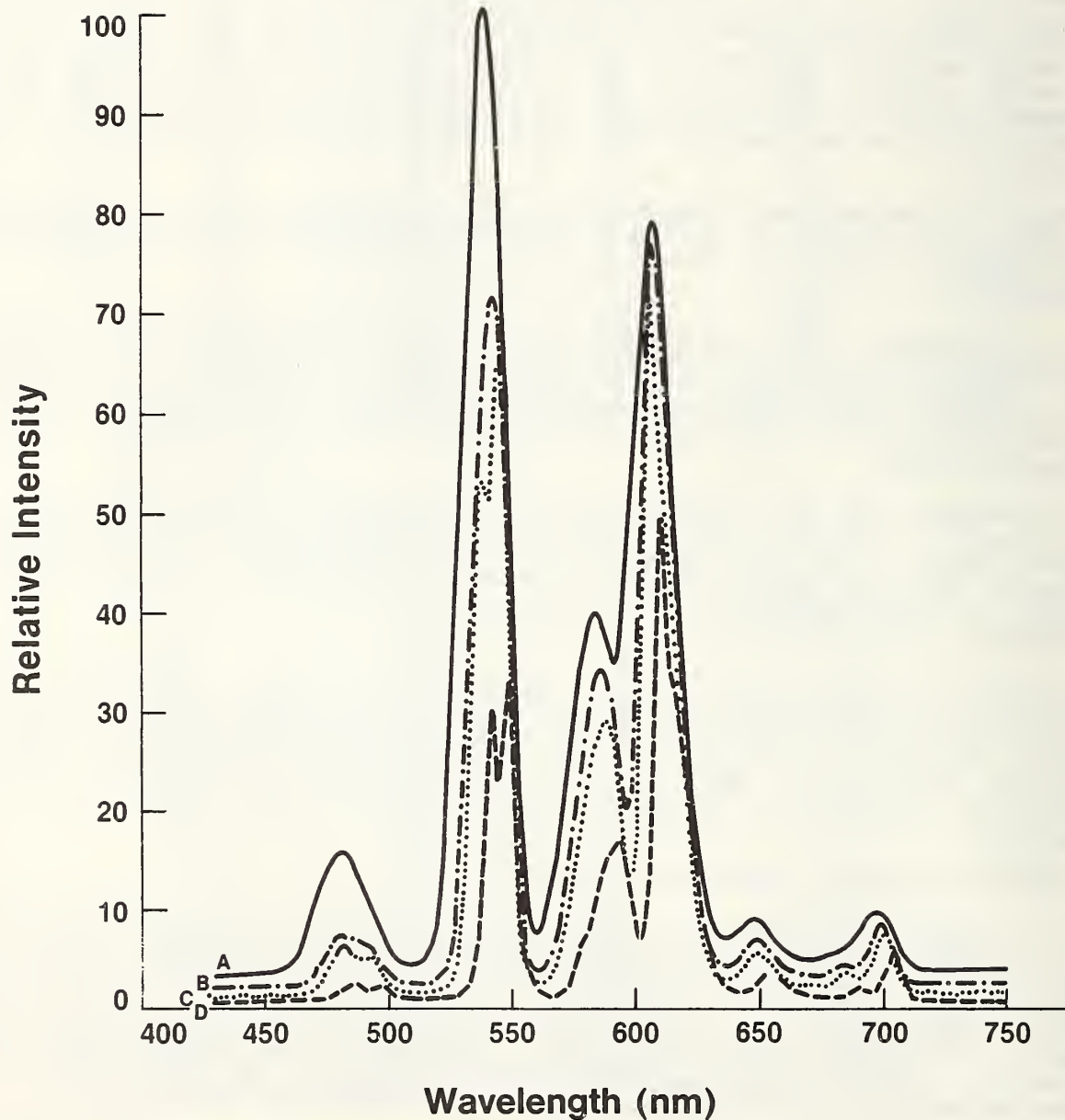
Figure 26. Luminescence spectra of glass melt K-1202 as a function of
monochromator slit widths using filter cube D (see table 1); A = 2 mm,
B = 1 mm, C = 0.5 mm, D = 0.2 mm.

where concentration, c is replaced with m/v (mass/volume). At a constant luminophor concentration, the mass of the luminophor should be proportional to the cube of the sphere diameter:

$$m \propto 4/3\pi r^3 \tag{7}$$

and since $I_L \propto$ mass from eq (6), then I_L has to be proportional to r^3. This relationship is verified for a melt in figure 27 which shows a straight-line relationship between I_L for the Tb and Eu peaks versus the sphere radius cubed. As shown in figure 28, the Eu/Tb ratio is independent of the sphere size with this method of bead preparation. The deviations from the straight line for beads with radii <5 μm are due to high measurement imprecisions resulting from excessive electronic noise and errors in radius measurement. It is recommended that beads with radii in the 10-20 μm range be used for optimal ratio measurements.
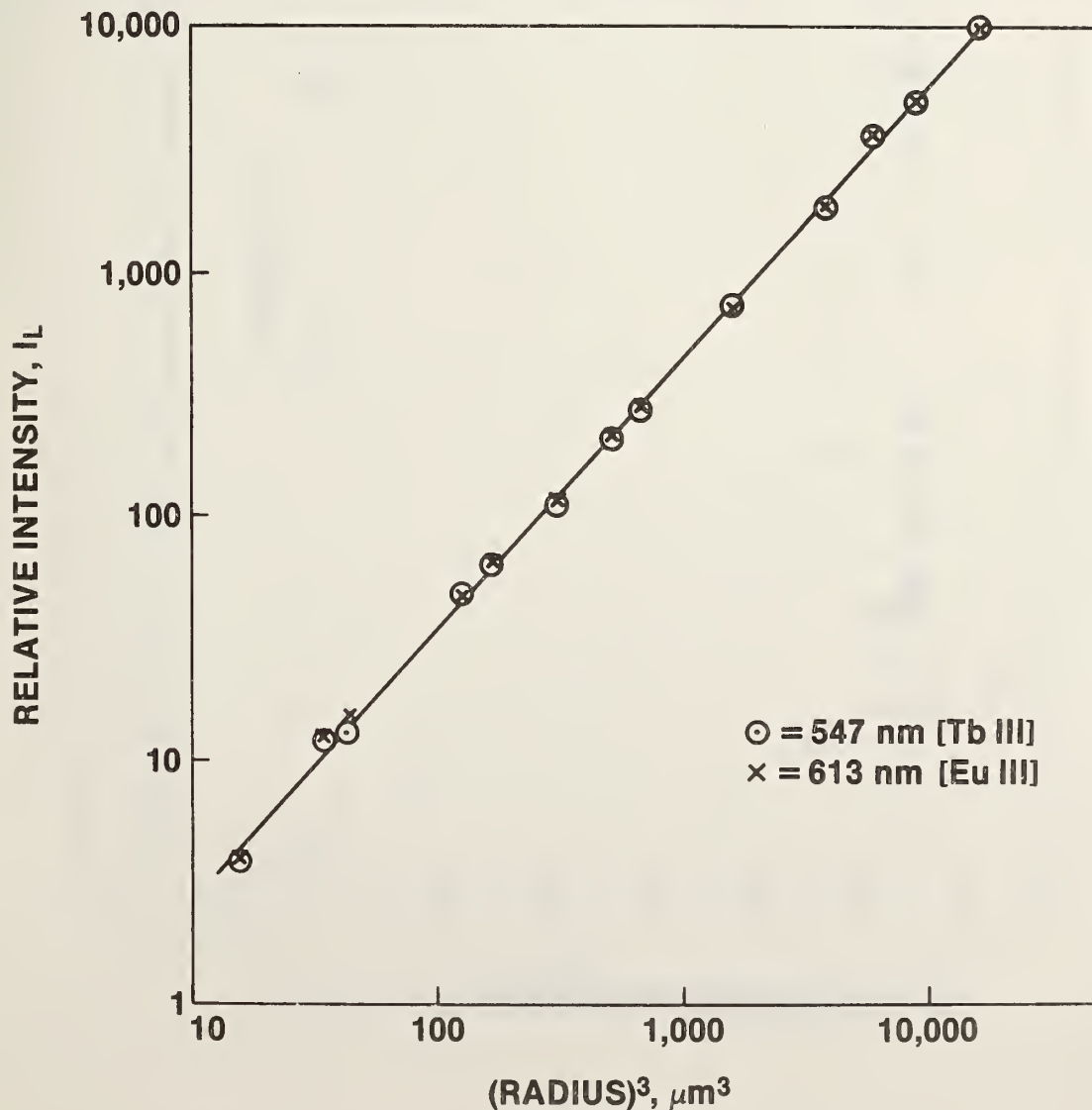
Figure 27. Plot of relative luminescence intensity versus the third power of particle radius.
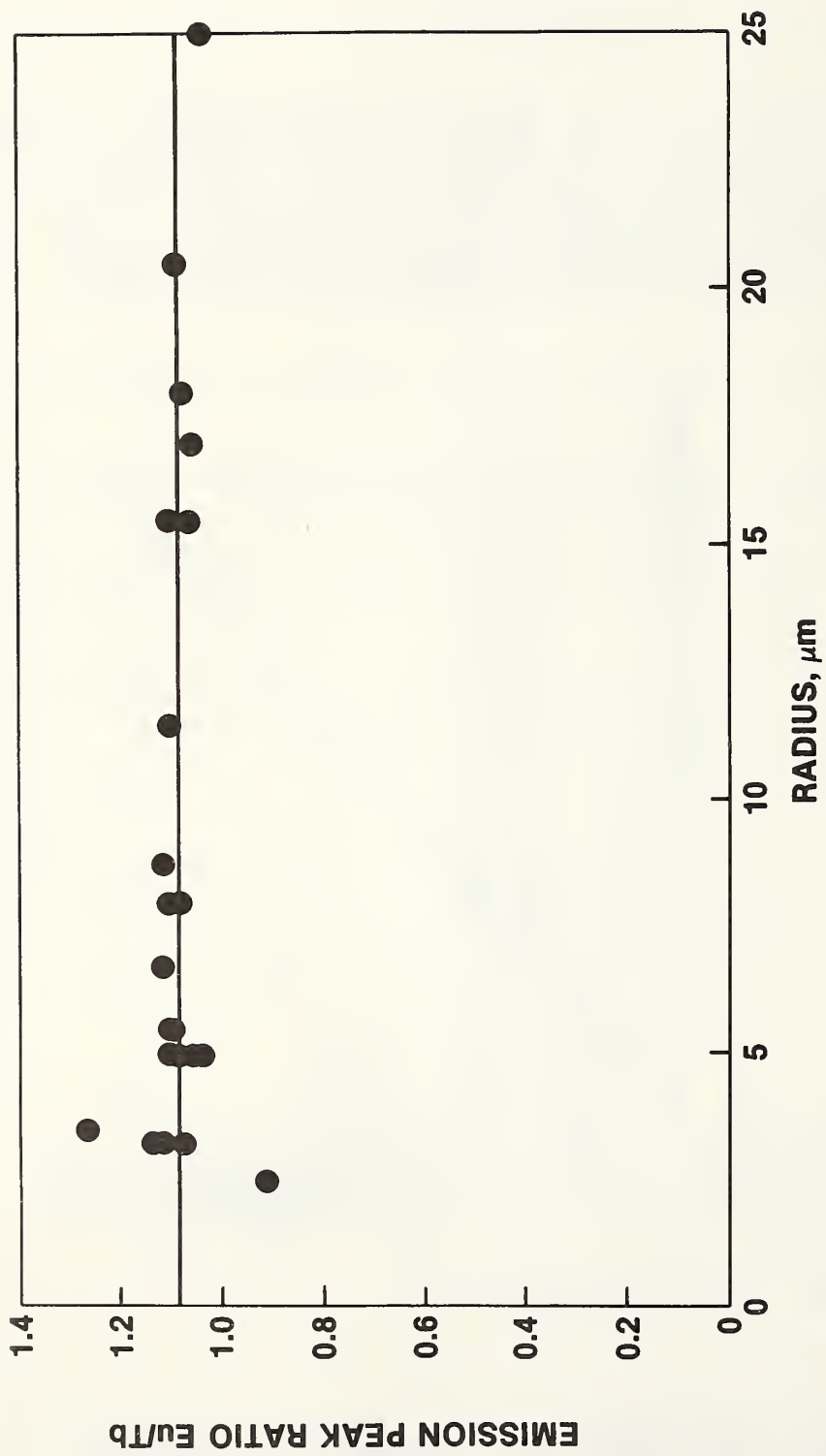
Figure 28. Plot of europium-terbium ratio versus the particle radius.

36

If the Eu/Tb peak ratio is plotted versus the [wt % Eu/wt % Tb], a linear relationship is observed (fig. 29) except for melt K-1125 (i.e., Eu/Tb concentration ratio = 1.5). We have not been able to establish a reason for the deviation observed for melt K-1125.

F. Reproducibility of Measurements

The identification of origin of any particular glass sphere doped with a pair of rare earths will depend upon a comparison of the concentration ratio of rare earths in the unknown glass sphere with that of a standard or known sample of the original tagged material. Consequently, it is important to know how reproducibly the ratio of rare earth concentrations in the glass can be measured.

Determinations were made on the effects of particle size, concentration ratio, operator, and measurement sequence on the variance of the measurement. An analysis showed no significant differences of variance from the parameter changes: sphere sizes with diameters 20 and 40 μm; two different operators; two different rare earth ratios (Codes K-1202 and 1198); and a comparison of within-day and between-day measurements (table 4). From these data it may be assumed that the method is fairly robust, although more detailed studies should be made. Pooling of all measurements shows a measurement imprecision of about 1 percent relative standard deviation of a single determination based on a series of 16 measurements.
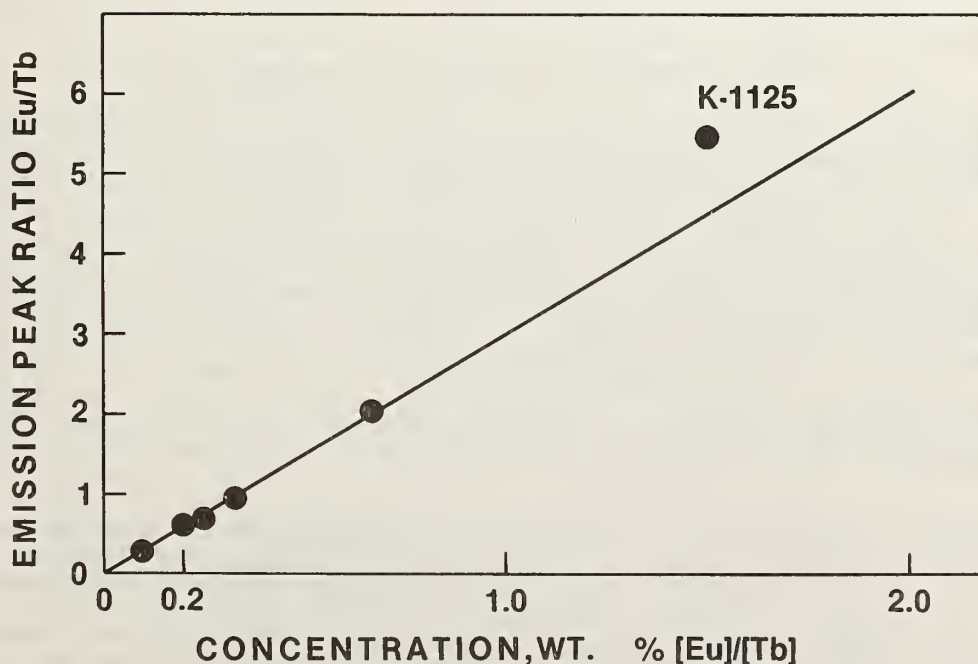
Figure 29.   Plot of europium-terbium ratio versus the weight percent
            ratio of europium to terbium.

37

Table 4. Effect of changing parameters of the measurement system

| | Peak ratios[a] | |
Variable/value	Average	Standard deviation
Operator 1	1.221	.018
Operator 2	1.219	.011
Particle size 41 μm	1.218	.016
Particle size 19 μm	1.222	.013
Measurement (within day)	1.216	.018
Timing (between days)	1.224	.010
Code K-1202	1.222	.016
Code K-1198	1.217	.013

[a]Average calculated from eight replications; standard deviation is for a single determination. Numbers for code K-1198 were normalized to that of K-1202.

IV. EXTENT OF UNIQUE TYPES OF PARTICLES

It is important to determine how many secured spaces can be identified uniquely. Therefore, it is necessary to determine the reproducibility that can be obtained in the measurement of the quantity of luminophors from the spectral data. As stated before, it is best to measure the ratio of the peak intensities of the two luminophors. In addition to the tests made in the previous section, measurements were made to determine what effect various methods of quantifying the spectral data had on reproducibility. The reproducibility of the ratios are measured by using three methods of processing the data: 1) graphical inspection, 2) digital peak height measurement with interpolation, and 3) a least squares fit of a Gaussian function to the data in the region of the peak. All showed a relative standard deviation of about 1 percent. It makes little difference upon the method used for processing the data at the level of reproducibility inherent in these data. It is always preferable if possible to process the data by computer in order to reduce blunders.

Based upon the analysis of variance and measurements of reproducibility in the previous section, one can expect to be able to distinguish a difference in peak intensity of about 3 percent. Therefore, each peak can be divided into ~30 parts. This would imply $(30)^2$ or 900 unique ratios less the redundancy generated by even multiples. A simple computer program was written to determine the number of unique ratios by eliminating redundancy. For a two-component system at 30 units of concentration for each component, 550 unique codes can be generated. At 20 units, 250 codes can be generated. For a three-component system at 10 units for each component, 840 unique codes can be generated.

38

V. TYPES OF PARTICLE DEPLOYMENT

In order to investigate the efficiency of detection of these particles by microscopic examination, it was necessary to develop a system that could put a known concentration of particles randomly on a glass slide. This involved a study of possible particle deployment methods.

Two media, liquid or gas, can be used for distributing the particles within the secured area. The liquid medium would be very useful for large areas and could be distributed as a mist or heavy spray. The liquid can contain an adhesive agent to aid in retaining the particles on a surface. Quite often, however, the particles will be electrostatically attracted to charged surfaces (e.g., nonconductors) and will adhere without an adhesive.

We elected to investigate the use of gaseous dispersion. This procedure has the attractive feature that the particles can be stored indefinitely as a powder in the dispersing mechanism with little likelihood of degradation that might result from dispersing the particles in a liquid. The dispersal technique selected for the conduction of the sensitivity experiments is described in the next section.

A. Apparatus and Experimental Procedure

A chamber approximately 1.5 m (5 ft) on each side was fabricated of aluminum angles. It was assembled so that a plastic sheet could be mounted totally within the frame such that no frame member was exposed to the inside of the chamber. In addition, sponge rubber strips were mounted on the bottom of the frame to fit flush with the floor which was also covered with a plastic sheet to make the floor of the chamber. The top was designed to fit flush with the frame by applying sponge rubber strips to the contacting surfaces. The center of the top contained a housing for the disperser system and a small fan. The fan was to be used to generate positive pressure within the chamber in the event that the plastic did not hang smoothly against the frame. However, with the design used, no difficulty of this type was observed and the fan was not used. The chamber was designed so that the plastic sheeting could be changed within a half hour.

The system for dispersal is shown in figure 30. The circular disc (D) acts as a deflector of the gas (N_2) stream and the particles are blown outward in all directions. The flowing gas stream produces a doughnut-shaped vortex that helps to mix the particles quite evenly over a space of about 2.25 m^2 (25 ft^2). The dispersal system is made of 1.3-cm (1/2-in) pipe with a 90° elbow fitting (P) that is loaded with a known weight of particles. A quick release valve is used to release the gas. The required amount of particulate matter was weighed directly into a section of the dispersal device, which was then mounted in place with a standard pipe connection. The dispersal device was aligned by eye to be parallel with the floor. Microscope slides appropriately labeled were then placed on the floor of the chamber (fig. 31) at the positions indicated in figure 32. The nitrogen pressure was adjusted to 5.50x10^5 Pa (80 psig) and the gas was turned on with a quick-acting lever valve and allowed to run for 5 s. The particles were allowed to settle for 15 min. (Preliminary tests indicated that at least 95 percent of all particles had settled by that time.)

After the particles settled, the top of the chamber was carefully removed so as not to jostle either the top or sides of the chamber. The chamber was then carefully tilted to expose the floor and allow easy removal of the glass slides. The slides were placed in a covered metal tray and transported to the laboratory for microscopic examination. (Plastic containers are unsatisfactory because static charges on the surface can draw particles from the glass slides.)

The chamber was constructed so that the plastic could be easily removed without producing contamination. Repeated tests for contamination of the top and sides of the chamber showed the presence of very few spheres. The plastic sheet on the floor of the chamber was replaced periodically. Evidently the chamber was large enough to prevent electrostatic attraction of the plume of particles that was produced.

B. Distribution of Particles

The distribution of spheres measured as an average of five separate runs normalized to unit weight of dispersed spheres is illustrated in figure 33. (For
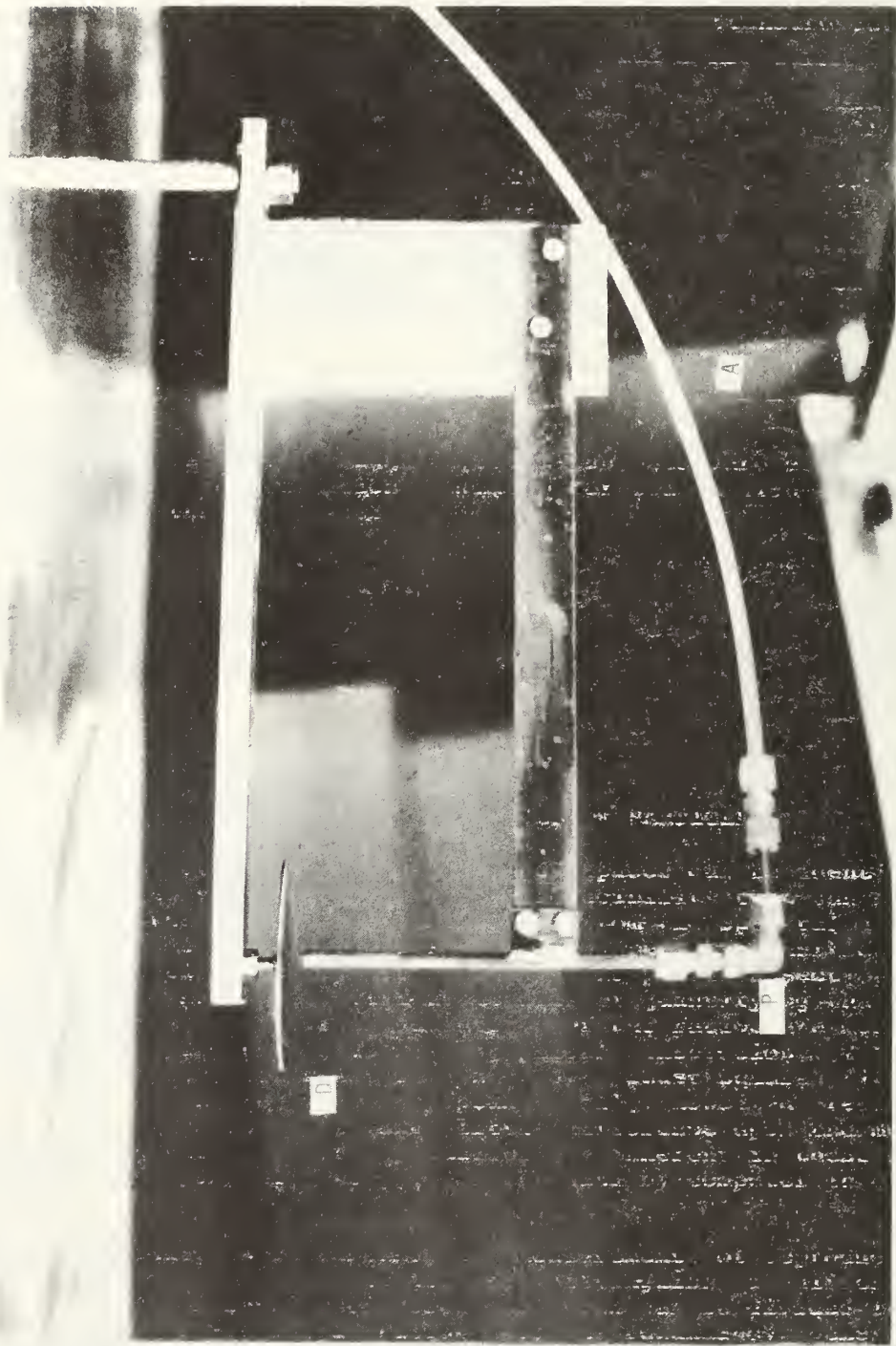
Figure 30.   Photograph of particle disperser; D = circular deflector disc;
P = pipe fitting in which particles reside; A = nitrogen pressure line.

40
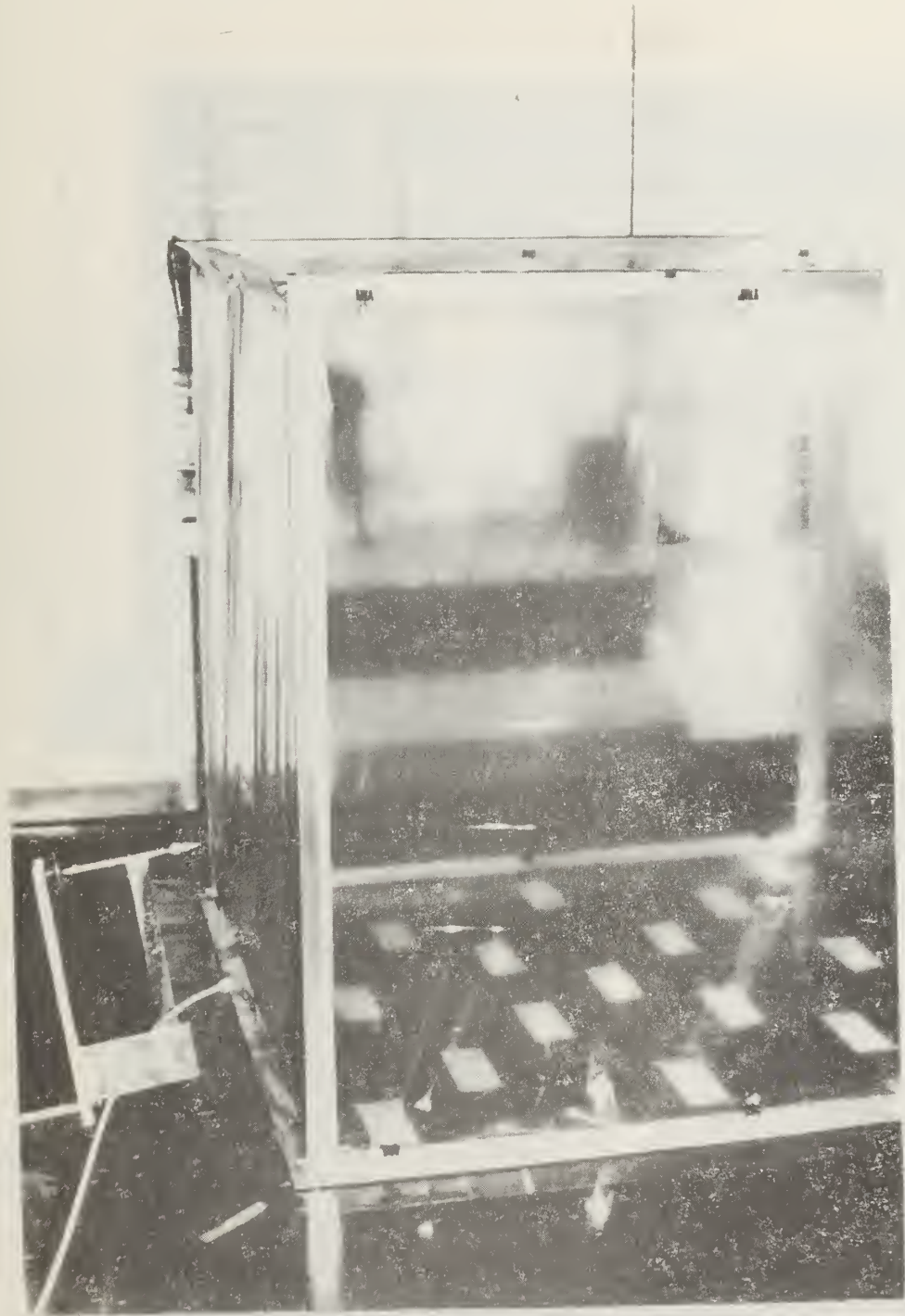
Figure 31a. Particle dispersal system; plastic covered chamber
showing positions of microscope slides.
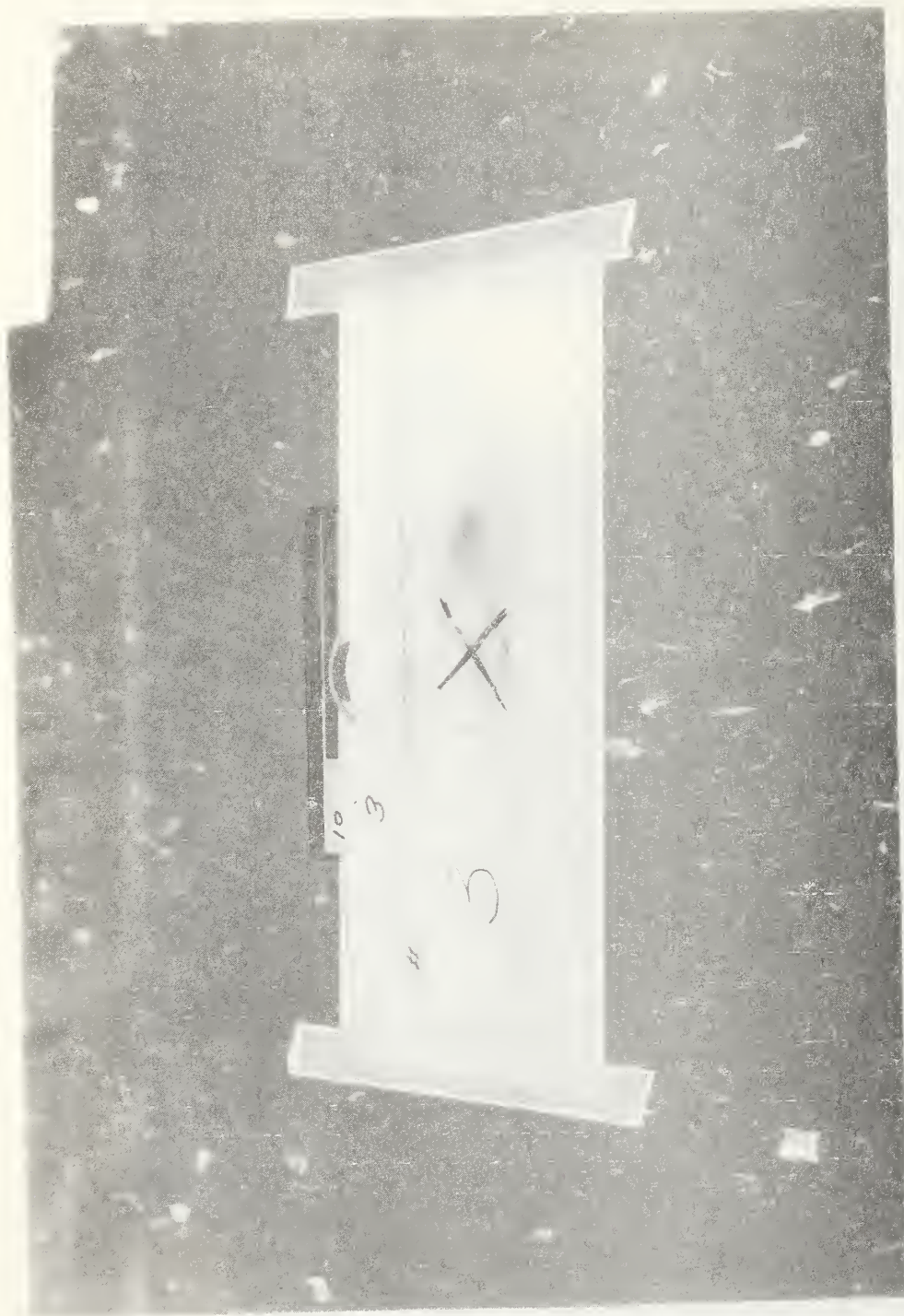
Figure 31b. Particle dispersal system; close-up showing microscope slide placed on inverted 50 mL beaker.

Figure 31c. Particle dispersal system; top of chamber showing mounted disperser with chamber in the background.

43
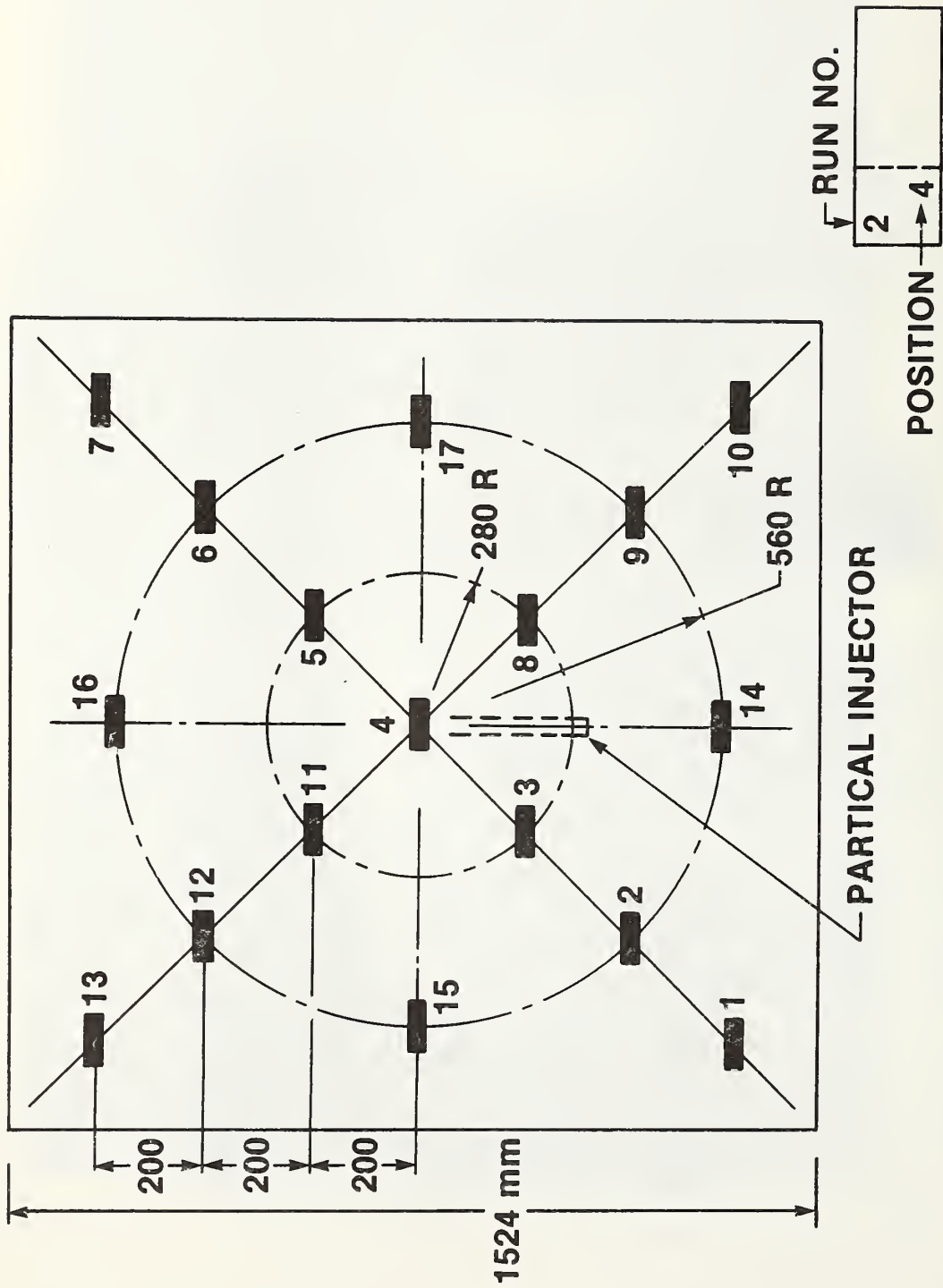
Figure 32. Diagram showing slide positions (dimensions in millimeters).
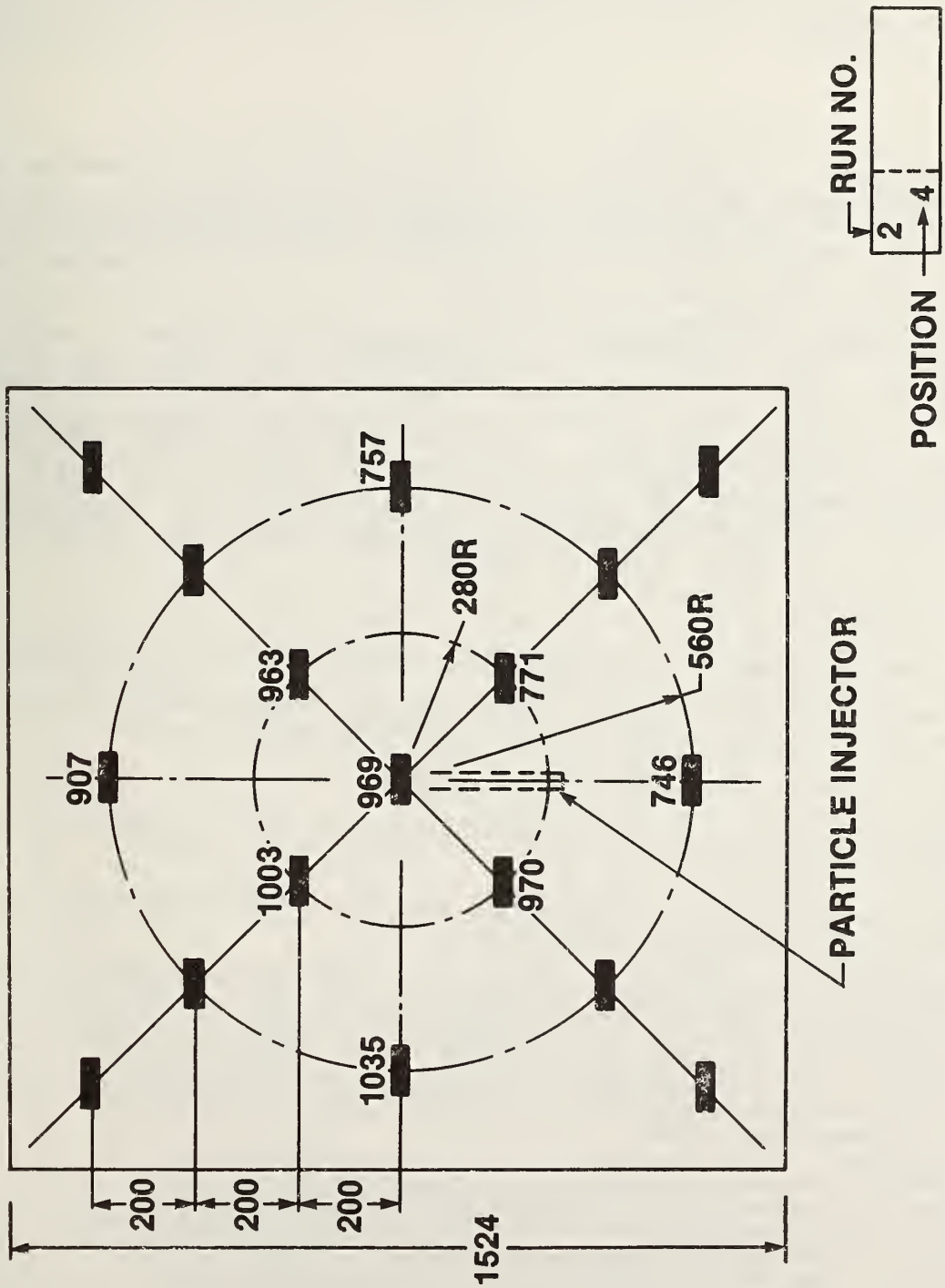
Figure 33. Test results of particle dispersal. Numbers are average of five runs; units = particles/cm²/g (dimensions in millimeters).

specifications on the glass spheres, see the next section.) The pooled relative standard deviation of the averages between runs using data from each of the nine positions is about 13 percent. The pooled relative standard deviation of the averages within a run and between positions is about 10 percent. The grand average over the replicates and positions (45 measurements) is 896 particles $cm^{-2} g^{-1}$ with a pooled relative standard deviation of 12 percent. These results are acceptable for such a dispersal system.

VI. DETECTION OF SPHERICAL PARTICLES

It is important to determine an approximate lower level of concentration of spherical particles that can be detected by microscopic examination. The simplest and best procedure for measuring the particles per unit area is to allow the particles to fall upon a surface as uniformly as possible and to measure the number of particles per unit area on a microscope slide. This was accomplished by using the system described in the previous section.

There are a number of factors that will determine the detectability of particles on the microscope slide. The size of the particles is very important, since the maximum resolving power of a microscope is about 1 µm. The type, size, shape, and number of the particles in the microscope field of view can adversely affect the selection of the desired particles. A decided advantage in their detection is the fact that the particles of interest are spherical and that they show a color (e.g., the luminescent radiation) when irradiated with ultraviolet light. However, it is the spherical shape that is most important, because it will be demonstrated that most house dust contains brilliantly luminescent particles when excited by ultraviolet light, but their shapes are irregular.

A. Limit of Detection

One can predict a limit of detection based upon the following assumptions:

1. The particles are dispersed randomly on the microscope slide and the law of probability for this system follows a binomial distribution.

2. Random fields of view (FOV) are inspected.

3. Eye fatigue limits the continuous inspection of a single microscope slide to 10 min.

4. Only a binary decision is considered; namely, the FOV under inspection has or has not a single particle of interest.

5. A selected particle will always be positively verified as a particle of interest after spectroscopic examination. Also, the observer is 100 percent efficient in detecting the presence of a particle in a field of view. The most practical size of particle to work with ranges between 10 - 20 µm in diameter. We have arbitrarily selected to work with particles that are one division wide within the optical graticule (16.7 µm). Therefore, calculations are based upon that size.

One needs to determine how many FOV can be inspected in 10 min. In practice, if the magnification was too high, eye strain increased significantly. It was found that with an objective setting of 25X and a 10X eyepiece, one could inspect 150 FOV in 10 min. At this magnification there are 950 FOV/cm^2. When there are a large number of FOV, and the probability of finding a particle is small, the Poisson distribution can be used. One can therefore calculate the minimum detectable particle density from the Poisson probability distribution function

$$P_{(r)} = \frac{(np)^r e^{-np}}{r'} \qquad (8)$$

where

      n = number of FOV measured
      p = probability of finding a particle in a single FOV
      r = the number of FOV's that are found to have a particle
  $P_{(r)}$ = probability of finding that r FOV contain a particle

Eq (8) reduces to

$$P_{(0)} = e^{-np} \tag{9}$$

since r must be 0 at the detection limit, and $p = \dfrac{N}{950}$ where N is the total number of particles per square centimeter. Substituting into eq (9) allows calculation of $P_{(0)}$ which is the probability of observing no particles in 150 FOV's when the total number of particles (in all 950 FOV's) is N.

If N = 4, $P_{(0)}$ = .53; N = 7, $P_{(0)}$ = .33; N = 14, $P_{(0)}$ = .11; N = 19, $P_{(0)}$ = 0.05. These results demonstrate that the particle density N particles/cm^2 can be quite low and still the probability of detecting a particle in the 150 FOV is reasonable, e.g., at N = 4, $1-P_{(0)}$ = .47.

B. Particle Dilution Experiments

It was thought desirable to verify experimentally these numbers for the detection limit. It was important to be able to distribute the particles as randomly as possible over the surface of the microscope slide. The test chamber proved to serve very well for this purpose.

One could experimentally measure the limit of detection by simply reducing the amount of dispersed particles, but this was deemed to be inadvisable because as the total mass of particles changed appreciably, it was suspected that the dispersal properties might vary. Therefore, we decided to dilute the luminescent glass particles with plain glass (blank) particles so that the total mass of particles dispersed is constant. The only complication might be in the relative particle size distribution. If the distribution were sufficiently different, the aerodynamics of the gas dispersal system might affect the blank particles in a manner unlike that of the luminescent particles. It was therefore necessary to measure the distribution of particle size. The size distribution was measured by using the microscope with a calibrated graticule while measuring the size of a particle in a randomly selected number of FOV. The data in table 5 represent those particles which fall within the size indicated ± 2 μm which is approximately two standard deviations for a single measurement. A total of 795 blank particles and 145 luminescent particles were measured. Table 5 shows the distribution relative to the number density in particles per square centimeter for four different sizes. The second column shows the mass fraction which is calculated by multiplying the size distribution cell number fraction by the cube of the particle diameter (assuming that the density of all particles is the same), and dividing by the sum of the cell products. Since it is relatively easy to detect 16.7 μm diam particles with the microscope, all subsequent measurements will relate to this particle size. There is probably a significant number density below 4 μm, but it is assumed that they are insufficient to affect the mass fraction. It can be seen from the table that the mass fraction for the blank (nonluminescent) particles is 0.38 and for the luminescent particles it is 0.61. For the dilution work it is necessary to convert from mass fraction, which is the mode used for diluting the luminescent particles with blank particles, to a number density because this is the measurement unit obtained from the microscope. From the distribution data of dispersed blank particles in figure 33, one obtains a grand average of 896, 16.7 μm diameter particles per square centimeter per gram with a relative standard deviation of the average of 12 percent based upon 45 measurements. Therefore, correcting for the mass fractions one should observe (89.6)x0.61/0.38 = 144 particles with 16.7 μm diameter per square centimenter per 100 mg of luminescent particles dispersed. Results of distribution experiments identical to that described in the previous section gave a grand average of 149 luminescent particles per square centimeter per 100 mg with a relative standard deviation of the average of 18 percent based upon nine measurements. Thus, it

47

appears that dilution by mass and verification by number density is a workable process.

The dilution experiments were made by weighing out the proper amount of blank glass particles and the luminescent-compound, doped-glass particles and by thoroughly mixing them. An aliquot was then weighed into the dispersal sample chamber.

Careful inspection of the particle distribution on the microscope slides showed no evidence of nonrandom particle distribution across the slide. Although a large amount of replication was not done, no evidence for nonrandom variation between runs was observed.

Glass slides were positioned as described above at positions 3, 4, 5, 6, 11, 14, 15, 16, and 17 (see fig. 32). Each dilution was dispersed as described. The slides were then examined using a microscope, random FOV were selected, and luminescent particles with a diameter of one division (16.7 μm diam) on the reticule were counted. The total area scanned was recorded and the number density calculated. Effort was made to keep the area measured close to 150 FOV.

The blank glass particles that were used are called glass reinforcement filter spheres and are distributed by Potters Industries, Inc., Carlstadt, NJ 07072, catalogue number 3000. These were passed through U.S. Screen Number, minus 325. Both types of particles (luminescent and blank) were observed to be very uniform spheres.

In figure 34 the results of the dilution experiments as a plot of the ratio of luminescent/blank particle number density calculated from mass dilution vs. the experimentally measured density ratio are shown in curve 1. Although the scatter in the data is significant, the experimental data agree with that calculated from the mass dilution within experimental error. At the lower ratios, the ability to distinguish between 10-15 particles/cm^2 and no particles is impaired as indicated in curve 2. It should be noted that at the calculated dilution to put 3 to 4 particles/cm^2 on the microscope slide, five of the nine slides did show 1 particle each. This agrees with calculations of the limit of detection.

Table 5. Frequency distribution of particles

Particle size, diameter (μm)	Number fraction of particles		Mass fraction of particles[a]	
	Blank	Luminescence	Blank	Luminescence
16.7	.07	.21	.38	.61
12.5	.13	.22	.33	.26
8.4	.34	.31	.25	.12
4.2	.46	.26	.04	.01

[a]Calculated from number fraction, F_N, and particle diameter, P, for each (i)th cell of distribution.

F_{m1} = mass fraction of first cell.

$$F_{m1} = \frac{F_{N1}P_1^3}{\Sigma F_{Ni}P_i^3}$$

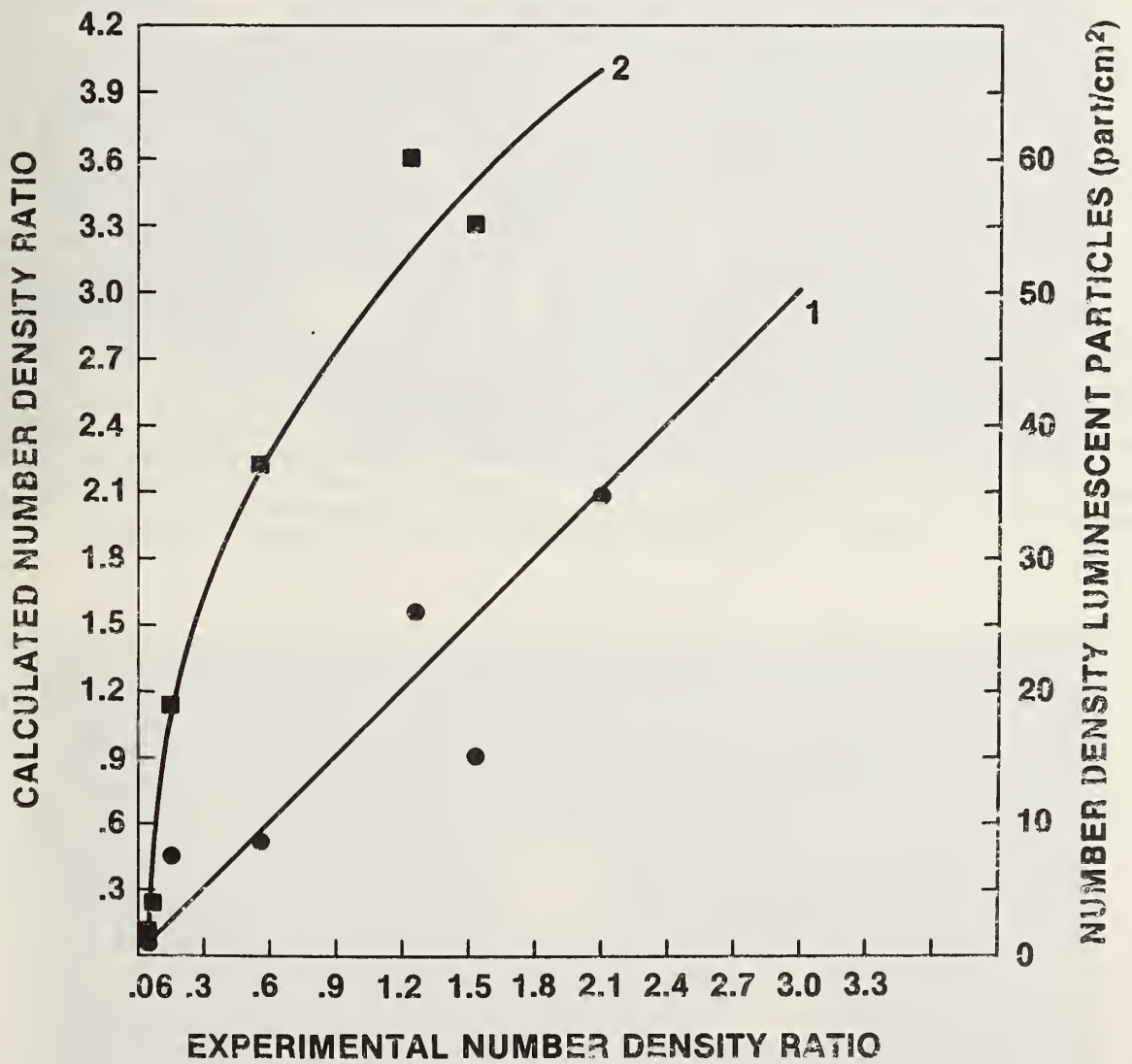Figure 34. Curve 1 (dots) – Ratio of number density (16.7 μm diam) luminescent to blank particles; calculated vs. experimental. Curve 2 (squares) – Experimental number density of luminescent particles vs. experimental ratio of number density luminescent to blank particles.

49

C. Detection of Particles in a Background

A series of experiments was devised to determine if detectability was affected by the presence of other particles. The first experiment involved the sequential dispersal of luminescent particles and 1.6 g of nonluminescent particles onto the slides without slide movement. Measurements were made on each of five microscope slides positioned at 3, 4, 5, 8, and 11 (see fig. 32). These data appear as rows 1 and 2 in table 6, respectively. Within the precision of these measurements, no significant difference can be observed.

A series of microscope slides were coated with a thin film of dust by pouring a thick layer of dust on the slide, then removing the bulk by tilting the slide and lightly tapping its edge. These slides were then placed in the positions indicated above for experiments 1 and 2, and luminescent spheres were dispersed over the dust layer. This result is shown in row 3(a) of table 6. Row 3(b) shows the same experiment except that a dilution of luminescent beads with blank beads was used. Appropriate normalization was made for the mass dilution ratios that were used, and the corrected result to zero dilution is shown in parenthesis.

The final experiment was identical to 3(a) except that a different dust was used. One can conclude from these experiments that blank glass particles do not affect detectability, but dust has the effect of reducing the efficiency of detection to about 60 percent. This cannot be considered to be a large decrease in efficiency and probably this lack of effect is due to the fact that the luminescent particles are spherical and have a very characteristic color while many of the dust particles are brightly luminescent but irregular in shape. A photograph of a luminescent particle in house dust is shown in figure 35. Here it is seen to be quite easy to pick out the circular shape from the background of odd shapes. However, in figure 36 a perfectly circular shape is found. It is even close to the correct color, but when the luminescence spectrum is measured (fig. 37), it is clear that it is not one of the tagged particles, but rather a sphere of pollen.

Table 6. Effect of background particles on
luminescent particle detectability

Experiment identification	Particle number density		Percent error
	p/cm^2g	error[a]	
1. Luminescent particles (K-1200)	864	75	9
2. Blank particle overlay	783	78	10
3. SRM dust			
(a) K-1200	542	38	7
(b) K-1200 dil	311 (520)[b]	(100)[b]	19
4. House dust	444	72	16

[a]Errors are the standard deviation of the average of five measurements.

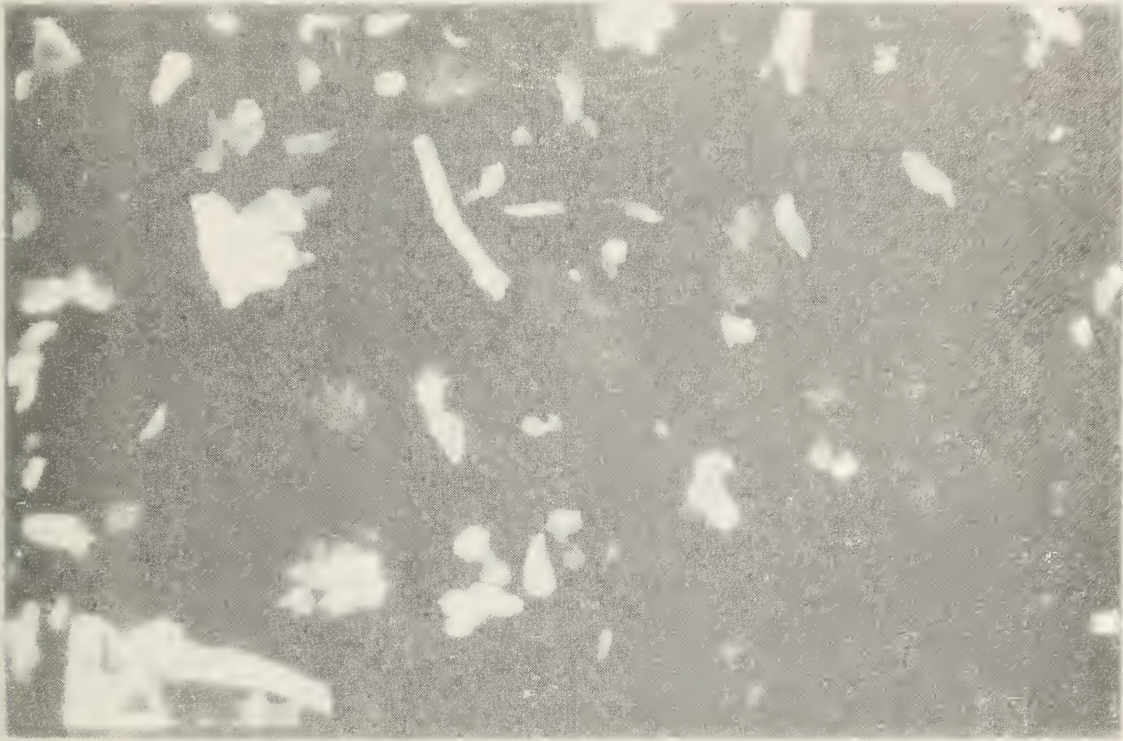[b]Corrected to undiluted value.

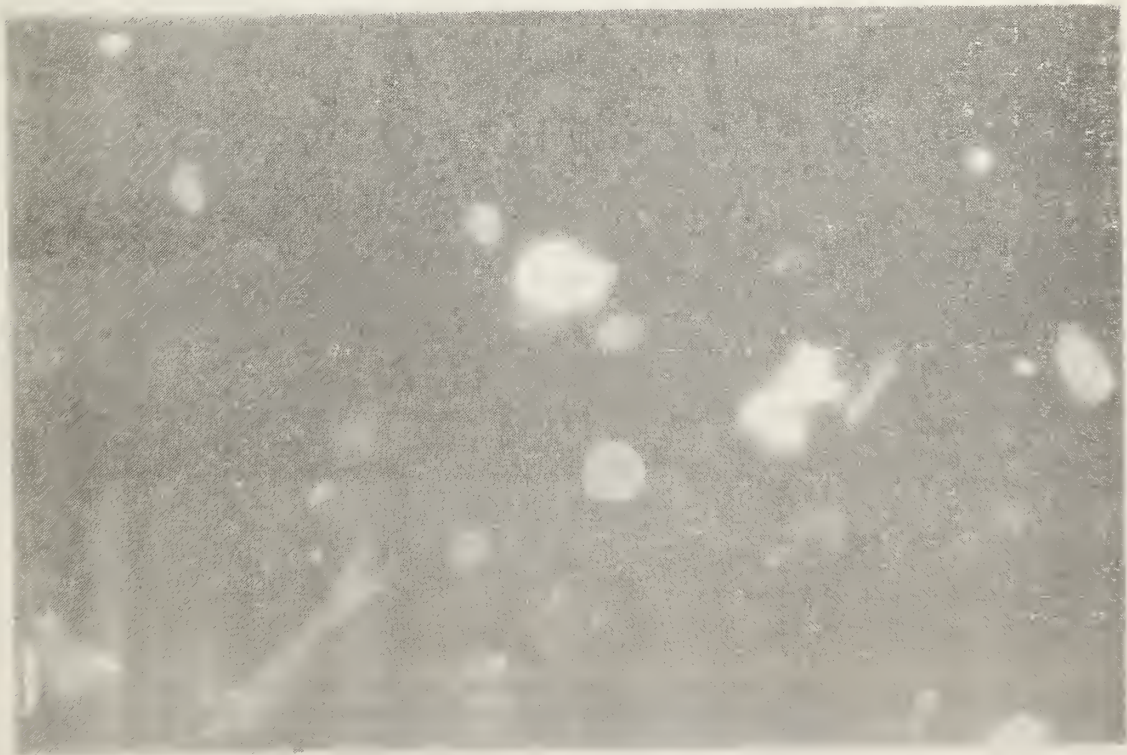Figure 35. Photograph of luminescent particles in house dust.

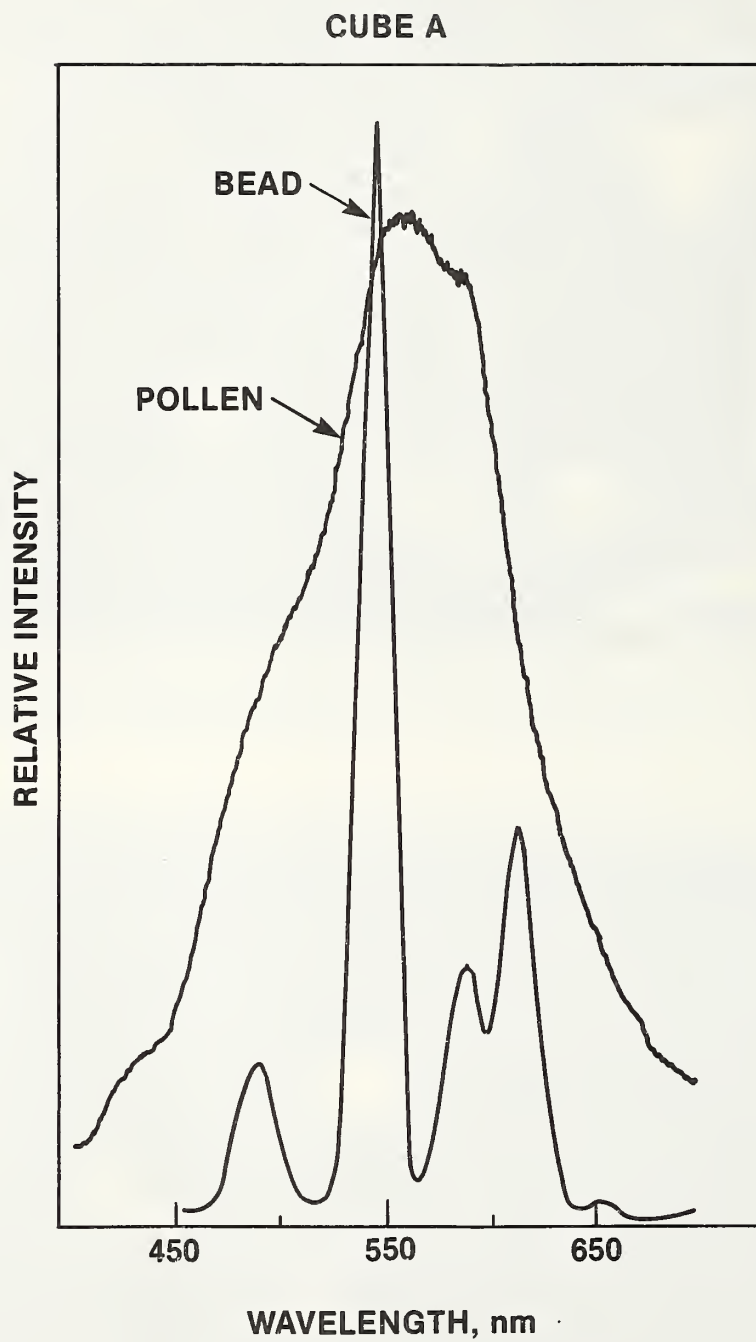Figure 36. Photograph of pollen grain and particles in house dust.

CUBE A

Figure 37. Luminescence spectrum of a pollen grain with K-1200 tagged particles for comparison.

D. Reflecting Glass Particles

A limitation of the particle tagging system is the long turnaround time from sampling a given area to the microscopic verification that there are coded particles in the sample. The best possibility would be to mount the apparatus in a mobile truck.

This particle tagging system can be enhanced by using retroreflector beads [11]. Retroreflector beads, available from 3 M Corporation are coated with aluminum over one-half of their surface. These particles act as miniature reflectors such that light incident on the particles will be reflected close to the angle of entry. Some studies of their optical properties show that the intensity of reflected light is not very great, and therefore, for light intensity used in normal automobile driving, some 60-100 m is the maximum distance that the reflected light can be seen [12]. The light is returned in the form of a ring about the entry axis [13]. A microscopic view of these retroreflecting microspheres that shows these rings is given in figure 38.

Mixing these particles with the coded ones or half coating the encoded particles would allow their detection by using a high intensity lamp that throws a beam of light about 10 cm wide. When the eye is placed close to a low intensity lamp such as a flashlight, a single 40 µm diam particle can be easily seen at a distance of 10 m in daylight away from the direct sun. Use of a small halogen lamp which provides a narrow beam of high-intensity light would allow very sensitive detection of the particles. Of course, it is possible that coated particles came from a legitimate source, such as a broken road sign or from the ubiquitous Scotch-lite tape. However, this can be considered improbable, and if one concludes that the presence of retroreflecting particles strongly suggests the presence of the tagged intruder, only those suspect samples need be taken to the microspectrofluorimeter for positive identification.

VII. PARTICLE SAMPLING TECHNIQUES

Two methods were investigated. One uses a vacuum cleaner type of device and the other uses adhesive tape. There are other possibilities such as a simple dust cloth or paper tissue that is swept over the surface to be sampled.

A. Vacuum System

The use of normal vacuum cleaners with a collecting bag was found to be unsatisfactory because of the porosity and thickness of the bag. It was not possible to observe particles at a density of 300 particles/cm^2 (16.7 µm diam) when removed by vacuum from a microscope slide.

A rather simple filter mechanism was devised from a commonly used filter system for chemical solutions. A glass frit was mounted in the base of an aluminum tube to which a vacuum pump was attached (fig. 39a). A filter mat was placed on the frit and an aluminum tube was screw-clamped on top, thereby holding the filter mat onto the surface of the glass frit. A tube and vacuum nozzle was attached to the top of the clamping tubes. The system is shown in figure 39b. It is very important that the flow of air through the filter be as laminar as possible· otherwise, the distribution of particles across the surface of the filter would be uneven. After trying several commercial filter holders without success, we resorted to the fritted glass support which gave a true laminar flow of air through the filter. A number of different filter materials were tried. A suitable one was determined to be Gelman Metricell Black 6N, 0.45 µm, 25 mm diam, Part No. 60511. The use of these filters produced a minimum of luminescent background, and the particles were well supported on the surface of the filter paper. The surface of the filter paper must be amply illuminated for microscopic examination. Luminescence spectra were easily obtained from particles on this filter paper [see fig. 40(A)].

The obvious major advantage of the vacuum system is that it increases the particle density and therefore improves detectability. Tests were made on the vacuuming of a glass slide. Transfer of particles from the slide was 100 percent, however, collection and detection on the millipore filter was only 50 percent efficient. Since the area of the millipore was smaller than the area of the glass slide, a net overall increase in detection using the vacuum cleaner as a
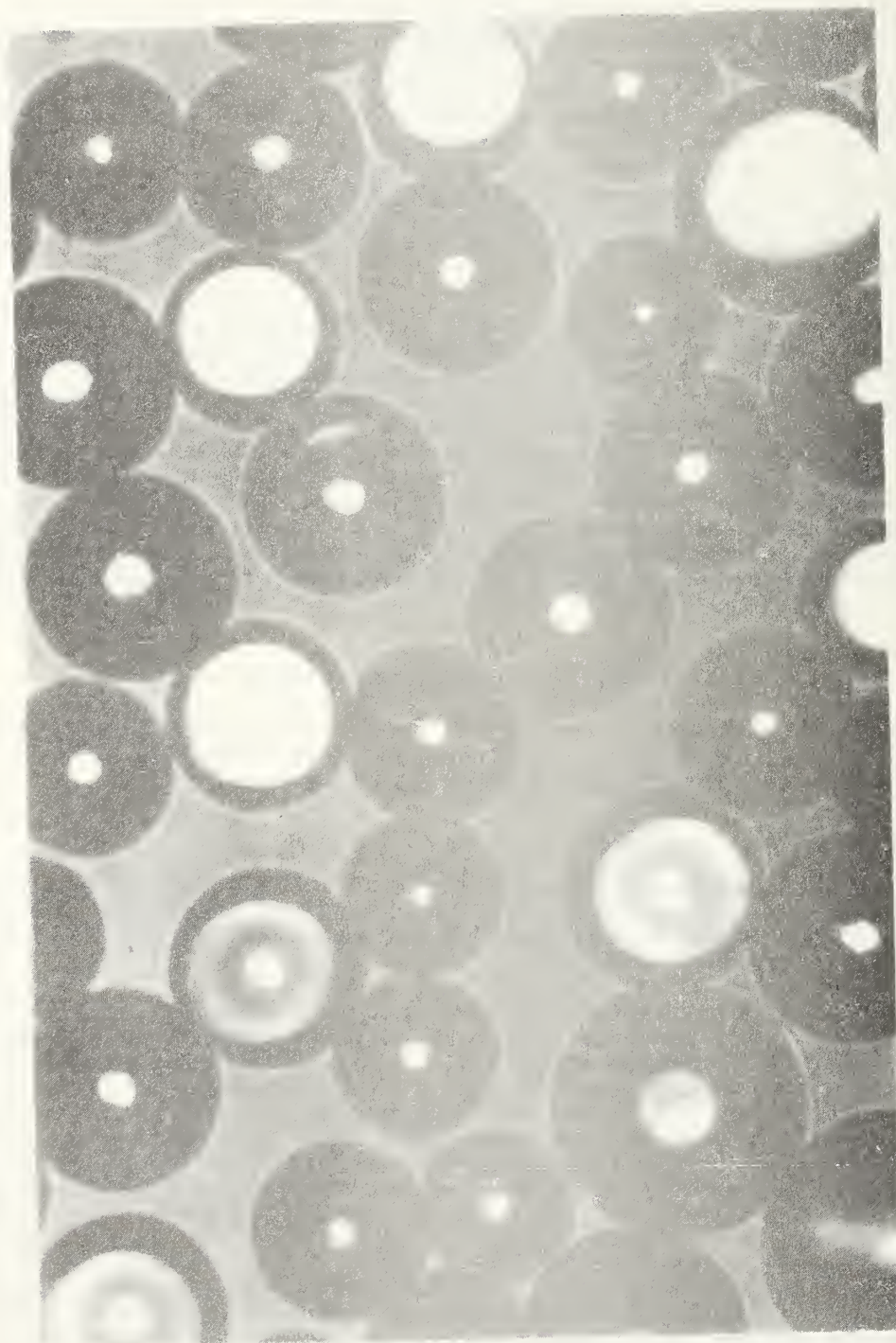
Figure 38. Photograph showing light-reflecting properties of the glass
sphere retroreflectors (diameters range from 40-85 μm).
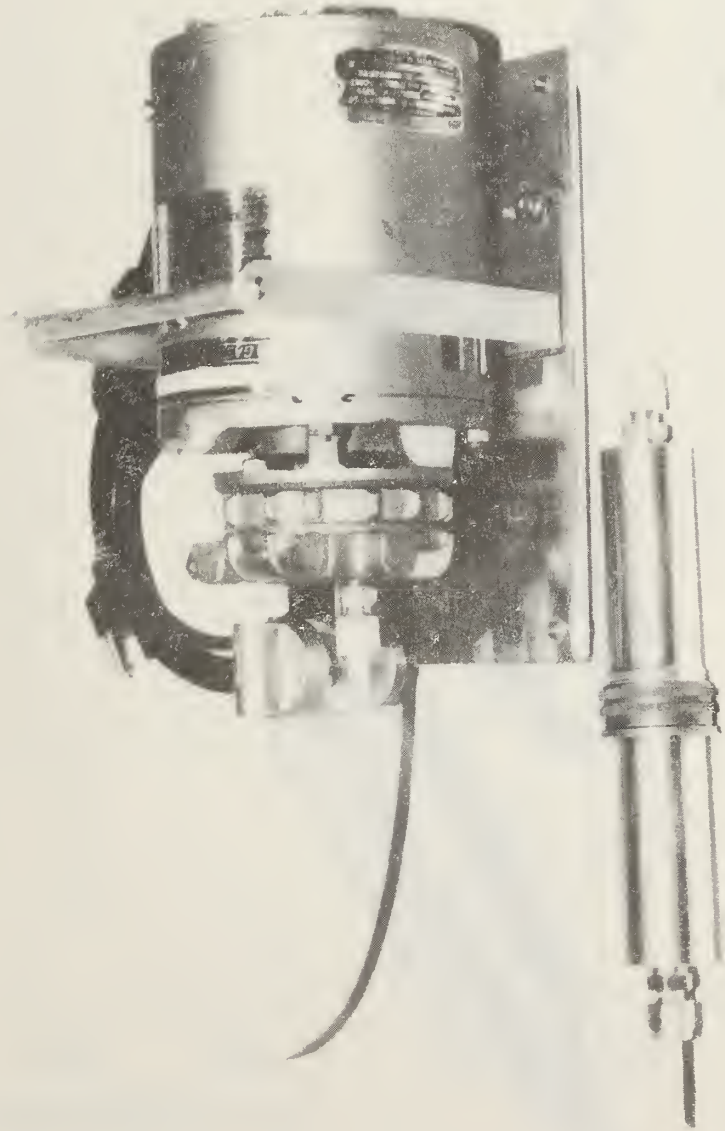
Figure 39a. Photograph of vacuum filter particle collection system: vacuum pump and filter housing.

55
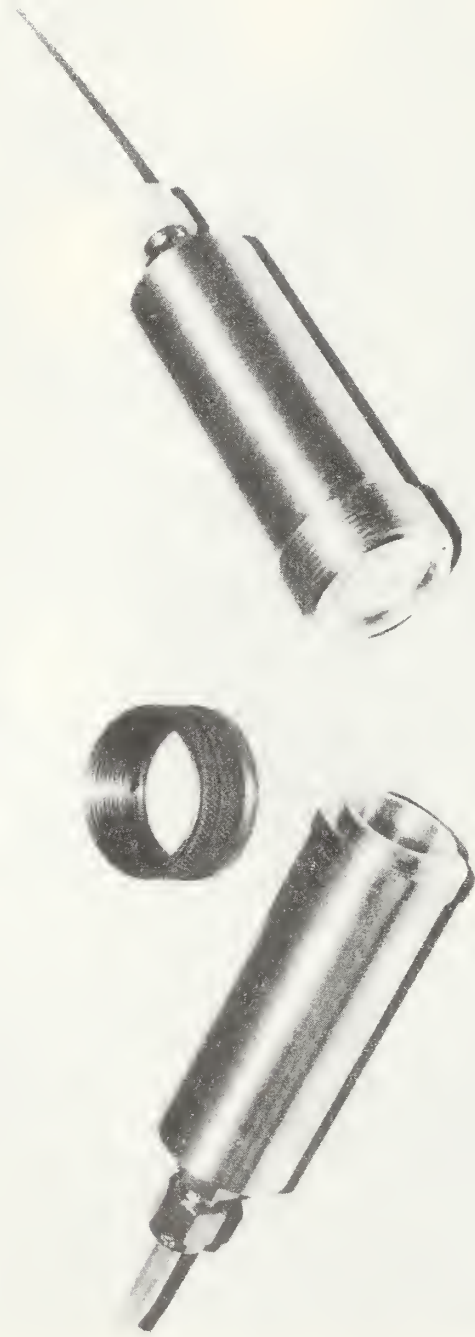
Figure 39b. Photograph of vacuum filter particle collection system; filter housing.
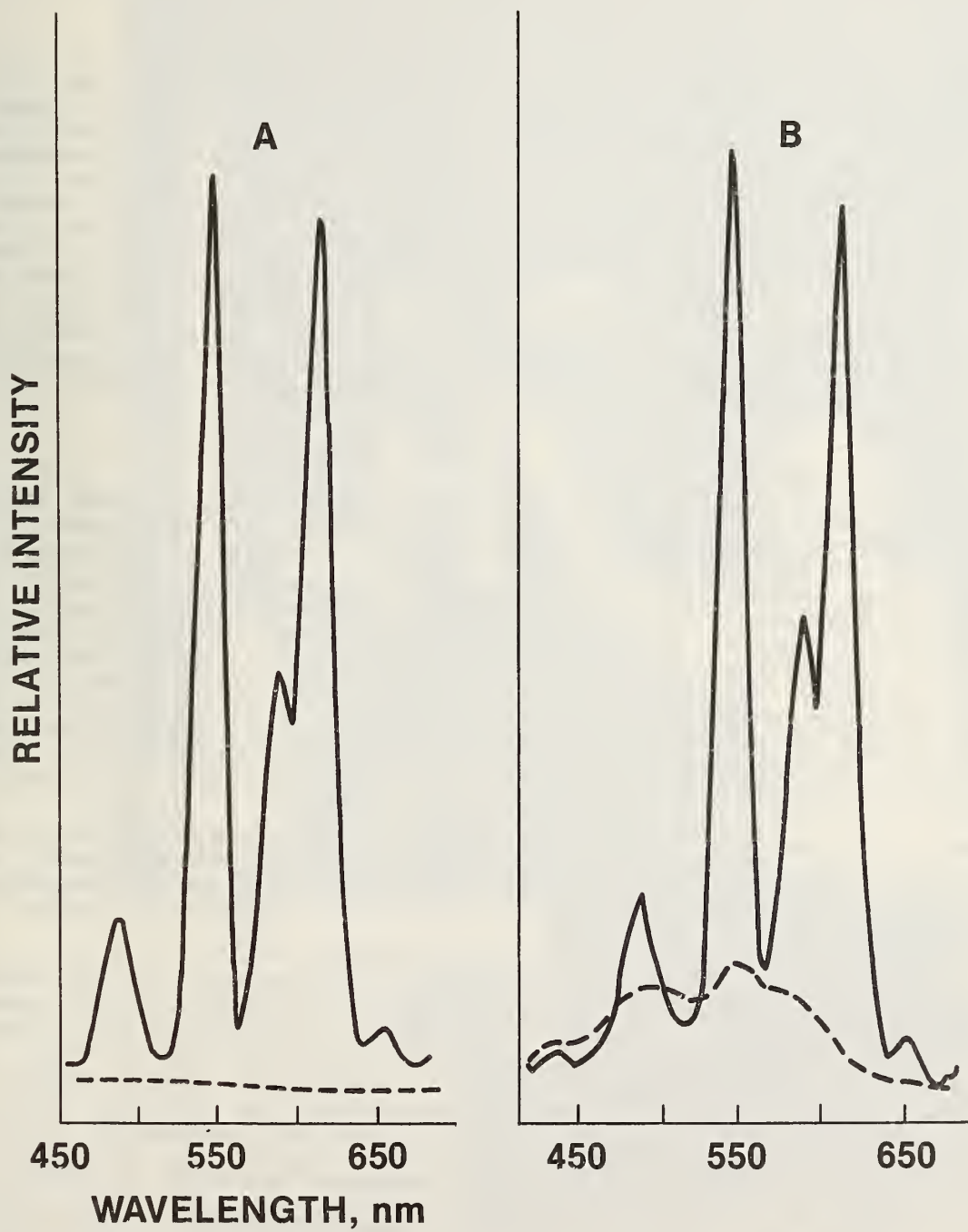
Figure 40. Spectra of luminescent particle (code K-1200) collected on: A) filter paper, and B) adhesive tape. Dashed lines indicate background.

concentrator results in a 1.5 times increase in number density. This factor can be easily increased by a factor of 10 by simply vacuuming more area, if the particles are evenly dispersed.

B. Adhesive Tape

Another method studied was the use of cellophane tape containing the usual adhesive material. One simply sticks the tape to the surface to be sampled, presses it firmly on the surface, and peels the tape from the surface with the particles embedded in the adhesive. The best procedure found was to use double-sided adhesive tape, to make good optical contact between the no-particle side of the tape and a glass slide, and to look at the particles with transmitted light. Optical contact is made by mechanically pressing the tape to the glass microscope slide. The cellophane effectively attenuates the ultraviolet excitation so the particles must be on the surface away from the slide. A series of experiments were performed by transferring particles from microscope slide to tape. A detection efficiency of about 50 percent was observed in transferring from particle densities of between 50-150 particles/cm^2. Of course, no gain in particle density can result from using this sampling technique. Again the spectrum from an individual particle on the tape is easily obtained [see fig. 40(B)].

C. Practical Tests

Using the two methods of particle collection, a general survey was made of our working laboratory where many of the particle experiments were performed. In addition, a pair of old shoes, a white shirt, and a black sweater were coated with particles in our test chamber to a level of about 350 particles/cm^2. Vacuuming of the clothing revealed hundreds of particles on the filter medium. Even though the clothing was worn for several days, many particles could still be picked up. Washing the clothing removed the particles. A few particles remained in the crack between the shoe leather and the sole even after several months of wearing the shoes. Sampling the experimental laboratory revealed particles on the floor of the balance room and around the balance where the mass dilutions were made. A few were found on the walls of the test chamber. Based upon these results, it appears that the particles adhere tenaciously to clothing, probably by electrostatic attraction.

Another test that simulated field conditions more closely was conducted at the Naval Weapons Supply Center, Crane, IN. The entire microspectrofluorimeter was disassembled, packed into a station wagon, and transported from NBS, Gaithersburg, MD to Crane, IN. The equipment was reassembled in a van in 3 h and verification of particles was made (see fig. 41).

The test involved the dispersal of the particles in concentrated liquid ammonia that was part of an ammonium chloride cloud-producing device which was being tested in an ammunition bunker. Based upon our test results we calculated that an even dispersal of 1 g of the coded particles throughout the ammunition bunker could be easily detected by our sampling techniques. Plastic strips were laid on the floor of the bunker in the manner shown in figure 42 to facilitate the sampling of the dispersed particles. About 4.2 g of the K-1200 code of particles containing europium and terbium in approximately equimolar quantities were placed in the ammonium chloride smoke generator. After firing the smoke generator and after the smoke had cleared (about 1 h), samples were collected from the plastic surfaces. Even though the plastic had become wet from the deliquescent ammonium chloride and moisture condensation on the cold floor, the tape sampling technique gave the results shown in figure 42. The numbers on the figure indicate the sampling locations and the number of particles per square centimeter that were collected at that point. The moisture totally prevented collection of the particles by the vacuuming technique. Because of the moisture on the plastic surface, we estimate that the collection efficiency was no more than 25 percent.

There were no problems in being able to distinguish the coded particles from the dirt and debris collected along with the particles. Separate laboratory tests showed that a coating of ammonium chloride on the particles did not affect the luminescence spectrum. However, an excessive white coating probably reduced the microscope particle detection efficiency although no quantitative measurements were made of the effect.
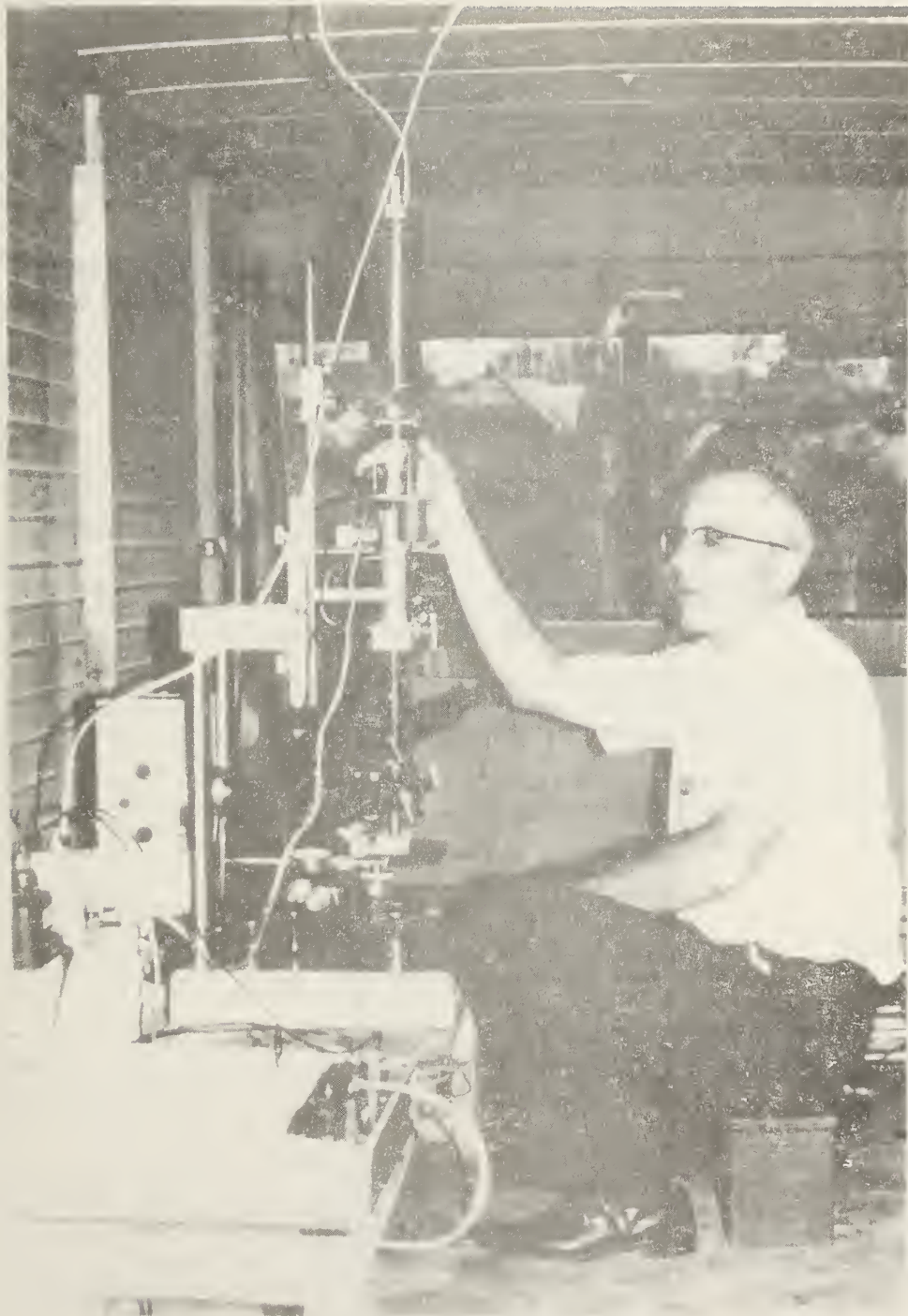
Figure 41. Photograph of the NBS microspectrofluorimeter in a
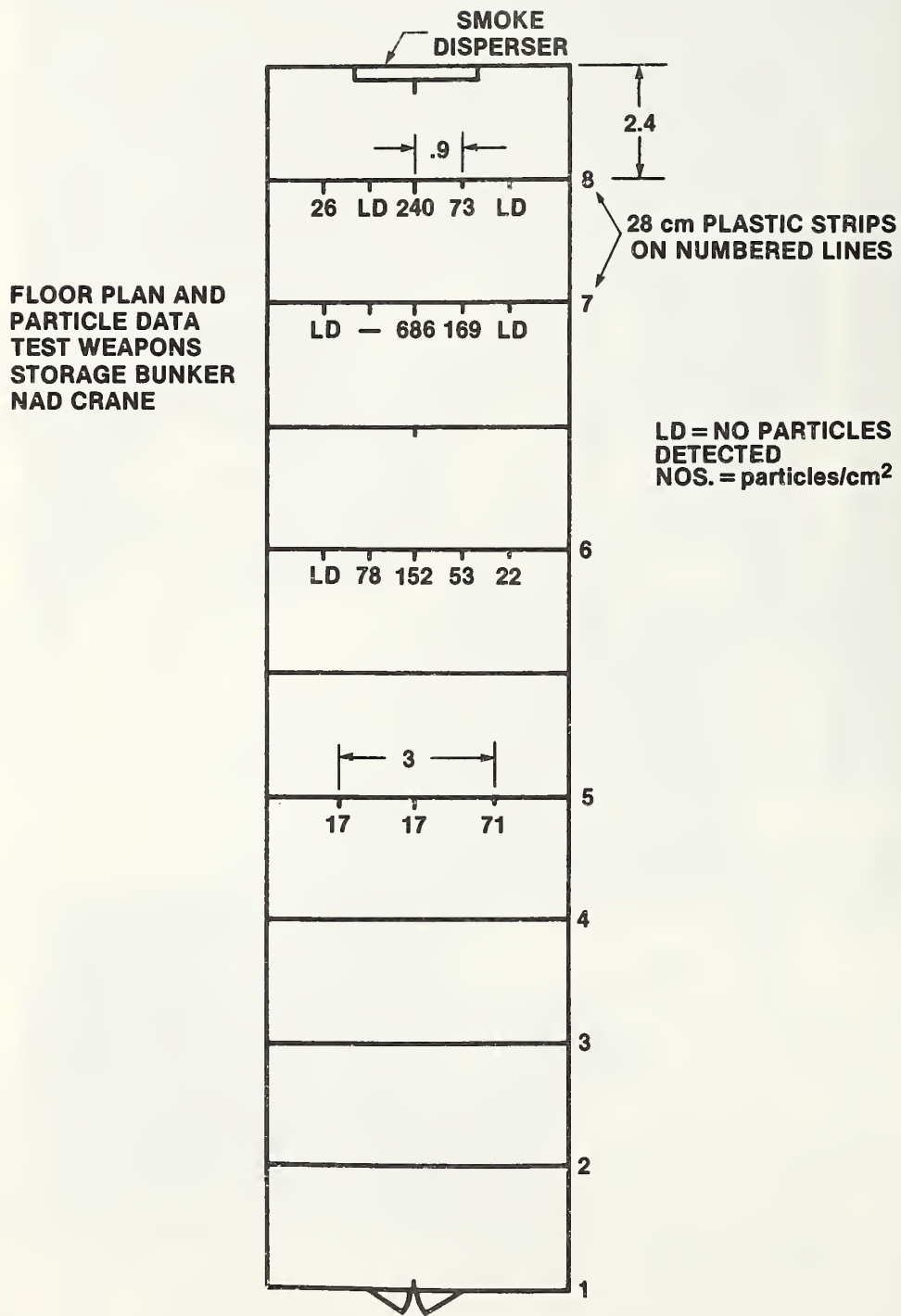van at the Naval Weapons Supply Center, Crane, IN.

Figure 42. Floor plan of ammunition bunker showing location of plastic strip and positions where sampling was performed along with the results in particles per square centimeter (dimensions in meters).

The field test demonstrated that the microspectrofluorimeter is sufficiently rugged to be used in the field, and that the particles can be unequivocally identified under field conditions in the presence of substantial amounts of dirt, moisture, HCl and NH$_4$Cl.

VIII. DESCRIPTION OF FIELD UNIT

The particle tagging system is at a sufficient stage of development to consider the assemblage of a field unit which could be placed in a van. A large suitcase can be used to house the necessary vacuum cleaner type of apparatus. The same suitcase can house a high intensity lamp although this is not included in the NBS kit.

DETAILED PROCEDURE FOR PARTICLE SAMPLING AND VERIFICATION

Particle Sampling

1. If light-reflecting particles have been incorporated into the tag, the high-intensity light should be used to illuminate the area under surveillance. It is important to keep the eye as close to the source of light as possible since the spherical beads act as retroreflectors. For example, a miner's-cap type of arrangement would be ideal.

2. If a likely area has been found, the particles can be collected using the vacuum system (fig. 39a). The pump uses 110 V ac; the filter clamps between the upper and lower housing (fig. 39b). The hose containing the copper wand is attached to the filter. Keeping the hose as short as possible is important because static charges can build up on the hose material and a substantial number of the collected particles will adhere to the inner surface of the hose.

If it is impractical to collect by vacuuming, cellulosive adhesive tape can be used. Adhesive tape coated on both sides provides the best optical contact with the microscope slide. The tape can be pressed onto the glass with the particle side up, by using a curved metal implement. Sufficient contact can be made so that few air bubbles are noticeable. Even though the particles are pressed into the adhesive by this technique they remain easily identifiable under microscopic examination.

Particle Verification

1. The microspectrofluorimeter is set up as follows:

    a. For a schematic of the apparatus refer to figure 3, and for a labeled photograph refer to figure 43.

    b. Place a sample of collected dirt or dust suspected of containing the tagged particle on a microscope slide. If the particles are on a filter medium, mount the filter on the slide; or if adhesive transparent tape is used, mount this on the slide.

    c. Turn the power switch on the excitation lamp power supply to "ON" position, wait 30 s, then depress the ignite button for 1/2 s. If the lamp does not light release the button and repeat after 30 s. Do not hold the button in for a long period of time, i.e., 5 s or longer. The "Lamp On" light will signal lamp ignition. Note: It is advisable to operate the light source for 1 h before use in order to stabilize its output intensity.

    d. The slide is scanned in as random a fashion as possible so that no FOV overlap. To minimize fatigue scanning should be no longer than 10 min. This time should allow the analyst to inspect about 150 FOV using 312X magnification (25X objective, 10X eyepiece, 1.25X lens).

    e. When a particle is located, its identity must be verified by measuring its luminescence spectrum, using the following procedure.

Photomultiplier

Monochromator

X-Y Focusing Optics

Measuring Aperture

Measuring Telescope

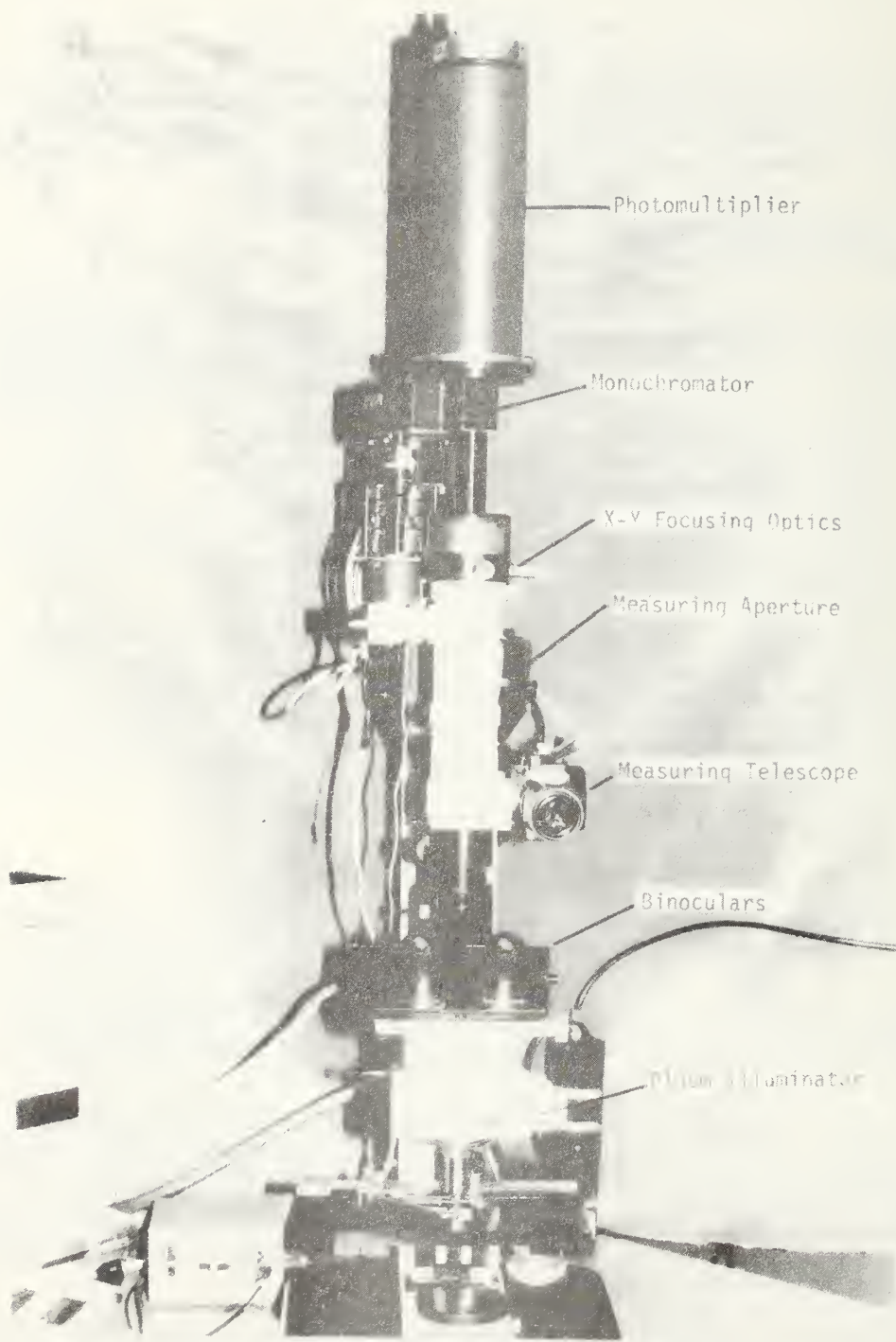Binoculars

Ploem Illuminator

Figure 43.   Photograph of microspectrofluorimeter (with pertinent
             controls labeled).

2. Turn on power supply to photomultiplier (PM) tube 1000-1300 V, the current amplifier (setting at 10^7), and the x-y recorder. Allow the lamp and electronic systems to idle for 1 h before taking measurements.

3. Place bead(s) to be examined on a glass slide and secure slide on microscope stage.

4. Viewing through the binocular eyepiece, focus the microscope using first the coarse, then the fine adjustments. Be careful not to drive the objective into the sample slide.

5. When a bead is found using the x and y stage adjustments, center the bead in the concentric circles seen through the binocular eyepiece.

6. Select the appropriate filter block by rotating the correct cube into position. Note: For each rare earth composition, there may be a different set of excitation and emission filters that will give the optimum peak intensities. These have to be tested experimentally for each standard particle.

7. Push in the lever that operates the beam splitter and observe the bead through the monocular eyepiece.

8. Refocus the bead and center it in the cross hairs seen through the monocular eyepiece.

9. With most of the light directed up the tube and with the side-mounted light on, adjust the field iris diaphragm so that the illuminated circular area is slightly larger than the image of the bead. This shows the image whose light will be transmitted to the monochromator. Note: The adjustment of the field size with the iris diaphragm is made by adding a small source of light to produce an image that superimposes on the microscope's monocular eyepiece.

10. Pull the beam splitter lever out to allow light to pass into PM tube. With the monochromator adjusted to a peak maximum, maximize the signal by adjusting the focusing lens. Note: The axis of the PMT focusing lens should be colinear with the optic axis of the microscope. This is best done by lateral movement of the lens with the two adjusting screws provided. Once this adjustment is made it should be unnecessary to readjust unless the optics have been disassembled.

11. Scan the emission spectrum with the scanning monochromator from ~430-750 nm while recording the output on the x-y recorder.

12. Readjust the mechanical stage so that a bead-free area of the slide is exposed and record a background spectrum. Note: A background "spectrum" should have very low intensity. If not, look for stray light entering the system. It might be possible for a strongly emitting particle to cause a distortion of the peak heights in the spectrum. The measurement should be repeated for both the standard and unknown at a different diaphragm setting (e.g., to change the amount of background light entering the optics). If the ratio of peak intensities changes, it may be necessary to move the particle to another location on the slide.

13. Repeating the above procedure, record an emission spectrum for a reference bead and again take a background spectrum.

14. Measure the peak-height maximum each for Eu and Tb, from the background level to the height of the peak and calculate a peak height ratio for the reference and unknown particles. If the spectral shapes of the reference and unknown look identical and the peak height ratios agree within 2 percent relative, a positive identification is indicated. Replicate measurements of both standard and unknown will statistically confirm the identity.

IX. FUTURE DEVELOPMENT OF THE SYSTEM

It is obvious that the process for identifying the presence of a tag is somewhat lengthy. However, the use of the retroreflecting beads should provide an answer to that problem because the particles can be rather easily seen at some distance that facilitates the scanning of a large area in a short time. This is of particular advantage when one wishes to follow a "hot" trail involving the immediate pathway that an intruder might have taken after setting off the alarm and releasing the tag material. The trail of the intruder would be illuminated by the retroreflecting spheres. Tests should be made with a high intensity lamp in bright sunlight to see if the retroreflecting spheres can still be easily seen. The obvious disadvantage is that the tag is not covert in the sense that anyone with the appropriate illuminator can locate the retroreflecting particles. Of course, the particle verification still requires the use of the microspectrofluorimeter which is not commonly available. The retroreflector particles can probably be admixed with the luminescent particles. There seems to be no advantage to having the luminescent particles coated with a reflecting substance. A low-cost light source, preferably battery-operated, to be used to detect the retroreflector particles needs to be developed.

Fluorescent chemical systems need to be developed to provide sufficient unique tagging codes for use at a large number of facilities, however, preliminary studies show that a sufficient number of codes can be generated.

More extensive studies should be made on the method of tagging the intruder. For example, thought should be given to the use of the particles in a paint that dries into a powdery film which causes tagging by contact with the painted surface. If a container housing the object to be protected were covered with the encoded luminescent particles, the intruder could not avoid contact. Inconvenience may outweigh the advantage of such a passive tagging method. For example, careful decontamination would have to be performed each time the protected item were moved.

Finally, through development of the technique, it should be possible to predict the proper areas for sampling. For example, during the limited practical testing done in this work, it was found that the crack between the shoe leather and sole is an excellent place to find a tag even though the tagging occurred months before the detection of the tag.

REFERENCES

[1]   DeVoe, James R. Intruder detection by chemical analysis. Memorandum report submitted to the Defense Nuclear Agency. Washington, DC: U.S. Dept. of Defense; 1977 June.

[2]   DeVoe, J. R.; Sweger, D. M.; Velapoldi, R. A. Intruder detection using trace constituent analysis. Progress report to Defense Nuclear Agency. Washington, DC: U.S. Dept. of Defense; 1978 April.

[3]   Harvey, E. N. A history of luminescence. Philadelphia, PA: The Amer. Phil. Soc.; 1957.

[4]   Stokes, G. G. Phil. Trans. Roy. Soc. London. A142, 463 (1852); Ibid. A143, 385 (1853).

[5]   (a) Parker, C. A. Photoluminescence of solutions. New York, NY: Elsevier Publishing Co.; 1968.

        (b) Binks, J. B. Photophysics of aromatic molecules. New York, NY: Wiley Interscience; 1969.

[6]   Ploem, J. S. Z. Wiss. Mikrosk. 68 129 (1967).

[7]   Velapoldi, R. A.; Travis, J. C.; Cassatt, W. A.; Yap, W. T. J. Microscopy. 103 293 (1975).

[8]   Seidle, A. R.; Velapoldi, R. A.; Erickson, N. Appl. of Surface Science. 3 229 (1979); J. Inorg. Nucl. Letters. 15 33 (1979).

[9]   Reisfeld, R.; Velapoldi, R. A.; Boehm, L. J. Phys. Chem. 76 1293 (1972); Reisfeld, R.; Honigbaum, A.; Michaels, G.; Hard, L.; Ish-Shalom, M. Israel J. Chem. 7 613 (1969).

[10]   Small, J. K.; Heinrich, K. F. J.; Fiori, C. E.; Myklebust, R. L.; Newbury, D. E.; Dilmore, M. F. Scan. Elect. Micros. 1 445 (1978).

[11]   This idea was first suggested to us by Dr. H. Webster, U.S. Naval Weapons Support Center, Crane, IN.

[12]   Stoudt, M. D. and Vedam, K. Applied Optics 17 No. 12 1855 (1978).

[13]   Stoudt, M. D. and Vedam, K. Applied Optics 17 No. 12 1859 (1978).

4. TITLE AND SUBTITLE

Intruder Tagging and Identification Using Luminescent Particles

5. AUTHOR(S)

J. R. DeVoe, R. A. Velapoldi, J. K. Langland, D. K. Hancock

11. ABSTRACT (A 200-word or less factual summary of most significant information. If document includes a significant bibliography or literature survey, mention it here)

This is the final report on the development of a unique particle tagging system that can allow one to follow the egress of a person who violates a secured area. The intruder comes into contact with glass beads (20 μm diam) which are of two types: one type acts as light reflectors allowing immediate visual detection; the second type contains rare earths whose emission spectra and quantity can be measured in a microspectrofluorimeter. Each site is tagged with beads containing a unique concentration ratio of two rare earths, thereby enabling hundreds of unique codes. The efficiency for detecting these particles has been measured and particle densities as low as 5 particles/cm^2 can be detected. Particle concentration techniques were also developed. Practical tests demonstrated the portability of the equipment and that this system is effective in such environments as normal buildings and houses as well as in an ammunition storage bunker.

12. KEY WORDS (Six to twelve entries; alphabetical order; capitalize only proper names; and separate key words by semicolons)

fluorescence; intruder tagging and identification; microspectrofluorimeter; particles; tagging material.